



REDE NORDESTE DE BIOTECNOLOGIA - RENORBIO  
UNIVERSIDADE FEDERAL DO ESPÍRITO SANTO - UFES  
PROGRAMA DE PÓS-GRADUAÇÃO EM BIOTECNOLOGIA

**LARYSSA PINHEIRO COSTA SILVA**

**APPLICATION OF GREEN NANOPARTICLES AND NANOCELLULOSE IN  
THE PRODUCTION OF SMART TEXTILES**

VITÓRIA, ES

2022

**LARYSSA PINHEIRO COSTA SILVA**

**APPLICATION OF GREEN NANOPARTICLES AND NANOCELLULOSE IN  
THE PRODUCTION OF SMART TEXTILES**

Tese apresentada ao Programa de Pós-Graduação em Biotecnologia (RENORBIO) – Ponto focal Universidade Federal do Espírito Santo, como requisito parcial para obtenção do título de Doutor em Biotecnologia.

Orientador: Marco Cesar  
Cunegundes Guimarães, D.Sc.

VITÓRIA, ES

2022

Ficha catalográfica disponibilizada pelo Sistema Integrado de Bibliotecas - SIBI/UFES e elaborada pelo autor

---

P654a Pinheiro Costa Silva, Laryssa, 1992-  
Application of green nanoparticles and nanocellulose in the production of smart textiles / Laryssa Pinheiro Costa Silva. - 2022.

117 f. : il.

Orientador: Marco Cesar Cunegundes Guimaraes.  
Tese (Doutorado em Biotecnologia) - Universidade Federal do Espírito Santo, Centro de Ciências da Saúde.

1. Nanopartículas. 2. Celulose. 3. Coco. 4. Fibras vegetais. 5. Tecnologia textil. I. Cunegundes Guimaraes, Marco Cesar. II. Universidade Federal do Espírito Santo. Centro de Ciências da Saúde. III. Título.

CDU: 61

---

**LARYSSA PINHEIRO COSTA SILVA**

**APPLICATION OF GREEN NANOPARTICLES AND NANOCELLULOSE IN  
THE PRODUCTION OF SMART TEXTILES**

Tese de Doutorado apresentada ao Programa de Pós-Graduação em Biotecnologia (RENORBIO) - Ponto focal Universidade Federal do Espírito Santo como parte dos requisitos para obtenção do grau de Doutor em Biotecnologia.

Aprovada em: \_\_\_ / \_\_\_ / \_\_\_\_

**BANCA EXAMINADORA**

---

Prof. Marco Cesar Cunegundes Guimarães  
Universidade Federal do Espírito Santo – UFES  
Orientador

---

Prof. Dr. Jairo Pinto de Oliveira  
Universidade Federal do Espírito Santo– UFES  
Examinador Interno

---

Prof. Diego Magalhães do Nascimento  
Centro Nacional de Pesquisa em Energia e Materiais – CNPEM  
Examinador Externo

---

Prof<sup>a</sup>. Dr<sup>a</sup>. Rosa Amalia Fireman Dutra  
Universidade Federal de Pernambuco - UFPE  
Examinador Externo



**UNIVERSIDADE FEDERAL DO ESPÍRITO SANTO**  
**Centro de Ciências da Saúde**  
**Programa de Pós-Graduação em Biotecnologia**  
**Rede Nordeste de Biotecnologia**

Ata da sessão da octagésima primeira defesa de Tese do Programa de Pós-Graduação em Biotecnologia da Rede Nordeste de Biotecnologia – RENORBIO, do Centro de Ciências da Saúde da Universidade Federal do Espírito Santo, da discente LARYSSA PINHEIRO COSTA SILVA, candidata ao título de Doutor em Biotecnologia. A defesa foi realizada às 13:00h do dia trinta e um de agosto do ano dois mil e vinte e dois, na Universidade Federal do Espírito Santo, por meio de videoconferência, conforme inciso 6º do Art. 51 Regulamento Geral da Pós-Graduação da UFES, aprovado na Resolução Nº 3-CEPE, de 28 de janeiro de 2022. O presidente da Banca, Marco Cesar Cunegundes Guimarães, apresentou os demais membros da comissão examinadora, os quais participaram remotamente da sessão de defesa, constituídos pelos Doutores: Jairo Pinto de Oliveira, da Universidade Federal do Espírito Santo, como membro titular interno; Diego Magalhães do Nascimento, Centro Nacional de Pesquisa em Energia e Materiais (CNPEM), membro titular externo à RENORBIO; Rosa Amália Fireman Dutra, Universidade Federal de Pernambuco, membro titular externo à Instituição Nucleadora UFES. Em seguida, cedeu a palavra à candidata que em 50 (cinquenta) minutos apresentou sua Tese intitulada “Application of green nanoparticles and nanocellulose in the production of smart textiles”. Terminada a apresentação, o presidente retomou a palavra e a cedeu aos membros da Comissão Examinadora, um a um, para procederem à arguição. O presidente convidou a Comissão Examinadora a se reunir em separado para deliberação. Ao final, a Comissão Examinadora retornou e o presidente informou aos presentes que a Tese havia sido APROVADA e que a aluna deve providenciar dentro do período de 60 dias, a versão final da Tese. O Presidente, então, deu por encerrada a sessão, e eu, Breno Valentim Nogueira, Coordenador da Nucleadora UFES do Programa de Pós-Graduação em Biotecnologia, lavrei a presente ata, que é assinada pelos membros da Comissão Examinadora. Vitória, 31 de agosto de 2022.

---

Prof. Dr. Marco Cesar Cunegundes Guimarães  
Universidade Federal do Espírito Santo – Orientador

---

Prof. Dr. Jairo Pinto de Oliveira  
Universidade Federal do Espírito Santo - Titular Interno

---

Profª. Drª. Rosa Amália Fireman Dutra  
Universidade Federal de Pernambuco - Titular Externo

---

Prof. Dr. Diego Magalhães do Nascimento  
Centro Nacional de Pesquisa em Energia e Materiais – Titular Externo



Campus Universitário Maruípe – Av. Maruípe, 1468 – Maruípe, Vitória – ES | 29047-185 |  
Tel. e Fax: (27) 3335-9501 | <http://www.biotecnologia.ufes.br/> | [renorbioes@gmail.com](mailto:renorbioes@gmail.com)




UNIVERSIDADE FEDERAL DO ESPÍRITO SANTO


**PROTOCOLO DE ASSINATURA**




O documento acima foi assinado digitalmente com senha eletrônica através do Protocolo Web, conforme Portaria UFES nº 1.269 de 30/08/2018, por  
MARCO CESAR CUNEGUNDES GUIMARAES - SIAPE 2622289  
Departamento de Morfologia - DM/CCS  
Em 02/09/2022 às 09:46

Para verificar as assinaturas e visualizar o documento original acesse o link:  
<https://api.lepisma.ufes.br/arquivos-assinados/554046?tipoArquivo=O>

Documento assinado digitalmente  
 ROSA AMALIA FIREMAN DUTRA  
Data: 16/09/2022 20:57:29-0300  
Verifique em <https://verificador.iti.br>

Documento assinado digitalmente  
 DIEGO MAGALHAES DO NASCIMENTO  
Data: 18/09/2022 20:21:27-0300  
Verifique em <https://verificador.iti.br>

Documento assinado digitalmente  
 JAIRO PINTO DE OLIVEIRA  
Data: 19/09/2022 08:34:19-0300  
Verifique em <https://verificador.iti.br>

A José Ronaldo Pinheiro Costa (*in  
memorian*) e à Audestina Patrícia da Silva Costa,  
por todo amor a mim dedicado.

## AGRADECIMENTOS

Desafio tão grande quanto escrever esta Tese, foi utilizar apenas duas páginas para agradecer a todas as pessoas que fizeram parte desta minha trajetória.

Início os agradecimentos aos meus pais, José Ronaldo Pinheiro Costa (*in memorian*) e Audestina Patricia da Silva Costa, que sempre primaram pela minha educação. Além de me oferecerem a oportunidade de estudar e estarem sempre ao meu lado, foram exemplo de força, dedicação e trabalho. Sinto-me orgulhosa e privilegiada por ter pais tão especiais.

Aos meus avós Odir Lucas Silva (*in memorian*) e Mariza de Carvalho Silva, por me amarem mesmo eu me ausentando dos almoços de fim de semana. Principalmente ao meu avô Odir, que sempre me ensinou que o maior bem que temos é o conhecimento.

Agradeço ao Prof. Dr. Marco Cesar Cunegundes Guimarães pela orientação, paciência, competência, profissionalismo e dedicação. Principalmente, por ter dado minha 1ª oportunidade na ciência, como aluna de Iniciação Científica (IC) em 2010. Obrigada por acreditar em mim, por sempre me incentivar e puxar minha orelha quando era preciso. Tenho certeza de que não chegaria até aqui sem o apoio do senhor.

Também agradeço aos meus orientadores de IC, Prof<sup>a</sup>. Dr<sup>a</sup>. Narcisa Imaculada Brant Moreira e Prof. Dr. Fausto Edmundo Lima Pereira, e ao meu orientador de mestrado, Prof. Dr. Fabio Ribeiro Braga, por todo apoio e conhecimento compartilhado. Embora o destino nos tenha traçado caminhos diferentes, ficaram as marcas de competência e respeito.

Aos membros da banca examinadora, Prof. Dr. Jairo Pinto de Oliveira, Dr. Diego Magalhães do Nascimento e Prof<sup>a</sup> Dr<sup>a</sup>. Rosa Amália Fireman Dutra, que tão gentilmente aceitaram participar e colaborar com esta tese. Ao Prof. Jairo, agradeço ainda pelas conversas, por estar sempre disposto a me ajudar e a me guiar.

À Prof<sup>a</sup>. Dr<sup>a</sup>. Glória Maria de Farias Viégas Aquije e ao técnico de laboratório LabPetro - Antônio Augusto Lopes Marins, que prontamente me auxiliaram na execução e interpretação das análises de AFM, Raman e FTIR.



Aos amigos Wanderson e Tadeu, pelos conhecimentos compartilhados, pelas risadas, ciladas e apoio constantes. Estamos juntos há mais de 12 anos, essa jornada sem a amizade de vocês não seria a mesma!

Agradeço ainda a todos os demais amigos e amigas do laboratório, Rafaela Spessemille, Luis Contreras, Flávio, Natane, Sady, Letícia, Pedro Cassaro, Alan, Bruno, Natália, Vanessa, Rayssa, Suely, Rodolfo, Gabriel, Ariany, Amanda, Jéssica Dutra, Caio, Heloisa, Luana, Marcelo, Miguel e Gustavo, obrigada pelo convívio, amizade e apoio demonstrado. Cada um dessa lista me ajudou a colocar um tijolinho na construção desse trabalho.

Aos amigos Ingrid (Gridizinha), Luiz Miguel, Iuly, Izack, Kamila, Tiago, Rebeca, Anelise, Leandra, Lilian, Glaucinha, Letícia, Martielo e Gregório. A crônica “Amigos”, de Vinícius de Moraes, descreve, de forma impecável, o quanto vocês são importantes para mim.

Gostaria de realizar um agradecimento especial ao meu noivo, Alexander Siqueira Silva, por todo amor, carinho, compreensão e apoio em tantos momentos difíceis desta caminhada. Obrigada por permanecer ao meu lado, por ser o meu porto seguro, por me fazer acreditar que chegaria ao final desta difícil, porém gratificante etapa, e principalmente, por me fazer feliz. Estou ansiosa para estar ao seu lado, junto com nossos futuros filhos e cachorros, o resto de nossas vidas!

Agradeço também aos Laboratórios parceiros, LUCCAR (UFES), LABPETRO (UFES), LABIOM (UFES), Química (IFES-Serra), Química (IFES-Vitória), Química (IFES-Aracruz).

Ao apoio institucional da Universidade Federal do Espírito Santo e do Departamento de Morfologia.

Ao Programa de Pós Graduação em Biotecnologia.

A FAPES pelo financiamento da pesquisa.

Por fim, agradeço a DEUS por poder citar todas estas pessoas neste momento tão importante. Obrigado por colocá-las tão caprichosamente em minha vida.

## ACKNOWLEDGMENT

As big a challenge as writing this thesis, it was to use only two pages to thank all the people who were part of my trajectory.

I would like to start by thanking my parents, José Ronaldo Pinheiro Costa (in memorian) and Audestina Patricia da Silva Costa, who always excelled in my education. In addition to offering me the opportunity to study and always being by my side, they were an example of strength, dedication, and work. I feel proud and privileged to have such special parents.

To my grandparents Odir Lucas Silva (in memorian) and Mariza de Carvalho Silva, for loving me even when I am away from weekend lunches. Mainly to my grandfather Odir, who always taught me that the greatest asset we have is knowledge.

I thank Prof. Dr. Marco Cesar Cunegundes Guimarães for his guidance, patience, competence, professionalism, and dedication. Mainly, for giving me my 1st opportunity in science, as a Scientific Initiation (IC) student in 2010. Thank you for believing in me, for always encouraging me and pulling my ear when I needed to. I'm sure I wouldn't have gotten this far without your support.

I also thank my IC advisors, Prof. Dr. Immaculate Narcissa Brant Moreira and Prof. Dr. Fausto Edmundo Lima Pereira, and to my master's supervisor, Prof. Dr. Fabio Ribeiro Braga, for all the support and shared knowledge. Although fate has traced different paths for us, the marks of competence and respect remain.

To the members of the examining board, Prof. Dr. Jairo Pinto de Oliveira, Dr. Diego Magalhães do Nascimento and Prof. Dr. Rosa Amalia Fireman Dutra, who so kindly agreed to participate and collaborate with this thesis. To Prof. Jairo, I also thank you for the conversations, for always being willing to help and guide me.

To Prof. Gloria Maria de Farias Viégas Aquije and the laboratory technician LabPetro - Antônio Augusto Lopes Marins, who promptly helped me in the execution and interpretation of the AFM, Raman and FTIR analyses.

To friends Wanderson and Tadeu, for their shared knowledge, laughter, pitfalls, and constant support. We've been together for over 12 years, this journey without your friendship wouldn't be the same!

I also thank all the other friends of the laboratory, Rafaela Spesseemille, L Contreras, Flávio, Natane, Sady, Letícia, Pedro Cassaro, Alan, Bruno, Natália, Vanessa, Rayssa, Suely, Rodolfo, Gabriel, Ariany, Amanda, Jessica Dutra, Caio, Heloisa, Luana, Marcelo, Miguel, and Gustavo, thank you for your friendship, friendship, and support. Each one of this lists helped me to lay a brick in the construction of this work.

To friends Ingrid (Gridizinha), Luiz Miguel, Iuly, Izack, Kamila, Tiago, Rebeca, Anelise, Leandra, Lilian, Glaucinha, Letícia, Martielo and Gregório. The chronicle “Amigos”, by Vinícius de Moraes, describes, impeccably, how important you are to me.

I would like to give a special thanks to my fiancé, Alexander Siqueira Silva, for all the love, affection, understanding and support in so many difficult moments of this journey. Thank you for staying by my side, for being my safe haven, for making me believe that I would reach the end of this difficult but rewarding stage, and above all, for making me happy. I look forward to being by your side, along with our future children and dogs, for the rest of our lives!

I also thank the partner Laboratories, LUCCAR (UFES), LABPETRO (UFES), LABIOM (UFES), Chemistry (IFES-Serra), Chemistry (IFES-Vitória), Chemistry (IFES-Aracruz).

To the institutional support of the Federal University of Espírito Santo and the Department of Morphology.

To the Graduate Program in Biotechnology.

FAPES for funding the research.

Finally, I thank GOD for being able to name all these people at this very important moment. Thank you for placing them so whimsically in my life.

"If you can't fly, run.  
If you can't run, walk.  
If you can't walk, crawl,  
but keep going anyway."  
(Martin Luther King Jr.)

## RESUMO

SILVA, L.P.C. Aplicação de nanopartículas verdes e nanocelulose na produção de têxteis inteligentes. 2022. 59f. Tese – Programa de Pós-Graduação em Biotecnologia, UFES, Espírito Santo. Brasil.

As atividades têxteis causam grandes impactos negativos e muitas vezes irreversíveis ao meio ambiente. Esses impactos decorrentes da produção percorrem toda a cadeia produtiva têxtil: desde o plantio do algodão até a confecção da peça. Ao longo da cadeia produtiva têxtil, os impactos ambientais envolvem contaminação do solo, consumo de água, de energia, emissões atmosféricas de poluentes e resíduos sólidos. Por outro lado, os consumidores estão cobrando cada vez mais produtos sustentáveis e, após o surgimento da pandemia do novo coronavírus, estão adotando estilo de vida higiênicos mais rigorosos. A celulose é uma das matérias-primas orgânicas mais abundante e renovável que existe. Além de sua disponibilidade e sustentabilidade, ela apresenta baixo custo e alta resistência. Por meio de ação química, física e enzimática é possível transformar a celulose em nanocelulose. A nanocelulose apresenta vantagens como biodisponibilidade, biocompatibilidade e alta capacidade de funcionalização. Aqui, propomos uma rota sustentável, para produção de nanocelulose e direcionamos nossos esforços para produção de tecidos inteligentes, com ação antimicrobiana, utilizando nanocelulose obtida de resíduo do agronegócio (fibra de coco), funcionalizada com nanopartículas oriundas de processos verdes.

**Palavras-chave:** Cellulose nanogels, fibra de coco, nanopartículas verdes, atividade antimicrobiana, tecidos inteligentes.

## ABSTRACT

SILVA, L.P.C. Application of green nanoparticles and nanocellulose in the production of smart textiles. 2022. 59f. Thesis – Postgraduate Program in Biotechnology, UFES, Espírito Santo. Brazil.

Textile activities cause major negative and often irreversible impacts on the environment. These impacts resulting from production run through the entire textile production chain: from the planting of cotton to the making of the garment. Along the textile production chain, environmental impacts involve soil contamination, consumption of water, energy, atmospheric emissions of pollutants and solid waste. On the other hand, consumers are increasingly demanding sustainable products and, following the emergence of the new coronavirus pandemic, are adopting stricter hygienic lifestyles. Cellulose is one of the most abundant and renewable organic raw materials in existence. In addition to its availability and sustainability, it has low cost and high strength. Through chemical, physical and enzymatic action, it is possible to transform cellulose into nanocellulose. Nanocellulose has advantages such as bioavailability, biocompatibility and high functionalization capacity. Here, we propose a sustainable route for the production of nanocellulose and direct our efforts towards the production of intelligent fabrics, with antimicrobial activity, using nanocellulose obtained from agribusiness residue (coconut fiber), functionalized with nanoparticles from green processes.

**Palavras-chave:** Cellulose nanogels, coconut fiber, green nanoparticles, antimicrobial activity, smart fabrics.

## LIST OF ABBREVIATIONS AND ABBREVIATIONS

NC – Nanocellulose

NCC – Cellulose nanocrystals or nanocrystalline cellulose

NCF – Cellulose Nanofibers or Nanofibrillated Cellulose

BC – Bacterial Nanocellulose

NP – Nanoparticles

TEM – Transmission electronic microscopy

SEM – Scanning Electron Microscopy

AFM – Atomic Force Microscope

DLS – Dynamic light scattering

XRD – X-Ray Diffraction

NMR – Nuclear magnetic resonance

FIRT – Fourier Transform Infrared Spectroscopy

DOE – Design of Experiments

DS – Dry mass

CNF-G – Cellulose nanofiber gel

CNC -G – Cellulose nanocrystal gels

AuNP – Gold nanoparticles

## SUMMARY

<b>1. INTRODUCTION AND OUTLINE OF THE STUDY.....</b>	<b>17</b>
<b>2. THEORETICAL BACKGROUND.....</b>	<b>19</b>
2.1. COCONUT FIBER.....	19
2.2. CELLULOSE.....	20
2.2.1. Cellulose extraction methods.....	23
2.3. NANOCELLULOSE.....	26
2.3.1. Nanocellulose Applications.....	28
2.4 GOLD NANOPARTICLES SYNTHESIZED WITH POMEGRANATE EXTRACT (AUNP-POMEGRANATE).....	31
2.5 SMART TEXTILE.....	32
<b>3. CHAPTER 1 – CELLULOSE EXTRACTION.....</b>	<b>34</b>
<b>4. CHAPTER 2 – PRODUCTION OF NANOCELLULOSIS.....</b>	<b>48</b>
<b>5. CHAPTER 3 – ANTIBACTERIAL ACTIVITY OF NANOCELLULOSIS     FUNCTIONALIZED WITH GREEN NANOPARTICLES.....</b>	<b>63</b>
<b>6. CHAPTER 4 – SMART TEXTILE.....</b>	<b>84</b>
<b>7. CONCLUSIONS AND PERSPECTIVES.....</b>	<b>101</b>
<b>8. REFERENCES</b>	
<b>9. ATTACHMENTS</b>	
9.1. CONFERENCE CONTRIBUTIONS	
9.2. ADDITIONAL INFORMATION	
9.2.1. Economic impact	
9.2.2. Socio-environmental impact	
9.3. Scientific outreach	



## **INTRODUCTION AND OUTLINE OF THE STUDY**

Textile activities have great consequences on the environment (Kishor et al., 2021). Making the entire garment manufacturing process sustainable, from the plantations that will give rise to the raw material of the garments to the carbon emission in the delivery logistics is one of the great challenges faced by this industry (Idumah et al., 2020).

Consumers have been demanding more responsibility from brands in relation to damage to nature and are more attentive to a hygienic lifestyle. These concerns became even more evident after the emergence of the new coronavirus pandemic.

Cellulose is one of the most abundant and renewable organic raw materials in existence. In addition to its availability and potential sustainability, it has low cost, biodegradability, biocompatibility, and high resistance (Balea et al., 2019). These features enable a wide variety of applications in various fields of industry.

Plant cell walls consist of lignocellulose, a structure composed mainly of cellulose, hemicellulose, and lignin. From the cellulose found in plant cells, it is possible to produce nanocellulose (Salimi et al., 2019).

Nanocellulose or cellulose nanoparticles (NC) are cellulose elements with one dimension smaller than 100 nm (Benini et al., 2018), which can combine the advantages of cellulose with those of nanomaterials (high surface area in relation to mass and unique optical properties). Thus, NC has advantages over the cellulose polymer, such as: high surface area, greater rigidity, light weight, high strength, and the extraordinary ability to interact with neighboring species such as water and inorganic and polymeric compounds (Balea et al., 2019).

Some authors have already described the possibility of using nanocellulose in the synthesis of antimicrobial materials (Li et al., 2018), drug delivery (Lam et al., 2012), biosensors (Junka et al., 2014), civil engineering (Cao et al., 2015), bioadhesives (De France et al., 2017), and water purification (Carpenter et al., 2015; Liang et al., 2016; Tang et al., 2019).

Here we propose a 100% ecological route to produce nanocellulose without the use of chemicals or organic solvents. We focus on the production of smart fabrics

with antibacterial action, using nanocellulose obtained from agribusiness residues (coconut fiber), functionalized with green nanoparticles obtained from pomegranate peel extract (Figure 1).

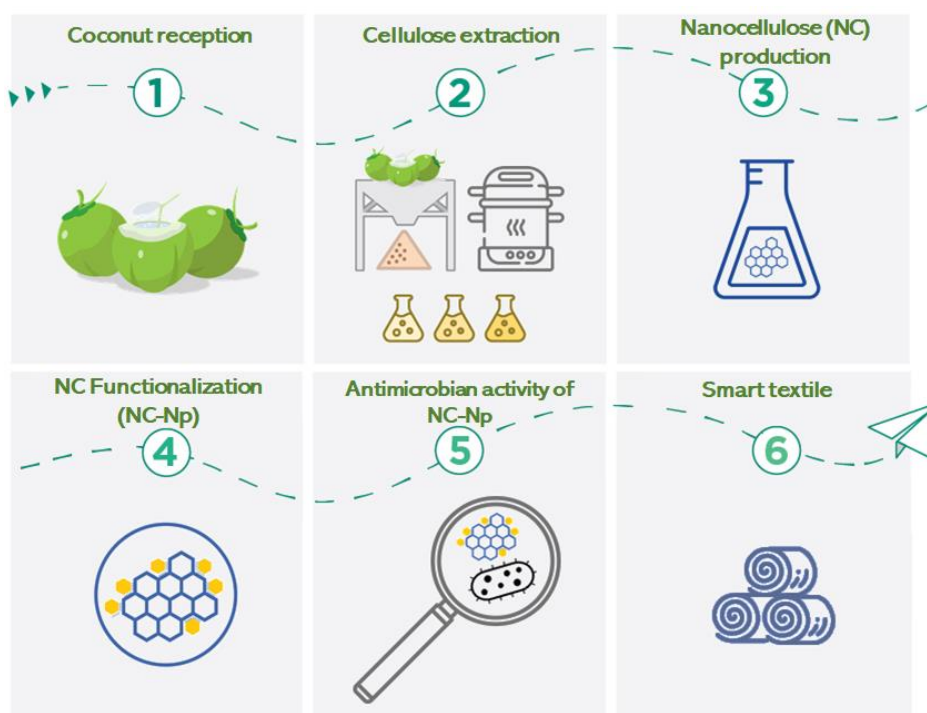


**Figure 1.** Experimental outline of the thesis. The first part of the thesis focuses on the extraction of cellulose (step 1-2). The second part deals with the production and functionalization of nanocellulose (step 3-5). The third part focuses on creating smart fabrics (step 6).

## 2. THEORETICAL BACKGROUND

### 2.1. Coconut fiber

Coconut fiber is obtained from the fruit of the coconut tree (*Cocos nucifera*), a member of the Arecaceae family (palm family), widely cultivated in tropical countries. Coconut is formed by the pericarp (part that surrounds the seed), epicarp (shell), mesocarp (fiber), endocarp (hard shell around the seed), and albumen (endosperm) (Almeida et al., 2013).

*Cocos nucifera* is cultivated in around 90 countries, with Indonesia, the Philippines, and India being the world's largest producers. Together, they account for 72.8% of all world production. The international market uses the fruit mainly for the production of copra (dry pulp) and oil. In Brazil, the crops are intended for the production of coconut water – from green coconut – and dried coconut derivatives: fresh dried coconut, grated coconut, coconut milk, and coconut oil (Brainer et al., 2018).

Brazil is the fifth largest producer of coconut in the world, with a planted area of approximately 215.7 thousand hectares (Brainer et al., 2018). The growing consumption of green coconut water resulted in a large production of solid residue formed by the fibrous husks. The fibrous coconut husk represents between 80-85% of the gross weight of the fruit and is responsible for 60% of the volume of domestic waste generated in some areas of the Brazilian coast (Sinsinwar et al. 20018). Furthermore, when this material is disposed of in landfills and dumps, it is a potential emitter of greenhouse gases (methane) (Nunes et al. 2007).

In the state of Rio de Janeiro, during the summer, around 12,000 t/month of coconut waste is produced. Therefore, the need for initiatives that take into account its use is rather important. These fibers can be used in the production of low-cost materials, in addition to contributing to the reduction of solid waste (Ishizaki et al., 2006).

Around 5 to 6 million tons of coconut fibers are produced annually around the world, but only 10% of this material is commercially reused (Tripathi et al., 2017).

Coconut fiber can be used in agriculture as fertilizer and in industry, in the process of making bags, brushes, mats, rugs, ropes, mattresses, insulation panels, packaging, and car seats (Mondal et al., 2014; Rencoret et al., 2013).

Chemically, coconut fiber is constituted by 3.1% of extractive materials, 37.3% of cellulose, 20.3% of hemicellulose, 32.2% of lignin and 6.8% of mineral material (ash) (Almeida et al. 2013). However, it is worth noting that these values may vary slightly according to seasonal conditions, age and plant variety, as demonstrated by Corradine et al. in 2009.

## **2.2. CELLULOSE**

In 1838, the French chemist Anselm Payen identified, for the first time, cellulose in the cell walls of plants, after chemically treating plant tissues with acids and ammonia, followed by extraction with water, alcohol, and ether (Bhat et al., 2019, Klemm et al., 2015).

Cellulose is the most abundant natural polymer produced in the biosphere, with an estimated annual production of more than  $7.5 \times 10^{10}$  tons (Giese et al., 2015). According to the Brazilian Tree Industry (2020), Brazil is one of the world's largest producers of cellulose and in 2018 it produced more than 21 million tons.

Plants are the main source of cellulose (eucalyptus, cotton, rice husk, banana rachis, and sugarcane bagasse), although it can also be extracted from some marine animals (Tunicados), fungi, and bacteria (Acetobacter, Rhizobium, Agrobacterium, Sarcina, Pseudomonas, Achromobacter, Alcaligenes, Aerobacter and Azotobacter) (Mohamed et al., 2017).

Cellulose is classified as a long-chain linear homopolymer with variable molecular weight, whose empirical formula is  $(C_6H_{10}O_5)_n$ . It is formed by the union of 10,000 to 15,000  $\beta$ -D-glucose units, through  $\beta$ -1,4-glycosidic bonds (Figure 1). This type of  $\beta$  configuration linking glucose residues is what makes the formation of such long straight chains possible; a crucial feature for molecules that perform structural functions (Marti-Martinez, 2018).

Two glucose molecules joined by  $\beta$ -1,4-glycosidic bonds form the disaccharide cellobiose. Therefore, cellobiose is considered the repeating unit of cellulose (Bhat et al., 2019).

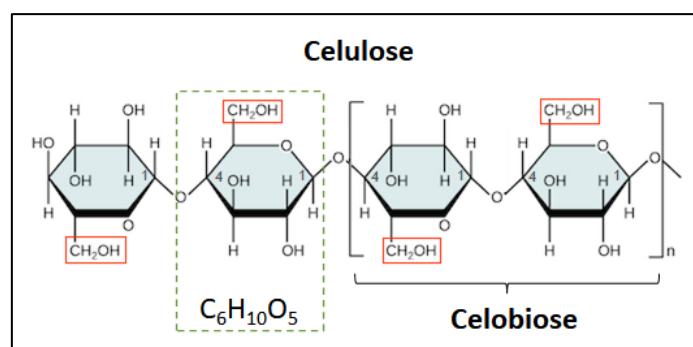


**Figure 1.** Cellulose molecule, highlighting the cellulose chain monomer and cellobiose units joined by  $\beta$ -1,4-glycosidic bonds. (Adapted from the OpenStax College, Biology 2e).

Each monomer in the cellulose chain has three free hydroxyls, divided into primary (C6) and secondary (C2 and C3) hydroxyls (Figure 1). These hydroxyls can form intramolecular hydrogen bonds and intermolecular bonds (Figure 2) (Liu et al., 2021). These two types of hydrogen bonds, together with van der Waals forces, allow the formation of basic structures called elementary fibrils.

Elementary fibrils, composed of cellulose molecules, have highly ordered (crystalline) and disordered (amorphous) regions. Thus, cellulose can be considered a semi-crystalline material with several polymorphic forms (I, II, III, and IV), depending on the nature and the chemical and/or physical treatment received (Figure 2). Cellulose I is the structure found in native cellulose; it has parallel packing of the hydrogen bond network and is formed by two allomorphs  $I\alpha$  and  $I\beta$ . Type II cellulose comes from the chemical regeneration of type I cellulose by dissolving it in a solvent or swelling it in an acidic or alkaline solution; it is composed of different antiparallel packing arrangements of the hydrogen bond network. Type III cellulose can be obtained from the ammonia treatment of cellulose I or II, while type IV cellulose is the modification of cellulose III by heating it up to 260 °C in glycerol (Phanthong et al., 2018).

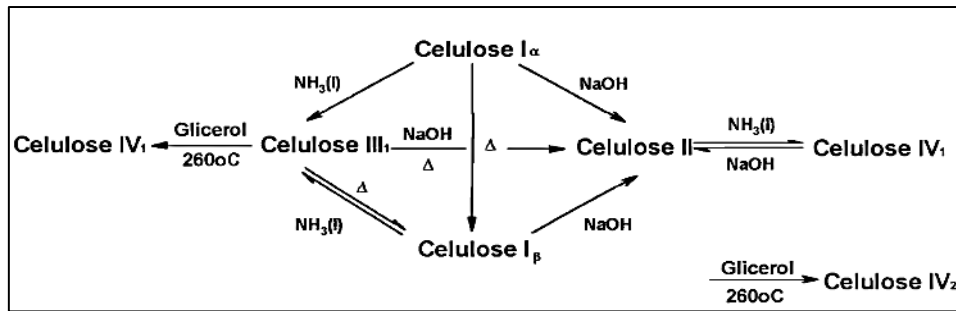


**Figure 2.** Polymorphic forms of cellulose resulting from chemical and/or physical treatment (Ruiz, 2004).

The association of several cellulose fibrils form larger units, three-dimensional (3D) networks known as cellulose microfibrils (Golmohammadi et al., 2017). Microfibrils build cellulose macrofibrils and these, in turn, give rise to cellulosic fibers (Marti-Martinez, 2018).

Thanks to the complex inter- and intra-molecular hydrogen bonds, cellulose is a fibrous polymer, resistant and insoluble in water. Furthermore, it is a renewable, non-toxic, and inexpensive material and is therefore considered an alternative to non-degradable fossil fuel-based polymers (Hu et al., 2018).

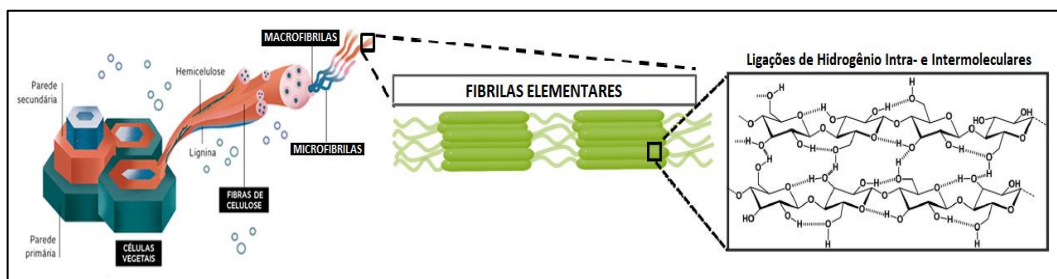


**Figure 2.** Cellulose structure. (Adapted from Giese et al. 2014; Revista Pesquisa FAPESP, 2017)

In some cases (e.g., in cotton capsules), cellulose is present in an almost pure state. However, a large part is fixed in a matrix of other structural biopolymers, mainly hemicellulose and lignin, which comprise 20-35% and 5-30% of the plant's dry weight, respectively. These interactions with the matrix are a structural feature that limits the use of whole and untreated biomass materials (Lynd et al. 2012). Thus, several types of treatments have been used to obtain cellulose.

Rosa et al. (2010) and Machado et al. (2014) used 2% sodium hydroxide and 1.7% sodium hypochlorite to extract cellulose from coconut fiber, an agribusiness residue.

### 2.2.1 Cellulose extraction methods

Vegetable fibers are basically composed of cellulose, hemicellulose, lignin, pectin, and extractives (fats, proteins, and inorganic salts). Cellulose corresponds to 40 to 90% of the fiber's weight. It is responsible for the strength of this structure, because of its high degree of polymerization and molecular orientation. Cellulose is a linear crystalline homopolymer formed by  $\beta$ -D-glucose units joined by glycosidic bonds (Albinante et al., 2012).

Hemicellulose is a complex branched heteropolysaccharide composed of D-glucose, D-galactose, D-mannose, D-xylose, L-arabinose, D-glucuronic acid, and 4-O-methyl-glucuronic acid (Figure 3). Its branched structure allows the interaction with cellulose, thus providing stability and flexibility to the aggregate. Compared with cellulose, hemicellulose is more susceptible to acid hydrolysis. This reactivity is attributed to the amorphous character of these polysaccharides (Santos et al., 2012). Hemicellulose is a hydrophilic, amorphous molecule that represents approximately 30% of the fiber's weight (Albinante et al., 2012).

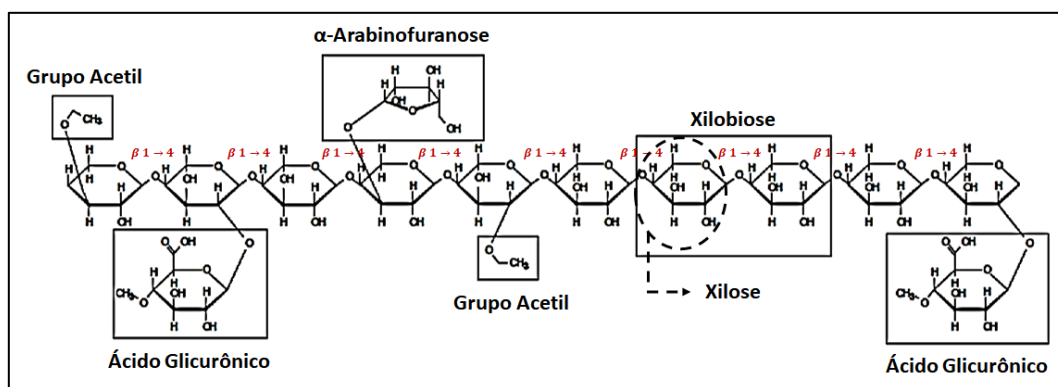


**Figure 3.** Schematic representation of hemicellulose structure (Adapted from Mussato et al., 2012).

The second largest bulk component of vegetable fiber is lignin. It accounts for about 35% of the fiber's weight and is associated with cellulose and hemicellulose

in the composition of lignocellulosic materials. It is an amorphous, hydrophobic macromolecule with high molar mass (Albinante et al., 2012).

Lignin is a natural aromatic polymer, formed mainly by three types of phenylpropane units: guaiacyl (G), syringe (S) and p-hydroxyphenyl (H), linked by aryl ether and carbon-carbon (CC) bonds (Figure 4) (Soares et al., 2017). This amorphous resin acts as a permanent bonding agent between cellulose fibers to provide physical (impact, compression, and flexion) and chemical (biological or aging reactions) strength to the structure (Zhang et al., 2017). The strength of the bond between cellulose fibers and lignin is amplified by the existence of covalent bonds between the lignin chains and the constituents of cellulose and hemicellulose (Silva et al., 2009). Although the main structural characteristics of lignin have already been studied in various aspects, it is not possible to accurately determine its structure, since it has a complex and heterogeneous composition (Chen et al., 2019).

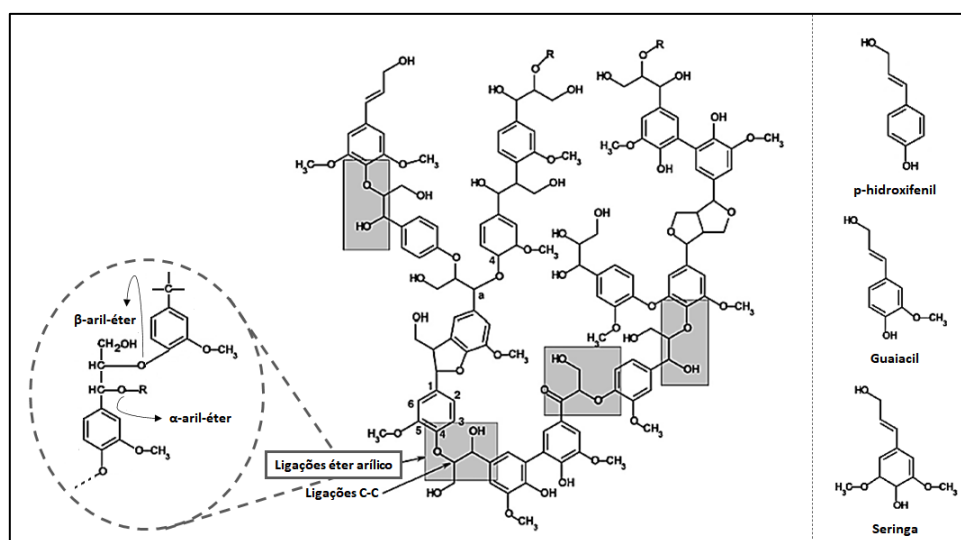


**Figure 4.** Schematic representation of a generic structure of lignin and its guaiacyl (G), syringe (S), and p-hydroxyphenyl (H) monomers (Adapted from Power et al., 2011).

Therefore, to obtain cellulose, it is necessary to isolate cellulose fibers, that is, to carry out the dismemberment of the lignin-cellulose-polyose complex. This process of removing lignin and hemicellulose without disintegrating cellulose is known as pulping. Pulping can be carried out using physical (by crushing and grinding), chemical (using alkaline chemical agents, diluted acids, oxidizing



agents, and organic solvents), biological (using enzyme) or a combination of these methods (Maldonado-Bustamante et al., 2017; Lee et al., 2014).

Among the possible types of cellulosic fiber treatments, chemical treatment is the most efficient and economical method for biomass deconstruction. While physical treatment and thermal methods are less efficient and consume more energy than chemical methods, the use of enzymes for biological treatment is expensive and takes longer (Lee et al., 2014).

Currently, the most used chemical pulping method is the Kraft process, which uses active chemical agents such as sodium hydroxide (NaOH) and sodium sulfide (Na<sub>2</sub>S) and heating around 160 °C. This chemical process allows the removal of a large part of the lignin, as cleavage reactions occur in the α-aryl ether and β-aryl ether bonds through hydroxide and hydroxysulfide anions that cleave the lignin macromolecule into smaller fragments soluble in aqueous and alkaline media (Silva et al., 2009).

After the pulping process, the cellulose pulp shows a dark color; thus, despite its efficiency, the pulping cannot totally eliminate lignin (Baptista et al. 2008). The bleaching method clears the pulp from the previous step, in addition to helping the delignification (Simão et al., 2018).

Conventional bleaching processes involve the use of chlorine-based chemicals (chlorine, chlorine dioxide, sodium hypochlorite), as these chlorinated organic solvents are capable of solubilizing residual lignin fragments. The main disadvantage of these processes is the formation of toxic organic compounds, mainly dioxins and furans. For this reason, new Totally Chlorine-Free (TCF) bleaching processes have been developed, based mainly on peracids (Taflick et al., 2017).

As highly oxidizing species, peracids – especially peracetic acid and permonosulphuric acid – are currently considered excellent substitutes for chlorinated reagents. These reagents allow the production of cellulose pulps with greater strength and higher delignification rates, thus promoting lesser whiteness reversals after bleaching and decreasing cellulose degradation (Silva et al., 2009).

## 2.3 NANOCELLULOSE

Cellulose nanoparticles or nanocelluloses are cellulose elements with at least one dimension smaller than 100 nm (Benini et al., 2018). These compounds can be obtained through three distinct methods: mechanical (Thakur et al., 2021; Phanthong et al., 2018), chemical (Verma et al., 2021; Rasheed et al., 2020), and enzymatic (Alonso-Lerma et al., 2020; Pere et al., 2020). In all three, the goal is to eliminate the amorphous domains of cellulose.

Nanocelluloses are divided into three categories: nanocrystalline cellulose (NC), nanofibrillated cellulose (NF) and bacterial nanocellulose (BC). These three types of nanocellulose have the same chemical composition, differing in terms of morphology, size, crystallinity, origin, and extraction method (Salimi et al., 2019).

Nanocrystalline cellulose (NC), also known as nanocrystal, cellulose nanocrystal or cellulose nanowhiskers, is a nanomaterial with high strength usually extracted from cellulose fibrils by acid hydrolysis. It has a shape similar to fragmented rods, with 2-20 nm in diameter, 100-500 nm in length, and crystallinity around 54-88%. The high crystallinity of this material is due to its being composed mainly of crystalline regions of cellulose, since the amorphous parts are hydrolyzed and removed by acid while the crystalline parts are maintained (Figure 6) (Phanthong et al., 2018; Mishra; et al., 2019).

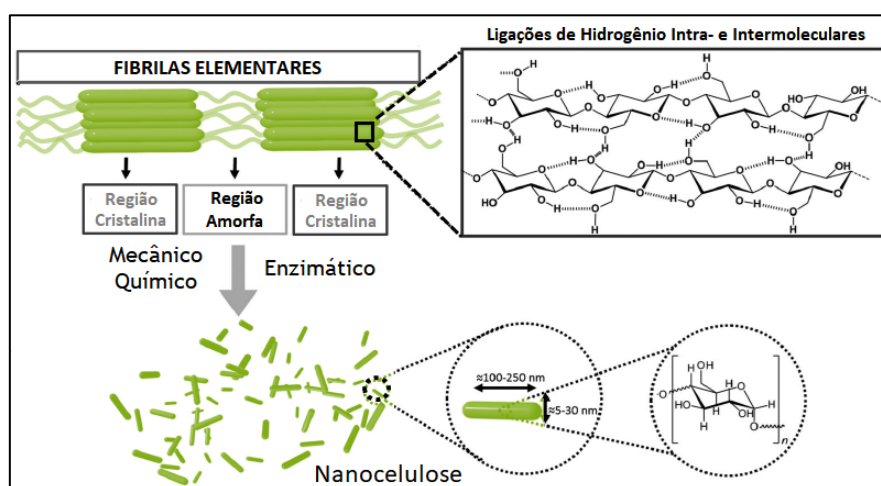


**Figure 6.** Nanocellulose production through the three main techniques: physical, chemical, and biological (Adapted from Giese et al., 2014).

Nanofibrillated cellulose (NF), also known as: microfibril, microfibrillated cellulose, cellulose nanofiber, and cellulose nanofibril, is a long and flexible nanomaterial, extracted from cellulose fibrils by mechanical methods. It has the form of long fibers with 1-100 nm in diameter and 500-2.000 nm in length. NF can be extracted from the cellulose chains by random cleavage of the fibrils, through the force applied by a mechanical process (Figure 6). Therefore, it is composed of crystalline and amorphous regions of cellulose. Compared with nanocrystalline cellulose, nanofibrillated cellulose has a longer length and higher aspect ratio (length/diameter), higher surface area, and larger extension of hydroxyl groups, which are easily accessible for surface modification (Phanthong et al., 2018; Rajinipriya et al., 2018).

Unlike NC and NF, which can be produced from lignocellulosic biomass, bacterial nanocellulose (BC) is formed by the accumulation of low molecular weight sugars synthesized by bacteria (e.g., *Gluconacetobacter xylinus*) in a few days. Thus, bacterial nanocellulose is always pure, without other components of lignocellulosic biomass, such as lignin, hemicellulose, and pectin. Bacterial nanocellulose has the same chemical composition as the two other types of nanocellulose. It comes in the form of twisted ribbons with average diameters of 20-100 nm and micrometric lengths (Phanthong et al., 2018).

Nanocellulose has attracted great interest in many scientific and technical areas as a potential sustainable natural material, with hundreds of possibilities in various industrial sectors. This is because it has several advantages related to its nanometric size (high surface area, excellent rigidity, unique optical properties, light weight, high strength, and the expressive interaction of these products with neighboring species, such as water, inorganic, and polymeric compounds); and properties inherent to cellulose, such as biodegradability, renewability and sustainability (Balea et al., 2019; Benini et al., 2018).

The characterization of nanocellulose is a very important stage of production, because from the data collected, such as physical-chemical, thermal, and morphological properties, one can foresee its possible applications, in addition to guaranteeing the quality of the product developed.

In the characterization of nanocelluloses, techniques such as TEM (Transmission Electron Microscopy) and AFM (Atomic Force Microscope) are used to assess morphology and size; zeta potential and DLS (Dynamic light scattering) to analyze surface charge, stability, and size; XRD (X-Ray Diffraction) and NMR (Nuclear Magnetic Resonance) to assess crystallinity; Thermo-gravimetry and DSC (Differential scanning calorimetry) to assess thermal properties; and FTIR (Fourier Transform Infrared Spectroscopy) to analyze the presence of hydroxyls on the nanomaterial's surface (Kleem et al., 2018).

Nanocellulose has already been produced from cellulose obtained from eucalyptus wood (Wang et al., 2012), sugarcane bagasse (Li et al., 2012), cotton (Morais et al., 2013), rice husk (Johar et al., 2012), and coconut shell (Rosa et al., 2010; Machado et al., 2014). It is important to highlight that the properties of nanocellulose (morphology, size, and degree of polymerization) depend not only on the isolation method applied, but also on the source from which it was isolated (Rajinipriya et al., 2018).

### **2.3.1. Nanocellulose applications**

Due to its excellent physical, chemical, and biological properties, such as: high surface area, low density, good mechanical and thermal properties, conductivity, scalability, low cost, biocompatibility, biodegradability, and low cytotoxicity, nanocellulose is considered a promising biopolymer for a wide range of applications.

This nanomaterial can be used in the food packaging (Abral et al., 2020), drug-delivery (Raghav et al., 2021), cosmetic additives (Chantereau et al., 2020), medical implants (Halib et al., 2018), paper (Xu et al., 2017), 3D printing (Badhe et al., 2020), wastewater treatment (Derami et al., 2019), biocatalysts (Bilal et al., 2019), bioenergy (Zhu et al., 2016), biosensor (Subhedar et al., 2021), and textile industries (Forsman et al., 2017; Eslahi et al., 2020).

The textile industry seeks technology to create more functional clothing, such as fire retardant, self-cleaning, and antimicrobial clothing (Norrurahim et al., 2021a). Nanotechnology has been an excellent tool to achieve these goals (Chauve et al., 2014).

In their book, Ngo et al. (2014) presented some possibilities for the application of nanotechnology in the textile industry: (1) self-cleaning and dirt-free textiles; (2) medical textiles with antimicrobial function; (3) military textiles that are capable of minimizing accidents, injuries, and infections; (4) automotive textiles that have anti-allergy, anti-static, better wear and tear resistance, and are self-cleaning; and (5) smart textiles that, when paired with an electronic device, allow the body's vital signs to be monitored.

Nanocellulose, in addition to presenting characteristics such as biocompatibility, high surface area, strength and flexibility, has been shown to be one of the most effective materials for filtering different microorganisms (Norrahim et al., 2021a; Elshafei et al., 2011). Thus, it can be employed to obtain fabrics with an antimicrobial function.

In recent years, nanocellulose-based antimicrobial materials have attracted a large number of applications in various areas of industry. In their review, Norrahim et al. (2021b) noted that research related to the term 'nanocellulose as antimicrobial material' over the past ten years has been increasing (Figure 7).

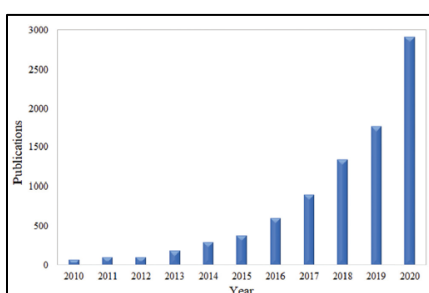


**Figure 7.** Total number of publications related to the term 'nanocellulose as antimicrobial material' (Source: Norrahim et al., 2021b).

In 2013, Jebali et al. demonstrated that nanocellulose fabrics conjugated with allicin and lysozymes have significant antibacterial activity against *Candida albicans*, *Aspergillus niger*, *Staphylococcus aureus*, and *Escherichia coli*. Sharma et al. (2020) highlighted the porosity of bacterial nanocellulose (BC) as a property to be explored in the antibacterial action of this nanomaterial.

Recently, Kokol et al. (2021) showed that cellulose nanofibers (CNFs) functionalized with hexamethylenediamine (HMDA) are not irritating to the skin and have an excellent antimicrobial property when adsorbed on viscose yarn.

Despite the versatility of nanocellulose functionalization and the consequent variety of applications in textiles, it is important to highlight that some challenges must be overcome for the application of this nanomaterial in textiles (Hassan et al., 2019). That is because most modifications to nanocellulose involve aggressive pretreatments. This usually affects its structural integrity and crystallinity, which can later change its mechanical properties on the textile surface (Chattopadhyay et al., 2016). Therefore, new modification processes and less aggressive chemicals need to be developed. Furthermore, some of the toxic chemical compounds are easily adsorbed by humans (Norrrahim et al., 2021a).

In this context, the functionalization of nanocellulose with metallic nanoparticles obtained by green synthesis can be a solution to the toxicity problem.

Nanoparticles (NP) have several unique properties due to their specific size, shape, composition, and higher surface area to volume ratio. These properties make them suitable to be used as nanomagnets, drug delivery systems, water disinfectants, catalysts, quantum dots for electronic devices, and pollutant remediation agents (Rana et al., 2020).

Biotech applications of NPs have expanded in the last decade due to their biocompatibility, anti-inflammatory and antimicrobial activity, effective drug delivery, bioactivity, bioavailability, tumor targeting, and bioabsorption (Salem et al., 2020).

Metallic nanoparticle is a term that refers to noble metals such as gold, silver, and platinum reduced to the nanoscale by the synthesis of nanoparticles (Jamkhane et al., 2019). Currently, researchers are focusing on metallic nanoparticles, nanostructures, and synthesis of nanomaterials because of their useful properties for catalysis (Gawande et al., 2015), polymer preparation (Moura et al., 2017), diagnosis and treatment of diseases (Le et al., 2017), and as biosensors (Hamdy et al., 2018; Barghouti et al., 2020).

NPs can be synthesized by various physical and chemical methods. The physical approach uses ultrasonication techniques, microwave irradiation (MW), and electrochemical methods. In the chemical approach, the main components are metallic precursors, stabilizing agents, and reducing agents (inorganic and organic). Reducing agents such as sodium citrate, ascorbate, sodium

borohydride ( $\text{NaBH}_4$ ), elemental hydrogen, Tollens reagent, N,N-dimethylformamide (DMF), and polyethylene glycol block copolymers can be used (Gour et al., 2019) .

Physical and chemical approaches to synthesize NP cause negative impacts on the environment and human health, because of their toxic metabolites and increased reactivity and toxicity of the particles. Thus, the green synthesis of NPs emerged as a solution to the problematic scenario of nanoparticle synthesis. This is because plant extracts (Keijok et al., 2019), fungi (Silva et al., 2017) and bacteria (Rajabairavi et al., 2017) can be used to reduce and stabilize nanoparticles (Gour et al., 2019).

Nowadays, green syntheses are preferred because they are safe, clean, inexpensive, and easily scalable for the well-constructed scale synthesis of NPs (Salem et al., 2020).

#### **2.4 GOLD NANOPARTICLES SYNTHESIZED WITH POMEGRANATE EXTRACT (AUNP-POMEGRANATE)**

Pomegranate (*Punica granatum L.*) is a fruit widely cultivated in all Mediterranean regions. It has been widely used in traditional medicine in America, Asia, Africa, and Europe for the treatment of different types of diseases (Basavegowda et al., 2013). Pomegranate fruit and rind are used against intestinal parasites, dysentery, and diarrhea. The juice and seeds are considered a tonic for the throat and heart. It can also be used to stop nose and gum bleeds and treat hemorrhoids (Shaygannia et al., 2015). Several studies report antioxidant (Ricci et al., 2006; Murthy et al., 2002), antibacterial (Prashanth et al. 2001; Alexandre et al., 2019), antifungal (Dahham et al., 2010), and antiviral (Salles et al., 2021; Angamuthu et al., 2019) properties for the constituents of this fruit. These include several fatty acids, sterols, triterpenes, anthocyanins, flavonoids, and tannins, which were identified and isolated from the juice of pericarps, leaves, and seeds (Abdelmonem et al., 2014).

Several studies have already reported the use of pomegranate extract for the synthesis of metallic NPs due to its high reducing properties (Patel et al., 2019; Yusefi et al., 2020; Hussein et al., 2021). Nadagouda et al. (2014) observed that pomegranate extract produced more uniform shapes and sizes of silver and gold

nanoparticles compared to turmeric, blueberry, blackberry, and tea/coffee extracts.

Lokina et al. (2014) reported that gold nanoparticles (AuNPs) synthesized from pomegranate extract show an excellent cytotoxic result against HeLa cancer cell lines at different concentrations and antibacterial activity against *Candida albicans* (ATCC 90028), *Aspergillus flavus* (ATCC 10124), *Staphylococcus aureus* (ATCC 25175), *Salmonella typhi* (ATCC 14028), and *Vibrio cholerae* (ATCC 14033).

Shahbazi and Shavisi (2018) demonstrated the ability of pomegranate essential oil to adhere to nano-chitosan films, conferring antibacterial/antioxidant characteristics to these materials.

## **2.5 SMART TEXTILES**

Textiles are everywhere and play an essential role in human society. In terms of function and application, the fabric of clothing can be considered the second skin of the human being.

With the development of flexible electronic technology and the closer interaction between people and the surrounding environment in the information age, smart fabrics have gradually become a people's desire (Honarvar et al., 2017).

Fiber is the most basic unit of fabric, used to obtain different patterns and styles of clothing by weaving technology. There are different types of chemical fiber, including polyester fiber, viscose fiber, cellulose nitrate fiber and polyamide fiber; with the intrinsic advantages of mildew, wear, light and easy drying resistance, respectively (Hindeleh et al., 1978; Wang et al., 1998; Colom et al., 2002; Huang et al., 2002).

To make fabrics more functional and intelligent, functional fibers have been widely studied and applied. Textile surface modification, including electrospinning, nanotechnologies, plasma treatment, polymerization, microencapsulation and sol-gel techniques, have been applied to impart some new functional properties to the textile, e.g. water repellent, thermal insulating, protection against radiation, flame retardant and antibacterial activity (Nadi et al., 2018; Emam et al. 2019; Li et al., 2021; Rivero et al., 2015).



Currently, antimicrobial textiles are very useful in environments and places prone to pathogenic microorganisms such as hospitals. Within the common public area, there are hotels, restaurants, or trains, where this type of fabric is highly demanded in towels, curtains and rugs. There is also a desire to apply this type of fabric in odor control (Gulati et al., 2022).

However, according to Shi et al. 2019, large-scale manufacturing can be regarded as one of the most critical issues for smart fabrics. In a long-term view, the materials used in these fabrics must be environmentally friendly and recyclable.

### 3. CHAPTER 1 – CELLULOSE EXTRACTION

#### Paper 1: DOE Optimization of cellulose extraction: transforming food waste in cellulose

Laryssa Pinheiro Costa Silva<sup>1</sup>, Pedro Henrique Cassaro Lirio<sup>1</sup>, Wanderson Juvencio Keijok<sup>1</sup>, Jairo Pinto de Oliveira<sup>1</sup> and Marco Cesar Cunegundes Guimarães<sup>1\*</sup>

<sup>1</sup> Federal University of Espirito Santo, Av Marechal Campos1468, Vitória, ES 29.040-090, Brazil.

\* Corresponding author: marco.guimaraes@ufes.br

#### Abstract

*Cocos nucifera* produces fruits with different food applications, from coconut water production to the production of grated coconut, coconut milk, and coconut oil. However, coconut fiber is not used much and ends up being discarded, accumulating in landfills. Here, we propose the extraction of cellulose from coconut fibers, seeking to put this agribusiness residue to good use. To arrive at a suitable production flow, we used DOE experimental planning. Cellulose fibers extracted from coconut were analyzed by quantitative cellulose analysis, Fourier transform infrared spectroscopy (FTIR), and scanning electron microscopy (SEM). Statistically, in the extraction process used, the variables concentration of hypochlorite and bleaching time were the most expressive. The best condition of cellulose extraction from coconut fibers observed was the lowest energy consumption, 1% NaOH, 20 minutes of autoclaving, 0.60% hypochlorite, and bleaching time of 8h 42min.

**Keywords:** Cellulose, coconut fibers, *Cocos nucifera*, DOE, factorial planning.

#### 1. Introduction

Approximately 40% of all food produced is wasted, from its cultivation to its final consumption. Although edible food waste volumes vary geographically, the proportion of food and agricultural waste generated at the pre-consumer level

represents a significant burden on the environment and remains a global challenge (Andler et al., 2018).

*Cocos nucifera* produces fruits with different food applications, from coconut water production to the production of grated coconut, coconut milk, and coconut oil. This palm is grown in about 90 countries, with Indonesia, the Philippines and India being the world's largest coconut producers. Together, they account for 72.8% of all world production (Brainer et al., 2018).

The "shell" of the green coconut, before complete maturation, corresponds to 85% of the gross weight of the fruit and has high humidity, which does not favor the application of coconut fibers in the processes of making bags, brushes, mats, rugs, ropes, mattresses, insulation panels, packaging, and automotive seats (Mondal et al., 2014; Rencoret et al., 2013), which usually employ the ripe fruit peel (Rosa et al., 2001). Therefore, this residue is discarded. Around 5 to 6 million tons of coconut fibers are produced annually around the world, but only 10% of this material is commercially reused (Tripathi et al., 2017).

The amount of coconut "husk" generated by the agroindustry is greater than the natural capacity of biomass degradation, resulting in a big problem of environmental pollution, since, normally, these residues are deposited in inappropriate places (Huamán-Pino, 2005). This stresses the need for initiatives that take its use into account. These fibers can be used in the production of low-cost materials, in addition to contributing to the reduction of solid waste (Ishizaki et al., 2006).

Chemically, coconut fiber is constituted by 3.1% of extractive materials, 37.3% of cellulose, 20.3% of hemicellulose, 32.2% of lignin, and 6.8% of mineral material (ash) (Almeida et al. 2013).

To improve the extraction of cellulose from coconut fibers is of great importance, as the forms of extraction reported so far are lacking where the control of the amount of cellulose extracted and yields are concerned.

Thus, the main objective of the present work was to achieve the ideal design for extracting cellulose from coconut solid waste. To do so, the concentration of sodium hydroxide and sodium hypochlorite used was analyzed, in addition to

autoclaving time, agitation, temperature, and washing of the fibers. The Design of Experiments (DOE) was used to treat all factors simultaneously to optimize cellulose extraction, in order to improve the understanding of significant variables and extract the most useful information. The evaluation of the cellulose extraction method developed was used as a way to overcome the energy difficulties that the traditional reuse of these residues presents.

## 2. Materials and Methods

**Materials.** Sodium hydroxide (NaOH), sodium hypochlorite (NaOCl), glacial acetic acid (CH<sub>3</sub>CO<sub>2</sub>H), nitric acid (HNO<sub>3</sub>), and absolute ethanol (Et-OH) were purchased from Sigma Aldrich Ltd and used as received without any further purifications. Deionized water from the Millipore Direct-Q® 3 water purification system was used in all experiments. The coconut fibers analyzed were donated by the company Marquinhos Água de Coco ®.

**Fiber preparation.** The fibers were abundantly washed in running water, left to dry in an oven at 60°C for 48 hours, ground in a mill with stainless steel blades, and sieved in 40-mesh sieves (Figure 1).

**Obtaining cellulose from coconut fibers.** In the pulping step, 10-g fiber samples were added to 400 mL of sodium hydroxide (NaOH) solution. The resulting solution was autoclaved. The fibers were then washed with distilled water until the complete removal of water-soluble agents. The bleaching step took place next, by adding the pulp formed, 100 mL of sodium hypochlorite, and 10 drops of glacial acetic acid. The resulting solution was placed under stirring at 250 rpm. The cellulose pulp was then filtered and oven-dried (40 °C) for 24 hours.

**Experimental conditions.** NaOH concentration, fiber soaking time (time in which coconut fibers will remain in contact with the NaOH solution), soaking temperature, autoclave time, sodium hypochlorite concentration, temperature, and reaction time, were determined by experimental design (DOE).

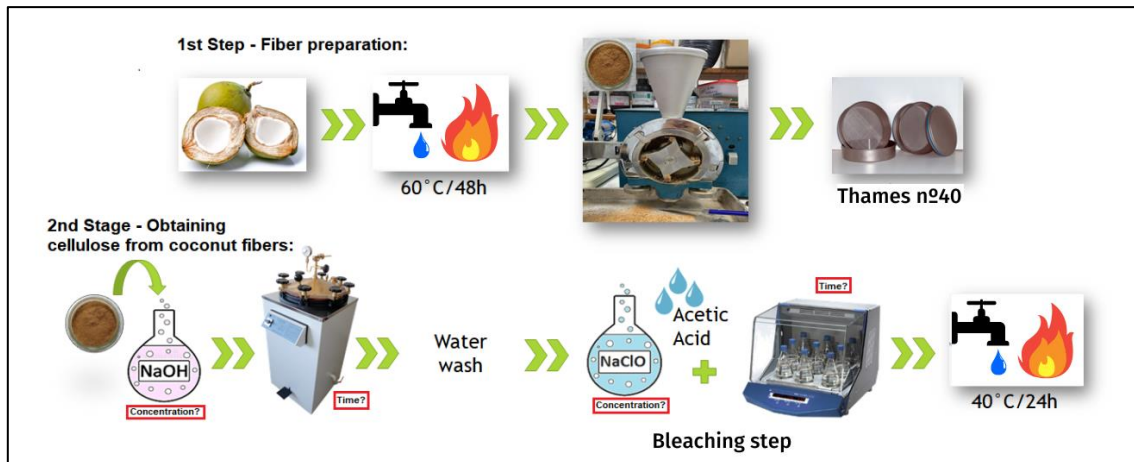


**Figure 1.** Extraction of cellulose from coconut fibers.

**Experimental design (DOE) and statistical modeling.** Initially, a literature search was carried out to decide the values of the parameters to be analyzed (Table 1). Then, a fractional factorial with 8 factors and 2 levels was performed (Table 2), followed by a full factorial combining 2 factors and 3 levels, with repetition of the central point (Table 3). The response variables used in both factorial designs were cellulose concentration ( $\text{mg cellulose g}^{-1}$  Dry Mass) and final weight (g). The results of each test run were evaluated in the “Statistica® 10 Graphical and Statistical Analysis Tool” based on main effects, interaction, ANOVA and a response table.

	<b>Plant material</b>	<b>NaOH conc. (%w/w)</b>	<b>Autoclave Time (min.)</b>	<b>NaOCl conc. (%v/v)</b>	<b>Bleaching Time and Temperature (h/°C)</b>
<b>Deepa et al., 2015</b>	Sisal, kapok, banana chips, pineapple and coconut leaf	2%	60 min.	Not applicable. Used NaClO <sub>2</sub> .	1h (70°C)
<b>Deepa et al., 2020</b>	Kapok	2%	Uninformed	Not applicable. Used NaClO <sub>2</sub> .	1h (70°C)
<b>Gouveia et al., 2009</b>	Sugar cane bagasse	Not applicable	30 min.	Not applicable	Not applicable
<b>Machado et al., 2017</b>	Coconut shell	2%	Unrealized	1,7%	6h (80°C)
<b>Machado et al., 2014</b>	Coconut shell	2%	Unrealized	1,7%	6h (80°C)
<b>Rosa et al., 2009</b>	Coconut shell	2%	Unrealized	Not applicable. Used NaClO <sub>2</sub> .	4h (25°C)
<b>Rosa et al., 2010</b>	Coconut shell	2%	Unrealized	Not applicable. Used NaClO <sub>2</sub>	4h (25°C)
<b>Benini et al., 2018</b>	<i>Imperata brasiliensis</i>	5%	Unrealized	Not applicable. Used NaClO <sub>2</sub>	2h (25°C)
<b>Mulinari et al., 2011</b>	Coconut shell	1%	Unrealized	Unrealized	Unrealized

**Table 1.** Bibliographic analysis of cellulose extraction parameters.

Factors	Levels		Answer Variables	
	A	B		
NaOH concentration (%w/v)	2	1	Cellulose concentration (mg cellulose g <sup>-1</sup> DM*)	Final weight (g)
Soaking Time (min.)	40	20		
Soaking Temperature (°C)	60	25		
Autoclave Time (h)	60	20		
NaOCl Concentration (%v/v)	1,70	0,85		
Bleaching Time (h)	6	1		
Bleaching Temperature (°C)	60	25		
Changing the NaOCl solution	4	1		

**Table 2.** Factor matrix of the fractional factorial experiment  $2^{8-2}$  (factor V) of cellulose extraction. \*DM, dry mass.

Factors	Levels			Answer Variables	
	A	B	C		
NaOCl Concentration (%v/v)	0.21	0.42	0.85	Cellulose concentration (mg cellulose g <sup>-1</sup> DM*)	Final weight (g)
Bleaching Time (h)	6	8	10		

**Table 3.** Factor matrix of the complete factorial experiment to obtain cellulose, its levels, and response. \*DM, dry mass.

**Determination of cellulose concentration.** Cellulose concentration was determined adapted to Brendel et al. (2000). Initially, 100 mg of ground samples were weighed into screw-capped glass tubes. Next, 2 mL of 80% acetic acid and 200  $\mu$ L of 69% nitric acid were added. The samples were carefully homogenized and placed in a water bath at 100 °C for 1 hour. After cooling, the samples were transferred to 15 mL Falcon tubes, to which 2.5 mL of 99% ethanol was added. The samples were then homogenized on a vortex shaker and centrifuged at 2,500 x g for 10 minutes at  $25 \pm 2$  °C and the supernatant carefully discarded. Then, the samples were washed following the sequence: (1st) 5 mL of 99% ethanol, to remove products degraded during the extraction; (2nd) 5 mL of deionized water, to remove traces of nitric acid; (3rd) 5 mL of 17% NaOH, remaining at rest at  $25 \pm 2$  °C for 10 minutes; (4th) 5 mL of deionized water; (5th) 2.2 mL of deionized water and 600  $\mu$ L of acetic acid, to eliminate persistent non-cellulosic materials; and (6<sup>th</sup>) 5 mL of deionized water. Between each washing step, the samples were

centrifuged at 2,500 x g for 10 minutes at  $25 \pm 2$  °C and the supernatants discarded. The samples were dried in an oven at 50 °C for 48 hours and weighed. Cellulose concentration was expressed in milligram of cellulose per gram of dry mass (mg cellulose g<sup>-1</sup> DM).

**Scanning Electron Microscopy (SEM).** Morphological and structural analysis of the fibers was performed by scanning electron microscopy (SEM). The fibers were metallized with gold for 2 minutes using argon as a carrier gas, dried, and analyzed in a ZEISS microscope, EVO MA10, with an electron acceleration voltage of 15 keV.

**Fourier transform infrared spectroscopy (FTIR).** The FTIR experiments were performed with attenuated total reflection (ATR), using a Cary 630 spectrometer (Agilent technology) equipped with a zinc selenide (ZnSe) crystal. The samples were dried and ground and their spectra recorded in the range from 4000 to 650 cm<sup>-1</sup> with a resolution of 4 cm<sup>-1</sup>. Absorption ratios were obtained by measuring the peak heights and normalizing them to the cellulose absorbance peak at 897 cm<sup>-1</sup>, which is due to the C<sub>1</sub>–H deformation of the glucose rings.

### 3. Result and Discussion

To establish the best condition for extracting cellulose from coconut fibers, a fractional factorial experiment, with 2 levels and 8 variables, and a complete factorial experiment, with 3 levels and 2 variables, were carried out.

The factors studied in the 2<sup>8-2</sup> fractional factorial included: 1- NaOH concentration (% w/v), 2- Fiber soaking time in NaOH (min), 3- Fiber soaking temperature in NaOH (°C), 4- Autoclaving time (min.), 5- NaOCl concentration (% v/v), 6- Bleaching time, 7- Bleaching temperature (°C), and 8- NaOCl solution change.

The authors Arsyad et al. (2015) Karthikeyan & Balamurugan (2012), Rosa et al. (2010), and Silva et al. (2015) discussed and highlighted the importance of the NaOH Concentration and NaOCl Solution Exchange factors in the extraction of cellulose in natural fibers. However, the Pareto charts (Figure 2) revealed that these parameters and parameters 2, 3, 7, and 8 were not statistically significant



for the response variables analyzed. Only factors whose p values fell under 0.05 were considered statistically significant.

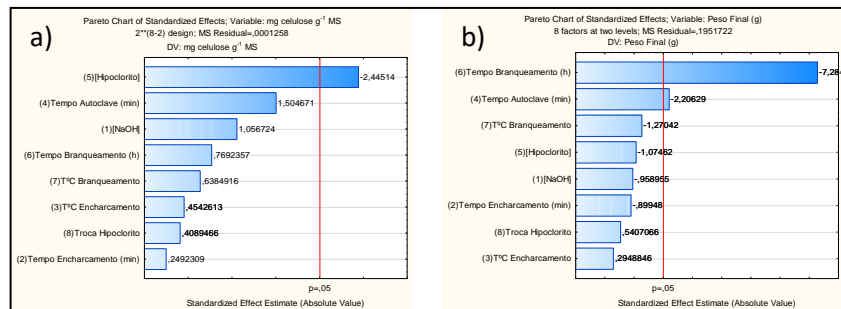


**Figure 2.** Pareto plots showing the significant variables affecting cellulose concentration (a) and final weight (b).

The Normal Effects Plot (Figure 3.A) indicates the magnitude, direction, and importance of the effects. Thus, among all the parameters analyzed as a function of Final Weight (g), Bleaching Time (h) was the most significant.

When analyzing the Marginal Means Graph (Figure 3.B) of the parameters autoclave time and bleaching time, which are significant factors in the Pareto graph (Figure 2.B), one can observe perfectly parallel lines, which indicate that the effect of interaction is not important between these two factors. Calado & Montgomery (2003)

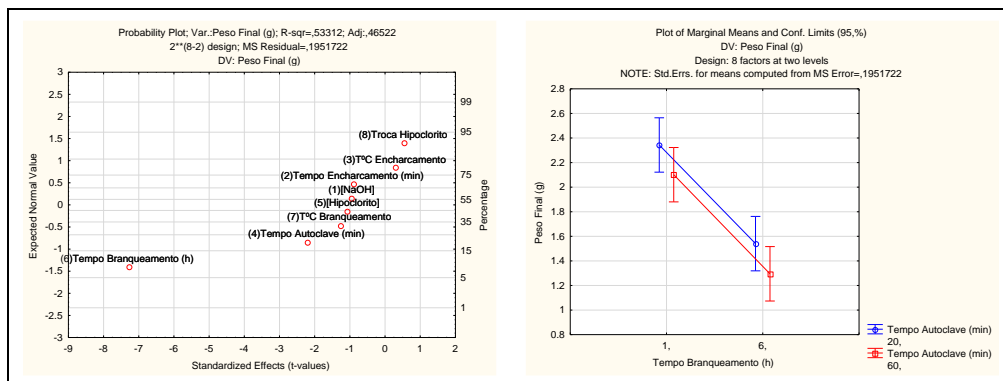


**Figure 3.** Normal Graph of Effects (a) and Graph of Marginal Means of the factors Hypochlorite Concentration (v/v%) and Bleaching Time (h) (b), in relation to final weight (g).

However, in the Marginal Means Graph of the factors Hypochlorite Concentration (v/v %) and Bleaching Time (h), in relation to the cellulose concentration (Figure 4), the lines in the different levels of Hypochlorite Concentration (v/v %) intersect. Therefore, the interaction effect between Hypochlorite Concentration (v/v%) and Bleaching Time (h) is important. Analyzing the direction of the lines in the graph,

one observes that the amount of cellulose is higher at the lower level of Hypochlorite Concentration (v/v%) and higher at the Bleaching Time (h).

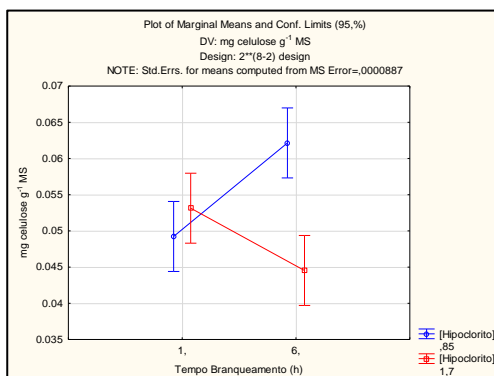


**Figure 4.** Graph of Marginal Means of the factors Hypochlorite Concentration (v/v%) and Bleaching Time (h) (b), in relation to cellulose concentration.

Thus, the factors studied in the full  $3^2$  factorial included: A – NaOCl concentration (% v/v) and B – Bleaching time (Table 4).

Execution Order	Blocks	Factors		Cellulose concentration (mg cellulose g <sup>-1</sup> DM*)	Final weight (g)
		NaOCl concentration (%v/v)	Bleaching Time (h)		
1	1	0.21	6	0.063	1.406
2	1	0.21	10	0.051	1.139
3	1	0.21	12	0.060	1.196
4	1	0.42	6	0.052	1.024
5	1	0.42	10	0.054	1.357
6	1	0.42	12	0.049	1.210
7	1	0.85	6	0.049	1.202
8	1	0.85	10	0.082	1.106
9	1	0.85	12	0.050	1.079
10	1	0.42	10	0.080	0.972
11	1	0.42	10	0.048	0.821
12	1	0.42	10	0.076	0.670

**Table 4.** Complete factorial design  $3^2$  of the experiment based on factors, levels, and response data (Slurry Concentration and Yield) to obtain the pulp. \*Dry Mass.

To obtain the optimal values for the two factors analyzed, the graph of the composite desirability function was built (Figure 5). Figure 5 shows the optimal point values of the 2 response variables – Cellulose concentration (0.06498 mg cellulose g<sup>-1</sup> DM) and Final weight (0.3811g) – and the operating conditions that

made that possible – Hypochlorite Concentration (0.60%) and Bleaching Time (8.0667h).

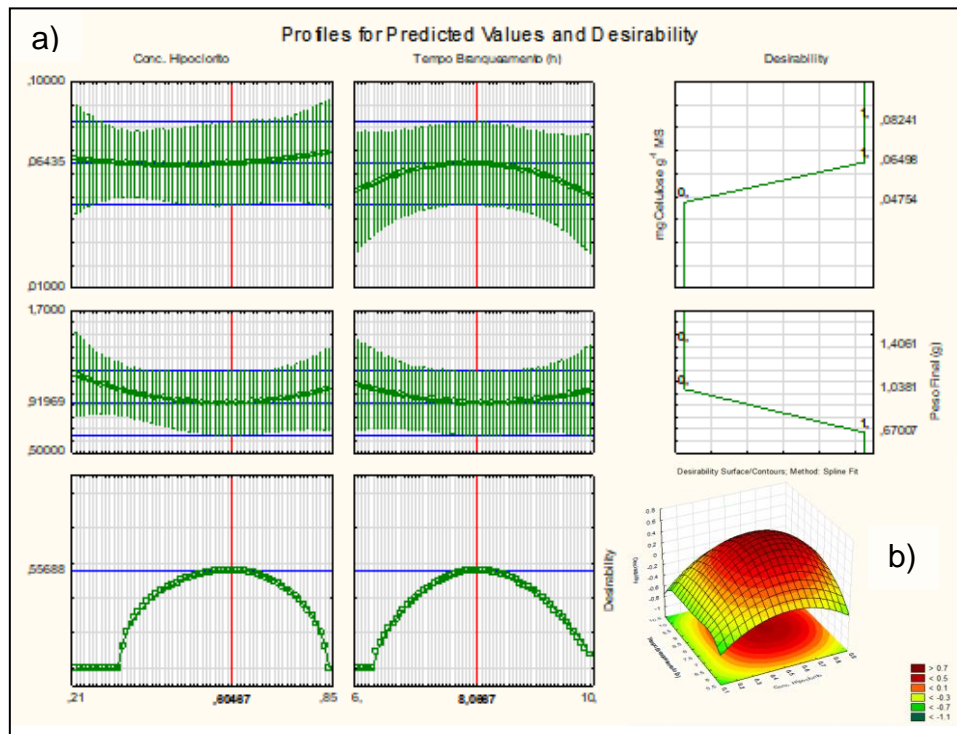


**Figure 5.** (a) Desirability function plot. Maximum response: cellulose concentration and intermediate response: final weight; (b) Response surface plot of the desirability function.

After statistical analysis, we identified that the best condition for extracting cellulose from coconut fibers was: 1% NaOH, 20 minutes of autoclaving, 0.60% hypochlorite, and bleaching time of 8.0667h. The final yield obtained was 1% (g cellulose/g dry fiber).

Figure 6 shows the difference in cellulose concentration between untreated coconut fiber (0.008 g cellulose/g DM) and coconut fiber after treatment with the optimal conditions (0.08 g cellulose/g DM).

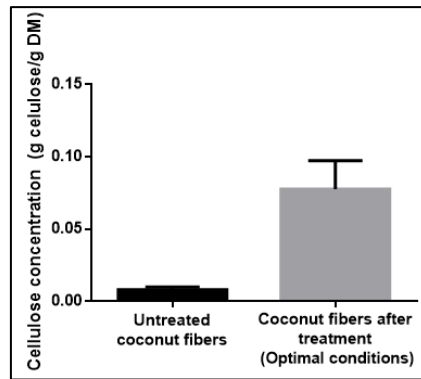


**Figure 6.** Bar graph comparing the difference in cellulose concentration between untreated coconut fibers and coconut fibers after treatment with optimal conditions.

FTIR spectroscopy revealed that lignin and hemicellulose were removed during the cellulose isolation process by analyzing their functional groups. The FTIR spectra of coconut fibers before and after treatment for cellulose extraction are shown in Figure 7.

In the FTIR spectrum, it was possible to verify the presence of an absorption band at  $897\text{ cm}^{-1}$ , characteristic of the  $\beta$ -glycosidic bond between glucose units; an elongation band at  $1030\text{ cm}^{-1}$ , attributed to the  $\text{-C-O-}$  group of secondary alcohols and ether functions present in the cellulose chain structure; an asymmetrical elongation signal  $\text{C-O-C}$  at  $1159\text{ cm}^{-1}$  characteristic of cellulose; elongation bands  $\text{O-H}$  at  $3330\text{ cm}^{-1}$  and  $\text{C-H}$  at  $2900\text{ cm}^{-1}$  referring to cellulose in the coconut fibers after treatment. Furthermore, signals related to lignin and hemicellulose, such as  $\text{CH}$  deformation outside the plane of lignin at  $771\text{ cm}^{-1}$ ,  $\text{CO}$  elongation of hemicellulose and lignin at  $1724\text{ cm}^{-1}$ , and  $\text{C=C}$  aromatic skeletal vibration of lignin at  $1609$  and  $1510\text{ cm}^{-1}$ , were absent (Rosa et al., 2010; Stuart et al., 2004; Fan et al., 2012)

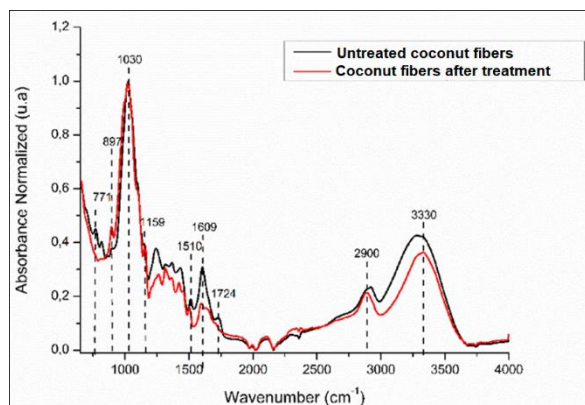


**Figure 7.** FTIR spectra of powdered coconut fibers, before (black) and after the cellulose extraction treatment (red).

When analyzing the images of treated fibers obtained by scanning electron microscopy (SEM), we observed that the treatment proposed eliminated globular particles, including the wax and fat layers that covered the entire structure of the coconut fiber (Figure 8), thus making the cellulose fibers stand out. These data corroborate the results from the quantitative fiber analysis. Despite the low final weight yield (1%), treated fibers have a concentration of cellulose (0.08 g cellulose/g DM) ten times greater than that of untreated fibers (Figure 6).

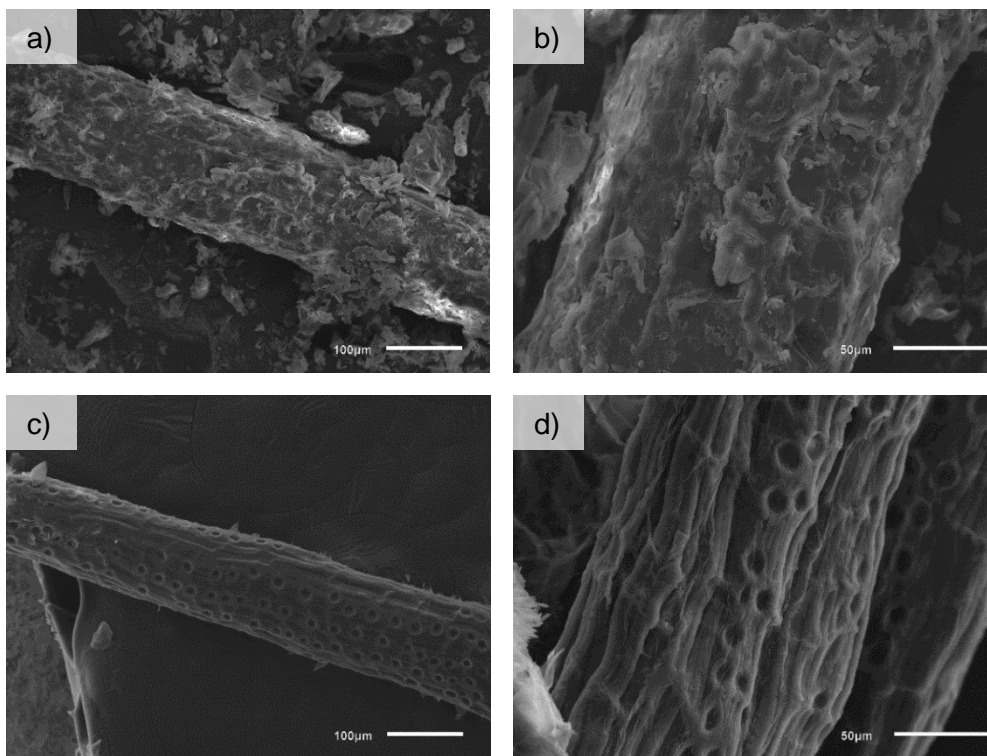


**Figure 8.** SEM images of coconut fibers before (a,b) and after physical-chemical treatment (c,d).

## Conclusion

The use of DOE for screening and optimization is an excellent tool for determining optimal pulp extraction conditions. The alkaline treatment for cellulose extraction has been frequently discussed in the literature; however, we observed that, in the extraction process adopted here, other variables were statistically more expressive, such as the concentration of hypochlorite and bleaching time. These steps have been previously described as adjuvants in the process of extracting cellulose from coconut fibers. The best conditions to extract cellulose from

coconut fibers were 1% NaOH, 20 minutes of autoclaving, 0.60% hypochlorite, and bleaching time of 8.0667h.

## References

1. Almeida, T. M.; Bispo, M. D.; Cardoso, A. R.; Migliorini, M. V.; Schena, T.; de Campos, M. C.; Machado, M. E.; López, J. A.; Krause, L. C.; Caramão, E. B. Preliminary studies of bio-oil from fast pyrolysis of coconut fibers. *Journal of agricultural and food chemistry*, 61(28), 6812–6821, 2013.
2. Andler, S.M., Goddard, J.M. Transforming food waste: how immobilized enzymes can valorize waste streams into revenue streams. *npj Sci Food*, 2:19, 2018.
3. Arsyad, M.; Pratikto, I.N.G.W; Irawan, Y.S. The morphology of coconut fiber surface under chemical treatment. *Matéria (Rio J.)*, 20:1, 169-177, 2015.
4. Benini, K.; Voorwald, H.; Cioffi, M.; Rezende, M. C.; Arantes, V. Preparation of nanocellulose from *Imperata brasiliensis* grass using Taguchi method. *Carbohydrate polymers*, 192, 337–346, 2018. <https://doi.org/10.1016/j.carbpol.2018.03.055>.
5. Brainer, M.S. de C. P. Produção de coco: o nordeste é destaque nacional. *Cad. Set. ETENE*, 3:61, 2018.
6. Brendel, O.; Losetta, P.P.M.G.; Stewart, D. A rapid and simple method to isolate pure alpha cellulose. *Phytochemistry Annal*, v. 11, p. 7-10, 2000.
7. Deepa, B., Abraham, E., Cordeiro, N. et al. Utilization of various lignocellulosic biomass for the production of nanocellulose: a comparative study. *Cellulose* 22, 1075–1090, 2015. <https://doi.org/10.1007/s10570-015-0554-x>
8. Deepa, B.; Abraham, E.; Cordeiro, N.; Faria, M.; Primc, G.; Pottathara, Y.; Leskovšek, M.; Gorjanc, M.; Mozetič, M.; Thomas, S.; Pothan, L.A. Nanofibrils vs nanocrystals bio-nanocomposites based on sodium alginate matrix: An improved-performance study. *Heliyon*, 6 (2), 2020. <https://doi.org/10.1016/j.heliyon.2020.e03266>.
9. Fan, M., Dai, D., Huang, B. Fourier transform infrared spectroscopy for natural fibres. *Fourier transform – Materials analysis*, InTech, 2012.
10. Gouveia, E. R.; Nascimento, R. T.; Souto-Maior, A. M.; Rocha, G. J. M. Validação de metodologia para a caracterização química de bagaço de cana-de-açúcar. *Química Nova* [online], 32 (6), 2009. <https://doi.org/10.1590/S0100-40422009000600026>
11. Huamán-Pino, G.; de Mesquita, L.M.S.; Torem, M.L.; Pinto, G.A.S. Biosorption of cadmium by green coconut shell powder. *Minerals Engineering*, 19:5, 380-387, 2006.
12. Ishizaki, M. H.; Visconte, L. L. Y.; Furtado, C. R. G.; Leite, M. C. A. M.; Leblanc, J. L. Caracterização mecânica e morfológica de compósitos de polipropileno e fibras de coco verde: influência do teor de fibra e das condições de mistura. *Polímeros*, 16(3), 182-186, 2006.
13. Karthikeyan, A.; Balamurugan, K. Effect of alkali treatment and fiber length on impact behavior of coir fiber reinforced epoxy composites. *Journal of Scientific & Industrial Research*, 71, 627-631, 2012.
14. Machado, B. A.; Reis, J. H.; Cruz, L. A.; Leal, I. L.; Barbosa, J. D.; Azevedo, J. B.; Druzian, J. I. Characterization of cassava starch films plasticized with

- glycerol and strengthened with nanocellulose from green coconut fibers. *African Journal of Biotechnology*, 16, 1567-1578, 2017. DOI:10.5897/AJB2017.15943.
15. Machado, B.A.S.; Reisb, J.H.O.; da Silva, J.B.; Cruz, L.S.; Nunes, I.L.; Pereira, F.V.; Druzian, J. I. Obtenção de nanocelulose da fibra de coco verde e incorporação em filmes biodegradáveis de amido plastificados com glicerol. *Quim. Nova*, 37(8): 1275-1282, 2014.
  16. Mondal, D.; Perween, M.; Srivastava, D.N.; Ghosh, P.K. Unconventional Electrode Material Prepared from Coir Fiber through Sputter Coating of Gold: A Study toward Value Addition of Natural Biopolymer. *ACS Sustainable Chem. Eng.*, 2, 3, 348–352, 2014.
  17. Mulinari, D.R.; Baptista, C.A.R.P.; Souza, J.V.C.; Voorwald, H.J.C. Mechanical Properties of Coconut Fibers Reinforced Polyester Composites. *Procedia Engineering*, 10, 2011. <https://doi.org/10.1016/j.proeng.2011.04.343>.
  18. Rencoret, J.; Ralph, J.; Marques, G.; Gutiérrez, A.; Martínez, Á.; del Río, J. C. Structural characterization of lignin isolated from coconut (*Cocos nucifera*) coir fibers. *Journal of agricultural and food chemistry*, 61(10), 2434–2445, 2013.
  19. Rosa MF, Medeiros ES, Malmonged JA, Gregorskib KS, Wood DF, Mattoso LHC, Glenn G, Orts WJ, Imam SH. Cellulose nanowhiskers from coconut husk fibers: Effect of preparation conditions on their thermal and morphological behavior. *Carbohydr. Polym.* 81(1):83-92, 2010.
  20. Rosa MF, Medeiros ES, Malmonged JA, Gregorskib KS, Wood DF, Mattoso LHC, Glenn G, Orts WJ, Imam SH. Cellulose nanowhiskers from coconut husk fibers: Effect of preparation conditions on their thermal and morphological behavior. *Carbohydr. Polym.* 81(1):83-92, 2010.
  21. Rosa, M. de F.; Medeiros, E. S.; Imam, S. H.; Nascimento, D. M.; Monteiro, A. K.; Malmonge, J. A.; Mattoso, L. H. C. Nanocelulose de fibras de coco imaturo para aplicação em nanocompósitos. *Embrapa Instr. Agro.*, 1- 4. 2009.
  22. Silva, E. J. da; Marques, M.L.; Velasco, F.G.; Fornari Junior, C.C.M.; Luzardo, F.H.M. Degradação da fibra de coco imersa em soluções alcalinas de cimento e NaOH. *Rev. bras. eng. agríc. ambient.*, 19:10, 981-988, 2015.
  23. Stuart, B.H. *Infrared Spectroscopy: Fundamentals and Applications*. Chichester, UK: John Wiley & Sons; 2004.
  24. Tripathi, A.; Ferrer, A.; Khan, S.A.; Rojas, O.J. Morphological and Thermochemical Changes upon Autohydrolysis and Microemulsion Treatments of Coir and Empty Fruit Bunch Residual Biomass to Isolate Lignin-Rich Micro- and Nanofibrillar Cellulose. *ACS Sustainable Chem. Eng.*, 5, 2483–2492, 2017.

#### 4. CHAPTER 2 – PRODUCTION OF NANOCELLULOSE

##### **Paper 2: Green production of nanocellulose gels and films from *Cocos nucifera***

Laryssa Pinheiro Costa Silva<sup>1</sup>, Pedro Henrique Cassaro Lirio<sup>1</sup>, Wanderson Juvencio Keijok<sup>1</sup>, Rafaela Spesseemille Valotto<sup>1</sup>, Adilson Ribeiro Prado<sup>2</sup>, Jairo Pinto de Oliveira<sup>1</sup> and Marco Cesar Cunegundes Guimarães<sup>1\*</sup>

<sup>1</sup> Federal University of Espirito Santo, Av Marechal Campos 1468, Vitória, ES 29.040-090, Brazil.

<sup>2</sup> Federal Institute of Espírito Santo, km 6.5 ES 010, Serra, Vitória, ES 29173-087, Brazil.

\* Corresponding author: marco.guimaraes@ufes.br

##### **Abstract**

About 5 to 6 million tons of *Cocos nucifera* (dwarf coconut) fibers are produced annually worldwide, but only 10% of this material is commercially recycled. The amount of coconut residue generated by the agro-industrial sector is greater than the natural capacity of biomass degradation, and this translates into an environmental amount. The wide availability of coconut fiber, added to the environmental problem generated, justify the use of this material as a source of raw material for obtaining nanocellulose gels. In this study, we show that an organic waste (coconut fibers) can be converted into nanocellulose gels, using mechanics combined with water. The nanomaterial obtained after the application of shear force was centrifuged and both the supernatant and sediment lyophilized. The nanomaterials were structurally characterized by scanning electron microscopy (SEM) and transmission electron microscopy (TEM), and the groups identified by Fourier transform infrared (FTIR) and Raman spectroscopy. The images produced by SEM and TEM highlight that two types of nanocellulose gels were produced: cellulose nanofiber gels (CNF-G), produced from the precipitate, and cellulose nanocrystal gels (CNC-G), produced from the supernatant. Thus, a sustainable and easily scalable process can be used to produce two types of high-market-value nanocellulose gels.

**Keywords:** *Cocos nucifera*, mechanical extraction, cellulose nanocrystals (CNC), cellulose nanofibers (CNF), TEM, and recovery of agro-industry waste.



## 1. Introduction

The species *Cocos nucifera* produces fruits with several food applications, such as coconut water, shredded coconut, and coconut oil [1,2,3]. However, the shell of the green coconut, before complete maturation, corresponds to 85% of the total weight of the fruit and has high humidity, which hinders the application of coconut fibers in the production of bags, brushes, mats, ropes, insulation panels, packaging, and car seats [4, 5]. This residue is, therefore, discarded. Although about 5 to 6 million tons of coconut fibers are produced annually around the world, only 10% of this material is commercially recycled [6].

The amount of coconut waste generated by the agroindustry sector is greater than the natural capacity of biomass degradation, and that translates into environmental pollution [7]. Thus, it is imperative to develop new initiatives that take the use of coconut waste into account. One of the alternatives discussed is the production of low-cost nanomaterials, which, in addition to contributing to the reduction of solid waste, can increase the added value of the final product [8].

Coconut fiber is made up of 37.3% cellulose, being, therefore, an attractive source for nanocellulose production. Nanocellulose or cellulose nanoparticles are elements derived from cellulose with at least one dimension smaller than 100 nm [9]. Morphologically, they can be differentiated as cellulose nanocrystals (CNC) or cellulose nanofibers (CNF), both with unique properties, such as high surface area [10, 11], ability to form a highly porous structure [12], excellent mechanical properties [13], low thermal expansion coefficient [14], low density [12], easy surface modification [15], high biodegradability [16], and biocompatibility [17, 18]. That results in a variety of applications, such as synthesis of antimicrobial materials [19], drug delivery [20], biosensors [21, 22], cement [23], and bioadhesives [24].

Nanocellulose can be obtained through three distinct approaches: mechanical [25, 26], chemical [27, 28], and enzymatic [29, 30]. In all three, the goal is to eliminate the amorphous domains of cellulose. In the production of CNF, the cleavage of the amorphous region of cellulose is aleatory, resulting in nanofibers with both crystalline and amorphous regions [31]. On the other hand, in the production of CNC the cleavage is directed, thus yielding a nanomaterial

composed exclusively of the crystalline region of cellulose [32]. It is common to have a combination of these approaches for the production of CNF and CNC, but this makes the process more expensive and time-consuming [33].

Some studies on the production of nanocelluloses from coconut fiber have already been carried out [34, 35]; however, they all used the chemical method for the production of cellulose nanocrystals. The mechanical extraction method was described only for the production of CNF [36, 37, 38, 39], suggesting the impossibility of applying this method for the production of nanocrystals. However, only the application of statistical models, aiming to exhaust the variables that affect the product, can prove the impossibility of producing CNF and CNC by this method. Recently, Kang et al. (2018) failed to produce CNF and CNC from cellulose pulp using only mechanical force, obtaining CNF and CNC only when a previously processed cellulose – microcrystalline cellulose – was used.

Here, we show that if the correct parameters determined by the Design of Experiments (DOE) method are employed, mechanical force combined with water can transform the cellulose pulp obtained from an organic residue (coconut fiber) into two types of nanocellulose gels: cellulose nanofiber gel (CNF-G) and cellulose nanocrystal gel (CNC -G).

## **2. Materials and Methods**

### **2.1. Materials**

Sodium hydroxide (NaOH), sodium hypochlorite (NaOCl), glacial acetic acid (CH<sub>3</sub>CO<sub>2</sub>H), nitric acid (HNO<sub>3</sub>), and absolute ethanol (Et-OH) were purchased from Sigma Aldrich Ltd and used as received without any further purifications. Deionized water obtained from Millipore Direct-Q® 3 water purification system was used for all experiments. Coconut fibers were donated by the company Marquinhos Água de Coco®.

### **2.2. Obtaining cellulose from coconut fibers**

Fibers were extracted from green coconuts, washed thoroughly in running water, oven-dried at 60 °C for 48 hours, ground in a mill with stainless steel blades, and sieved in 40-mesh sieves.

Fiber samples (10 g) were added to 400 mL of 1% sodium hydroxide (NaOH) and the resulting solution was autoclaved (20 minutes). The fibers were then washed with distilled water until the complete removal of water-soluble substances. To the resulting pulp were added 100 mL of 0.8% sodium hypochlorite and 10 drops of glacial acetic acid, and the mixture was stirred at 250 rpm for 8 hours and 4 minutes. The cellulose pulp was filtered and oven-dried (40 °C) for 24 hours.

## 2.5. Obtaining nanocellulose

Cellulose was mixed with ultrapure water and 1:10 glass spheres (4 mm) and submitted to ball grinding at 250 rpm in an orbital shaker. After milling, the samples were centrifuged at 4,000 rpm for 5 minutes. The supernatant and pellet were lyophilized and weighed. The amount of sample and stirring time were determined by Design of Experiment (DOE).

## 2.6. Design of experiment (DOE) and statistical modeling for the production of nanocellulose

The matrix of factors used in the experiment, its levels, and responses is shown in Table 1. We generated a full factorial combining 2 factors and 3 levels, with repetition of the central point, in which the response of each test (yield) was recorded (Table S1). The results of each test run were evaluated through the graphical and statistical analysis tool of the Statistica® 10 software, based on the main effects, interaction, ANOVA and a response table.

Factors	Levels			Responses	
	A	B	C		
Amount of sample (g)	1	3	5	Nanocrystal yield (g)	Nanofiber yield (g)
Time (h)	6	15	24		

**Table 1.** Matrix of factors, levels, and responses for the complete factorial design to obtain nanocellulose.

## 2.7. Nanocelullose characterization

### 2.7.1. Scanning Electron Microscopy (SEM)

The fibers were morphologically and structurally analyzed by scanning electron microscopy (JSM-6610LV, JEOL, USA inc.). The fibers were metallized with gold for 2 minutes, using argon as a carrier gas, being then dried and analyzed with an electron acceleration voltage of 15 keV.

### 2.7.2. Transmission Electron Microscopy (TEM)

Nanocellulose was dispersed in water to form a 0.2% suspension; a drop of this suspension was deposited on nickel grids covered with Formvar and dried under the hood at room temperature. Samples were observed at 80 kV (JEM-1400, JEOL, USA inc.) and dimensions determined using the Image J software.

### 2.7.3. Fourier Transform Infrared Spectroscopy (FTIR)

FTIR experiments were carried out with attenuated total reflection (ATR), using a Cary 630 spectrometer (Agilent technology) equipped with a zinc selenide (ZnSe) crystal. The samples were dried and ground and their spectra recorded in the range from 4000 to 650  $\text{cm}^{-1}$  with a 4  $\text{cm}^{-1}$  resolution. Absorption ratios were obtained by normalizing the peak heights to the cellulose absorbance peak at 897  $\text{cm}^{-1}$ , which results from the C<sub>1</sub>—H deformation of the glucose rings.

### 2.7.4. Raman Spectroscopy

Cellulose nanocrystals and nanofibers were characterized using Raman scattering (Raman Spectrometer Mira DS, Metrohm) in the 640-2000  $\text{cm}^{-1}$  range at a laser wavelength of 785 nm.

### 2.7.5. Energy dispersive x-ray (EDS)

The elemental composition of the sample was identified by energy dispersive x-ray spectroscopy (EDS), using a liquid nitrogen-based 30 mm detector (EDAX model). Although EDS and SEM analyses are usually integrated, for the former samples were not metallized.

### 2.7.6. X-ray diffraction (XRD)

The crystal structure of CNC was determined using X-ray diffraction (XRD). CNC samples were scanned in a  $2\theta$  region from 30° to 90° at 0.01° per minute, with a time constant of 2 s, using a D8 Advance (Brukeraxs) X-ray diffractometer. The crystallinity index (CrI) was determined through Eq. (1):

$$CrI = \frac{I_{crystalline} - I_{amorph}}{I_{crystalline}} \times 100$$

In which,  $I_{crystalline}$  is the peak intensity at  $2\theta \sim 22^\circ$  and  $I_{amorph}$  is the intensity of the minimum region at  $2\theta \sim 18^\circ$ .

### 3. Results and discussion

3.1. Design of experiment (DOE) and statistical modeling for the production of nanocellulose.

Several factors affect the synthesis of nanocellulose through the ball mill, such as the number and size of balls, the rotation speed, the state of the sample (dry or wet), the time, and the proportion balls:sample [26].

For the simultaneous production of nanocrystals and cellulose nanofibers, we performed a complete  $3^2$  factorial analyzing the factors time (h) and amount of sample (g), with repetition of 3 central points. We used as a response variable the final weight (g) of the nanocrystals and nanofibers produced. The optimal values for the response variable were 0.034 g and 0.272 g, for nanocrystals and nanofibers, respectively (Fig. 1A). The optimal operating conditions based on the factors time and amount of sample were 15.424 h and 3.1886 g, respectively (Fig. 1A). To assess whether there is a relationship between the maximum and minimum points with the desirable point, we observed a quadratic function in the three-dimensional response surface plot (Fig. 1B).

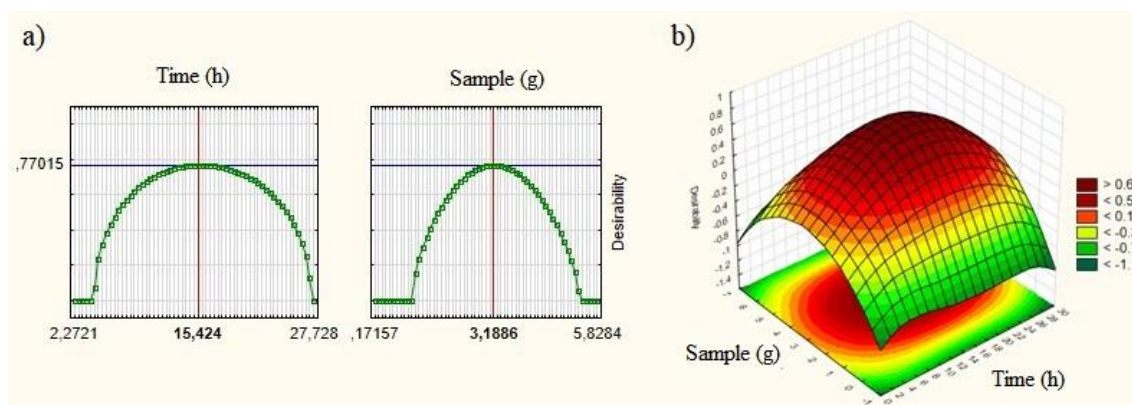


**Fig. 1.** (a) Desirability function plot. Maximum response for nanocrystals (g) and nanofibers (g); (b) Response surface graph of the desirability function.

### 3.2. Nanocellulose characterization

Nanofibers can be separated from cellulose nanocrystals by centrifugation because their longer length cause them to entangle and aggregate, precipitating upon centrifugation [40]. Thus, following the synthesis of nanocellulose, the samples were centrifuged and separated into precipitate (P) and supernatant (S),

which represented, respectively, 92.65% and 7.35% of the lyophilized material recovered.

### 3.3. Structural and Morphological analysis of nanocellulose (SEM and TEM)

The structural characterization of the lyophilized precipitate and supernatant was performed by scanning electron microscopy (SEM) and transmission electron microscopy (TEM).

Through SEM, we observed that the precipitate has a porous and fibrillar nature (Figure 2 A and C), like the nanofibers visualized by Lee et al. (2021). The hydrated structure presented a consistent gelatinous aspect (Figure 3A), and the images obtained by TEM (Figure 3C) revealed fibrillar structures with a diameter between 10-20 nm.

The image of the supernatant obtained by SEM (Figure 2B and D) shows an amorphous structure, consistent with the characteristic flake appearance after lyophilization [33]. Klem et al. (2005) found only CNF in the NC supernatant produced from cellulose pulp. This is due to the high degree of polymerization of this material, which implies that CNC cannot be produced by shear force alone. However, in addition to the hydrated structure with an inconsistent gelatinous aspect (Figure 3B), the TEM image (Figure 3D) shows CNC of 13.95 nm in diameter and 200 nm in length.



CNC are highly crystalline when the crystallinity index falls between 54 and 88% [45]; that of CNC obtained from coconut fiber was 58.74%.

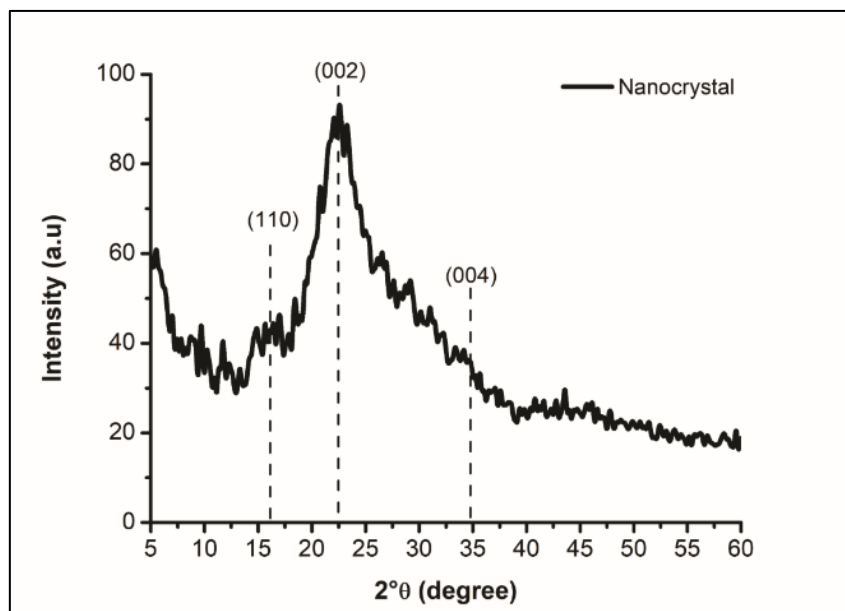


**Figure 7** XRD spectrum of nanocrystal samples

### 3.4. Fourier Transform Infrared Spectroscopy (FTIR)

To assess the elemental chemical composition of nanocellulose, Fourier transform infrared spectroscopy (FTIR) analysis was performed, as shown in Figure 4. The FTIR spectra confirm the absence of possible contaminants during the production of nanocellulose, as the same bands and signals observed in the analysis of cellulose extracted from coconut fiber were detected, namely 897, 1030, 1159, 2900, and 3330  $\text{cm}^{-1}$  [45, 46].



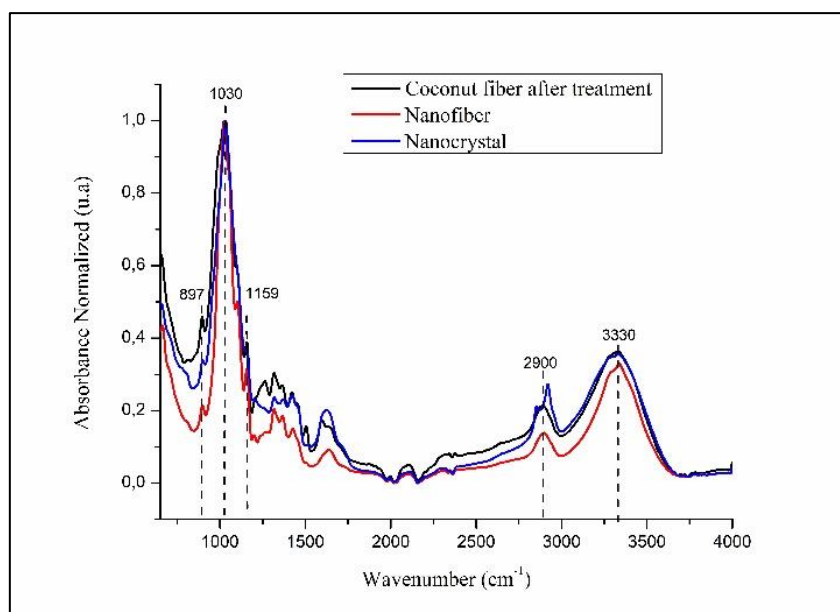


**Fig. 4.** FTIR spectra of powdered coconut fibers after cellulose (black), nanofiber (red), and nanocrystal (blue) extraction treatment.

### 3.5. Raman spectroscopy

Nanocelluloses have similar Raman spectra, but the Raman frequency, intensity, and shape of the vibration band can vary between cellulose nanofibers (CNF) and nanocrystals (CNC), because crystalline compounds are associated to higher intensities [47]. We observed that the Raman spectra of CNF and CNC are similar (Fig. 5), with bands at  $485\text{ cm}^{-1}$ ,  $900\text{ cm}^{-1}$ , and between  $1080\text{--}1097\text{ cm}^{-1}$ , associated with nanocellulose obtained from plant material [48]. However, the nanocrystal sample has a sharper resolution.

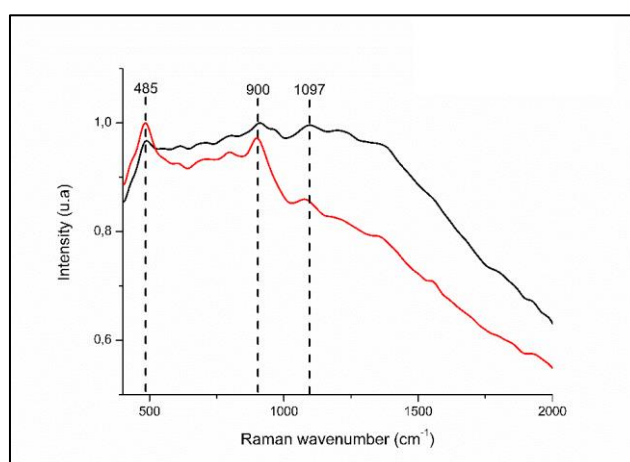


**Fig. 5.** Raman spectra of nanofibers (black) and nanocrystals (red).

## Conclusion

The use of organic waste as a raw material has several benefits. These materials can provide cost-effective products, low greenhouse gas emissions and, most importantly, a sustainable environment for a better life. With cellulose extracted from agribusiness residue, we produced high value-added nanomaterials – cellulose nanofiber gel (CNF-G) and cellulose nanocrystal gel (CNC-G) – using a sustainable technique, using only water and mechanical strength.

## References

1. Abitbol, T.; Rivkin, A.; Cao, Y.; Nevo, Y.; Abraham, E.; Ben-Shalom, T.; Lapidot, S.; Shoseyov, O. Nanocellulose, a tiny fiber with huge applications. *Current Opinion in Biotechnology* 39 (2016) 76-88.
2. Agarwal, U.P. (2017). Raman Spectroscopy of CNC- and CNF-Based Nanocomposites. In *Handbook of Nanocellulose and Cellulose Nanocomposites*; Kargarzadeh, H., Ahmad, I., Eds., Wiley-VCH Verlag: Weinheim, Germany; pp. 609–625.
3. Agarwal, U.P. (2019). Analysis of Cellulose and Lignocellulose Materials by Raman Spectroscopy: A Review of the Current Status. *Molecules*, 24(9), 1659-1675. <https://doi.org/10.3390/molecules24091659>
4. Almeida, T. M.; Bispo, M. D.; Cardoso, A. R.; Migliorini, M.V.; Schena, T.C.; Machado, M.E.; López, J. A.; Krause, L. C.; Caramão, E. B. Preliminary studies of bio-oil from fast pyrolysis of coconut fibers. *Journal of agricultural and food chemistry* 61 28 (2013) 6812–682.
5. Alonso-Lerma, B.; Barandiaran, L.; Ugarte, L.; Larraza, I.; Reifs, A.; Olmos-Juste, R.; Barrietabeña, N.; Amenabar, I.; Hillenbrand, R.; Eceiza, A.; Perez-Jimenez, R. (2020). High performance crystalline nanocellulose using an ancestral endoglucanase. *Communications Materials*, 1(57), 1-10. <https://doi.org/10.1038/s43246-020-00055-5>
6. Balea, A., Fuente, E., Blanco, A., & Negro, C. (2019). Nanocelluloses: Natural-Based Materials for Fiber-Reinforced Cement Composites. A Critical Review. *Polymers (Basel)*, 11(3), 1-33. <https://doi.org/10.3390/polym11030518>
7. Brainer, M.S. de C. P. Produção de coco: o nordeste é destaque nacional. *Caderno Setorial ETENE* 3 61 (2018) 1-25.
8. Brendel, O.; Losetta, P.P.M.G.; Stewart, D. (2000). A rapid and simple method to isolate pure alpha cellulose. *Phytochemistry Annal*, 11, 7-10.
9. Brígida, A.I.S.; Calado, V.M.A.; Gonçalves, L.R.B.; Coelho, M.A.Z. Effect of chemical treatments on properties of green coconut fiber. *Carbohydrate*

- Polymers 79 (2010) 832–838. Doi: <https://doi.org/10.1016/j.carbpol.2009.10.005>
10. Cao, Y.; Zavaterri, P.; Youngblood, J.; Moon, R.; Weiss, J. (2015). The influence of cellulose nanocrystal additions on the performance of cement paste. *Cement and Concrete Composites*, 56, 73-83.
  11. Chu, Y., Sun, Y., Wu, W., & Xiao, H. (2020). Dispersion Properties of Nanocellulose: A Review. *Carbohydrate Polymers*, 250, 116892.
  12. De France, K.J.; Hoare, T.; Cranston, E.D. (2017). Review of Hydrogels and Aerogels Containing Nanocellulose. *Chemistry of Materials*, 29, 11, 4609-4631.
  13. Di Giorgio, L.; Martín, L.; Salgado, P. R.; Mauri, A. N. (2020). Synthesis and conservation of cellulose nanocrystals. *Carbohydrate polymers*, 238, 116187-116197. <https://doi.org/10.1016/j.carbpol.2020.116187>
  14. Du, H.; Liu, W.; Zhang, M.; Si, C.; Zhang, X.; Li, B. Cellulose nanocrystals and cellulose nanofibrils based hydrogels for biomedical applications. *Carbohydrate Polymers* 209 (2019) 130–144.
  15. Fan, M.; Dai, D.; Huang, B. Fourier transform infrared spectroscopy for natural fibres. *Fourier transform – Materials analysis*, InTech, 2012.
  16. Golmohammadi, H.; Morales-Narváez, E.; Naghdi, T.; Merkoçi, A. (2017). Nanocellulose in Sensing and Biosensing. *Chemistry of Materials*, 29 (13), 5426-5446.
  17. Huamán-Pino, G.; de Mesquita, L.M.S.; Torem, M.L.; Pinto, G.A.S. Biosorption of cadmium by green coconut shell powder. *Minerals Engineering* 19 5 (2006) 380-387.
  18. Ishizaki, M. H.; Visconte, L. L. Y.; Furtado, C. R. G.; Leite, M. C. A. M.; Leblanc, J. L. Caracterização mecânica e morfológica de compósitos de polipropileno e fibras de coco verde: influência do teor de fibra e das condições de mistura. *Polímeros* 16 3 (2006) 182-186.
  19. Jordan, J. H.; Easson, M. W.; Dien, B.; Thompson, S.; Condon, B. D. (2019). Extraction and characterization of nanocellulose crystals from cotton gin motes and cotton gin waste. *Cellulose*, 26, 5959–5979.
  20. Junka, K.; Guo, J.; Filpponen, I.; Laine, J.; Rojas, O. J. (2014). Modification of cellulose nanofibrils with luminescent carbon dots. *Biomacromolecules*, 15(3), 876–881.
  21. Kang, X.; Kuga, S.; Wang, C.; Zhao, Y.; Wu, M.; Huang, Y. Green Preparation of Cellulose Nanocrystal and Its Application. *ACS Sustainable Chemistry & Engineering*, 6(3), 2954-2960, 2018.
  22. Karimian, A.; Parsian, H.; Majidinia, M.; Rahimi, M.; Mir, S. M.; Samadi Kafil, H.; Shafiei-Irannejad, V.; Kheyrollah, M.; Ostadi, H.; Yousefi, B. (2019). Nanocrystalline cellulose: Preparation, physicochemical properties, and applications in drug delivery systems. *International journal of biological macromolecules*, 133, 850–859.
  23. Kim, J.H.; Shim, B.S.; Kim, H.S.; Lee, Y. J.; Min, S. K.; Jang, D.; Abas, Z.; Kim, J.(2015). Review of nanocellulose for sustainable future materials. *International journal of precision engineering and manufacturing-green technology*, 2(2), 197–213. <https://doi.org/10.1007/s40684-015-0024-9>
  24. Klem, D.; Heublein, B.; Fink, H. P.; Bohn, A. (2005). Cellulose: Fascinating Biopolymer and Sustainable raw material. *Angewandte Chemie International*, 44, 3358 – 3393.

25. Kramer, F.; Klemm, D.; Schumann, D.; Heßler, N.; Wesarg, F.; Fried, W.; Stadermann, D. (2006). Nanocellulose polymer composites as innovative pool for (bio) material development. *Macromolecular Symposia*, 244, 136–148. <https://doi.org/10.1002/masy.200651213>
26. Lam, E.; Male, K. B.; Chong, J. H.; Leung, A. C.; Luong, J. H. (2012). Applications of functionalized and nanoparticle-modified nanocrystalline cellulose. *Trends in biotechnology*, 30(5), 283–290.
27. Le Bras, D.; Strømme, M.; Mihranyan, A. (2015). Characterization of dielectric properties of nanocellulose from wood and algae for electrical insulator applications. *The journal of physical chemistry. B*, 119(18), 5911–5917.
28. Lee, H.; Kim, S.; Shin, S.; Hyun, J. (2021). 3D structure of lightweight, conductive cellulose nanofiber foam. *Carbohydrate polymers*, 253, 117238–117250. <https://doi.org/10.1016/j.carbpol.2020.117238>
29. Li, J.; Cha, R.; Mou, K.; Zhao, X.; Long, K.; Luo, H.; Zhou, F.; Jiang, X. (2018). Nanocellulose-Based Antibacterial Materials. *Advanced Healthcare Materials*, 7(20), 1–16. <https://doi.org/10.1002/adhm.201800334>
30. Machado, B.A.S.; Reisb, J.H.O.; da Silva, J.B.; Cruz, L.S.; Nunes, I.L.; Pereira, F.V.; Druzian, J. I. Obtenção de nanocelulose da fibra de coco verde e incorporação em filmes biodegradáveis de amido plastificados com glicerol. *Quim. Nova*, 37(8): 1275-1282, 2014.
31. Mishra, S.; Kharkar, P. S.; Pethe, A. M. (2019). Biomass and waste materials as potential sources of nanocrystalline cellulose: Comparative review of preparation methods (2016 – Till date). *Carbohydrate Polymers*, 207, 418-427.
32. Lee H, Kim S, Shin S, et al. 3D structure of lightweight, conductive cellulose nanofiber foam. *Carbohydrate polymers*. 2021; 253, 117238–117250. [doi.org/10.1016/j.carbpol.2020.117238](https://doi.org/10.1016/j.carbpol.2020.117238)
33. Klem D, Heublein B, Fink HP, Bohn A. Cellulose: Fascinating Biopolymer and Sustainable raw material. *Angewandte Chemie International*. 2005; 44: 3358–3393. [doi.org/10.1002/anie.200460587](https://doi.org/10.1002/anie.200460587).
34. Nagarajana, K.J.; Balajia, A.N.; Ramanujamb, N.R. (2019). Extraction of cellulose nanofibers from *cocos nucifera* var *aurantiaca* peduncle by ball milling combined with chemical treatment. *Carbohydrate Polymers*, 212, 312–322. <https://doi.org/10.1016/j.carbpol.2019.02.063>
35. Osong, S. H.; Norgren, S.; Engstrand, P. (2016). Processing of wood-based microfibrillated cellulose and nanofibrillated cellulose, and applications relating to papermaking: a review. *Cellulose* 23, 93–123.
36. Pere, J.; Tammelin, T.; Niemi, P.; Lille, M.; Virtanen, T.; Penttilä, P.A.; Ahvenainen, P.; Grönqvist, S. (2020). Production of High Solid Nanocellulose by Enzyme-Aided Fibrillation Coupled with Mild Mechanical Treatment. *CS Sustainable Chemistry & Engineering*, 8 (51), 18853–18863.
37. Phanthong, P.; Reubroycharoen, P.; Hao, X.; Xu, G.; Abudula, A.; Guan, G. (2018). Nanocellulose: Extraction and application. *Carbon Resources Conversion*, 1(1), 32-43.
38. Rajinipriya, M.; Nagalakshmaiah, M.; Robert, M.; Elkoun, S. (2018). Importance of Agricultural and Industrial Waste in the Field of Nanocellulose and Recent Industrial Developments of Wood Based

- Nanocellulose: A Review. *ACS Sustainable Chemistry & Engineering*, 6 (3), 2807–2828.
39. Rasheed, M.; Jawaid, M.; Parveez, B.; Zuriyati, A.; Khan, A. (2020). Morphological, chemical and thermal analysis of cellulose nanocrystals extracted from bamboo fibre. *International journal of biological macromolecules*, 160, 183–191.
  40. Rencoret, J.; Ralph, J.; Marques, G.; Gutiérrez, A.; Martínez, Á.; Río, J. C. del. Structural characterization of lignin isolated from coconut (*Cocos nucifera*) coir fibers. *Journal of agricultural and food chemistry* 61 10 (2013) 2434–2445.
  41. Rosa, M. F.; Medeiros, E. S.; Malmonged, J. A.; Gregorskib, K. S.; Wood, D. F.; Mattoso, L. H. C.; Glenn, G.; Orts, W. J.; Imam, S. H. (2010). Cellulose nanowhiskers from coconut husk fibers: Effect of preparation conditions on their thermal and morphological behavior. *Carbohydrate Polymers*, 81(1), 83-92.
  42. Saba, N., Mohammad, F., Pervaiz, M., Jawaid, M., Alothman, O. Y., & Sain, M. (2017). Mechanical, morphological and structural properties of cellulose nanofibers reinforced epoxy composites. *International journal of biological macromolecules*, 97, 190–200.
  43. Shojaeiarani, J.; Bajwa, D.; Shirzadifar, A. A review on cellulose nanocrystals as promising biocompounds for the synthesis of nanocomposite hydrogels. *Carbohydrate Polymers* 216 (2019) 247–259.
  44. Xiao Y, Liu Y, Wang X, et al. Cellulose nanocrystals prepared from wheat bran: Characterization and cytotoxicity assessment. *International Journal of Biological Macromolecules*. 2019; 140:225-233; doi.org/10.1016/j.ijbiomac.2019.08.160.
  45. Thakur, V.; Guleria, A.; Kumar, S.; Sharmad, S.; Singh, K. (2021). Recent advances in nanocellulose processing, functionalization and applications: a review. *Materials Advances*, 2, 1872–1895.
  46. Trache, D.; Tarchoun, A.F.; Derradji, M.; Hamidon, T. S.; Masruchin, N.; Brosse, N.; Hussin, M. H. (2020). Nanocellulose: From Fundamentals to Advanced Applications. *Frontiers in Chemistry*, 8, 392-412.
  47. Tripathi, A.; Ferrer, A.; Khan, S.A.; Rojas, O.J. Morphological and Thermochemical Changes upon Autohydrolysis and Microemulsion Treatments of Coir and Empty Fruit Bunch Residual Biomass to Isolate Lignin-Rich Micro- and Nanofibrillar Cellulose. *ACS Sustainable Chemistry & Engineering* 5 (2017) 2483–2492.
  48. Verma, C.; Chhajed, M.; Gupta, P.; Roy, S.; Maji, P. K. (2021). Isolation of cellulose nanocrystals from different waste bio-mass collating their liquid crystal ordering with morphological exploration. *International journal of biological macromolecules*, 175, 242–253.

**Paper 2: Green production of nanocellulose gels and films from *Cocos nucifera***

**Supplementary material**

Run order	Blocks	Factors		Nanocrystals Yield (g)	Nanofiber Yield (g)
		Amount of sample (g)	Time (h)		
1	1	1	6	0,024	0,111
2	1	5	6	0,019	0,147
3	1	1	24	0,016	0,173
4	1	5	24	0,018	0,174
5	1	3	2,27	0,034	0,159
6	1	3	27,73	0,033	0,147
7	1	0,17	15	0,005	0,0
8	1	5,83	15	0,01	0,146
9 (C)	1	3	15	0,031	0,272
10 (C)	1	3	15	0,028	0,215
11 (C)	1	3	15	0,029	0,243

**Table S1.** Complete factorial design  $3^2$  with repetition of the central point of the experiment based on factors, levels and response data (Nanocrystal and nanofiber yield), to obtain nanocellulose.

## 5. CHAPTER 3 – ANTIBACTERIAL ACTIVITY OF NANOCELLULOSE FUNCTIONALIZED WITH GREEN NANOPARTICLES

### Paper 3. High antibacterial activity against *Staphylococcus aureus* and *Pseudomonas aeruginosa* using nanocellulose hybridized with Pomegranate (*Punica granatum L.*) nanoparticles

Laryssa Pinheiro Costa Silva<sup>1</sup>, Natane Aparecida de Oliveira<sup>1</sup>, Rafaela Spesseemille Valotto<sup>1</sup>, Flávio Cunha Monteiro<sup>1</sup>, Luiz Alberto Contreras<sup>1</sup>, Wanderson Juvencio Keijok<sup>1</sup>, Tadeu Ériton Caliman Zanardo, Ricardo Shuenk<sup>2</sup>, Jairo Pinto de Oliveira<sup>1</sup> and Marco Cesar Cunegundes Guimarães<sup>1\*</sup>

<sup>1</sup> Federal University of Espírito Santo, Av Marechal Campos 1468, Vitória, ES 29.040-090, Brazil.

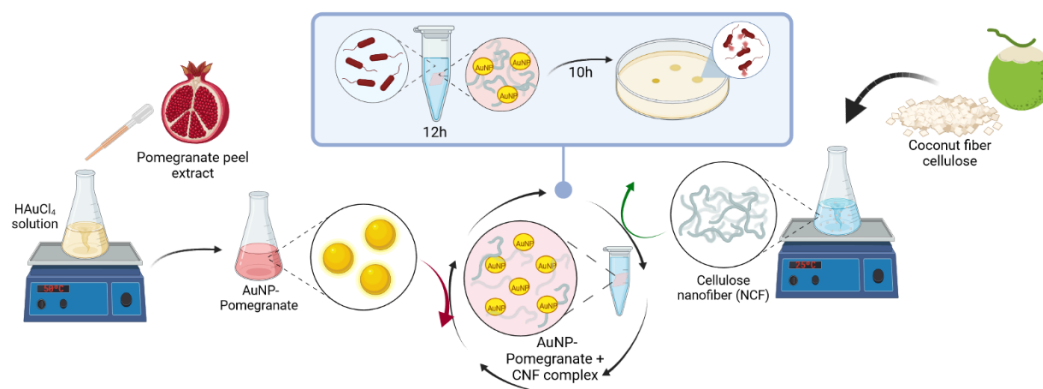
\* Corresponding author: [marco.guimaraes@ufes.br](mailto:marco.guimaraes@ufes.br)

#### Abstract

Environmental concern has increased the search for new biodegradable materials and materials derived from renewable resources. Cellulose nanofiber (CNF) combines the properties of cellulose (e.g., biocompatibility and biodegradability) with the high surface area of nanomaterials. It can serve as a polymeric matrix for inorganic agents in the form of nanoparticles. Gold nanoparticles (AuNPs) have physicochemical stability and can be easily functionalized with bioactive organic molecules. Here, we synthesized, characterized, and investigated the antimicrobial activity of the AuNP-Pomegranate + CNF complex. The complex formed is stable, non-cytotoxic, and has considerable antibacterial activity against strains of *Staphylococcus aureus*, *Escherichia coli*, and *Pseudomonas aeruginosa*, which makes it suitable for application in the health area.

**Keywords:** Nanocellulose; Cellulose nanofiber; Gold nanoparticles; Pomegranate nanoparticle; Antimicrobial activity.

## Graphical Abstract



### 1. Introduction

Cellulose is a linear homopolymer whose production reaches up to  $10^5$ - $10^{10}$  tons per year. It is among the most abundant, renewable, low-cost, biocompatible, and biodegradable polymers in the world, and can replace synthetic materials (Kumari et al., 2019). Cellulosic materials with at least one dimension smaller than 100 nm are referred to as nanocellulose. Nanocellulose combines the properties of cellulose with the high surface area of nanomaterials (Benini et al., 2018).

The growing demand for cost-effective, high-performance renewable materials makes nanocellulose attractive for advanced applications in many industries, such as food packaging and healthcare (Roig-Sanchez et al., 2019). Nanocellulose can also act as a polymer matrix for organic or inorganic agents in the form of nanoparticles and nanotubes (Zhang et al., 2020; Bacakova et al., 2020).

Gold nanoparticles (AuNPs) are more stable compared with other metallic noble metal nanoparticles (Cu, Hg, Ag, Pt), although the former have weaker antibacterial activity (Mokammel et al., 2022). This property can be improved by forming compounds of AuNPs with other antibacterial agents.

Pomegranate (*Punica granatum L.*) fruits grow in warm climates and their peels have been historically applied as herbal remedies to treat flu, allergy, inflammation, and parasitic and microbial infections (Naeem et al., 2020). Pomegranate peel extract contains numerous bioactive constituents such as polyphenols, flavonoids, and tannins that have potent antioxidant and antimicrobial mechanisms (Gad et al., 2021).



Compounds in which AuNPs are combined with cellulose nanofibers have great potential to be used as components in a wide range of products. These may include protective equipment (particularly in healthcare settings) (Zhou et al., 2020), food packaging (Abdalkarim et al., 2021), textiles (Zhou et al., 2018), drug carriers (Tian et al., 2022), in ultrafiltration (Jiang et al., 2019), and wound dressing (Nezhad-Mokhtari et al., 2020).

In this study, we synthesized, characterized, and investigated the antimicrobial activity of the AuNP-Pomegranate+CNF complex. The antibacterial activity of the complex was observed in *Staphylococcus aureus* (ATCC 29213), *Escherichia coli* (ATCC 25922), *Enterococcus faecalis* (ATCC 29212), and *Pseudomonas aeruginosa* (clinical sample 64B) strains. Our results indicate that the AuNP-NF complex is stable, non-cytotoxic, and has antimicrobial activity against gram-positive and gram-negative bacteria. These features make it an excellent material for possible applications in the health area.

## **2. Materials and Methods**

### *2.1. AuNP synthesis*

#### 2.1.1 Preparation of plant extract

The aqueous extract of pomegranate peel was produced by infusing 10 g of crushed peels in 50 mL of ultrapure water at 90 °C (Ahmad et al., 2012). The system was kept under orbital agitation (400 rpm) in a round-bottomed flask coupled with a Graham condenser for 20 minutes. The resulting solution was filtered using 0.45- $\mu\text{m}$  quantitative filter paper. The filtrate was then vacuum-filtered using 0.22- $\mu\text{m}$  membranes, poured into an amber bottle, and kept under refrigeration.

#### 2.1.2 Reduced AuNP synthesis with pomegranate peel extract

Gold nanoparticles were synthesized by reduction method using 10 mL of a  $2.5 \times 10^{-4}$  mol.L<sup>-1</sup> HAuCl<sub>4</sub> solution (Sigma-Aldrich) and 100  $\mu\text{L}$  of pomegranate extract at 56 °C under 400 rpm for 5 minutes. The resulting solution was cooled in an ice bath until cold.

## 2.2 Characterization of AuNP-Pomegranate

AuNP formation was confirmed by color changes in the solution and by localized surface plasmon resonance (LSPR), using a UV–Vis spectrophotometer (Evolution® 300 ThermoScientific) at a resolution of 1 nm and scanning between 230-800 nm. For morphological characterization, AuNPs were placed on a Formvar-coated copper grid (Ted Pella Inc., Redding, CA, USA) and examined by transmission electron microscopy (TEM) using a JEOL microscope (JEOL, Inc., Peabody, MA, USA), model JEM1400, operating at 120 V with lanthanum hexaboride filament (LAB6). The size distribution and zeta potential of the particles were determined using dynamic light scattering (DLS) combined with the interaction of random Brownian motion and the electrical field movement of the particle suspensions (Litesizer 500). To investigate which organic compounds may be associated with AuNPs, we performed Fourier-transform infrared spectroscopy (FTIR) (Agily 630). The concentration of the AuNPs formed was determined by Inductively Coupled Plasma Mass Spectrometry (ICP-MS – model NEXION300D, USA) and that of the extract on the AuNP surface by spectrophotometry (Evolution® 300 ThermoScientific), using the equation (Eq.1) obtained through the calibration curve of the pomegranate extract performed at 373 nm (Fig. S1).

$$\text{Eq. 1. } y = 0.7913x + 0.0653$$

In which x is the concentration of the extract and y is the absorbance of the AuNP solution at 373 nm.

### 2.1 Assessment of cell viability in the presence of AuNPs

Cell viability in the presence of AuNP-Pomegranate was assessed using the MTT (3-(4, 5-dimethylthiazol-2-yl)-2,5-diphenyl tetrazolium) assay as described by Mosmann (Mosmann et al., 1983). The test was performed using L-929 ATCC® CRL-6364™ normal fibroblasts and HaCat MRC-5 ATCC® CCL cell lines. The cells were seeded in flat-bottomed 96-well plates ( $2 \times 10^4$  cells.ml<sup>-1</sup>) and incubated for 24h at 37 °C in a humidified atmosphere (5% CO<sub>2</sub>) for adhesion. Dilution series (42.7; 21.35; 10.67; 5.34; and 2.67 µg/mL) of AuNP-Pomegranate were added to the plates, which were incubated under the same conditions for another 24h to determine the IC<sub>50</sub>. Camptothecin (10 µM) was used as a positive

control. After incubation, 100  $\mu$ L of MTT (5 mg/mL in PBS) (1:3) was added to the plates, which were further incubated for 2 h. Subsequently, the excess of MTT was aspirated and the formazan crystals formed were dissolved in 100  $\mu$ L of dimethyl sulfoxide (DMSO). The absorbance proportional to the number of viable cells was measured at 595 nm using a microplate reader (Molecular Devices, Spectra Max 190, USA). The experiments were performed in triplicate and the percentage of inhibition calculated by equation 2 (Eq.2):

$$\text{Eq.2. } \%inhibition = \left( \frac{\text{Sample intensity}}{\text{Control intensity}} - 1 \right) \times 100$$

Data were analyzed using the GraphPad Prism 7 program for non-linear regression analysis, in which the average inhibition ( $IC_{50}$ ) was obtained at the different concentrations of AuNPs tested.

## 2.2. *Production of cellulose nanofiber film*

Cellulose extracted from coconut fiber (3.26 g) was mixed with ultrapure water (100 mL) and 4-mm glass spheres (62 g) and submitted to ball grinding at 250 rpm in an orbital shaker at 25  $^{\circ}$ C. After milling, the samples were centrifuged 5 times at 4,000 rpm for 5 minutes. The pellet was lyophilized and stored protected from moisture.

## 2.3. *Formation of the AuNp-Pomegranate + Cellulose Nanofiber complex*

Nanofibers (0.001 g) were immersed in 1 mL of AuNP-Pomegranate at three different concentrations (C1: 42.7; C2: 128.1; and C3: 256.2  $\mu$ g/mL) for 24h/150 rpm/25  $^{\circ}$ C, protected from light. The material was then centrifuged twice at 4,000 rpm/ 5 min and resuspended in ultrapure water to remove possible AuNPs that did not adhere to the cellulose nanofiber. The material was dried in an oven at 37  $^{\circ}$ C for 36h and sterilized by UV radiation.

## 2.4. *Characterization of the AuNp-Pomegranate + CNF Complex*

### 2.4.1. Transmission Electron Microscopy (TEM)

AuNp-Pomegranate + CNF complex samples were dispersed in water to form a 0.2% suspension, of which a drop was deposited on nickel grids covered with Formvar and dried at room temperature. Samples were observed at 80 kV (JEM-1400, JEOL, USA inc.).

#### 2.4.2. Energy dispersive x-ray (EDS)

The elemental composition of the sample was identified by energy dispersive X-ray spectroscopy (EDS) using a 30 mm liquid nitrogen-based detector (model EDAX). For the EDS analyses – which are built-in features of SEM – the samples were not metallized.

#### 2.4.3. Inductively Coupled Plasma Mass Spectrometry (ICP-MS)

The total concentration of AuNP-Pomegranate adsorbed on the surface of the nanocellulose was determined using ICP-MS (model NEXION300D, USA). The nanocellulose-nanoparticle (NC-NP) solution (1 mL) was added to 1 mL of aqua regia (1 nitric acid (HNO<sub>3</sub>): 3 hydrochloric acid (HCl)) and the mixture allowed to stand for 1 hour. Then, 0.5 mL of the resulting solution was diluted in 9.5 mL of ultrapure water and analyzed by ICP-MS.

#### 2.4.4. Dynamic light scattering (DLS) and zeta potential measurements.

The size distribution and the zeta potential of the particles were determined using dynamic light scattering (DLS) combined with the interaction of random Brownian motion and the electrical field movement of the particle suspensions (NPA152 Zetatrac, Microtrac Instruments, York, PA, USA). Measurements were performed at neutral pH. Each sample was measure in triplicate and the averages reported.

### 2.2 NC-NP antimicrobial activity

#### 2.2.2. Hohenstein challenge test

In this study we used two Gram-positive bacteria [*Staphylococcus aureus* (ATCC 29213) and *Enterococcus faecalis* (ATCC 29212)] and two Gram-negative bacteria [*Escherichia coli* (ATCC 25922) and *Pseudomonas aeruginosa* (clinical sample 64B)] strains.

NC-NP samples were previously sterilized with UV radiation for 15 minutes.

The antimicrobial efficacy of NC-NP was evaluated according to the Hohenstein challenge test (AATCC-100) (Tong et al., 2018). NC-NP samples (0.001 g) were added to 1 mL of nutrient broth containing  $1.0 \times 10^3$  CFU/mL of bacteria (Jafary et al. 2015). The flasks were then incubated at 37 °C, with a rotation speed of

120 rpm for 10 h. After the incubation period, the viable cell count was performed using the drop technique, inoculating 10  $\mu$ L of the sample diluted in nutrient agar. The antimicrobial activity of NC-NP was evaluated by making a plate count of each sample after 12 h. The tests were performed in triplicate. The antimicrobial efficiency of the sample in terms of percentage of growth was determined in relation to the negative control (nanocellulose film without AuNPs).

The percentage of reduction in bacterial colonies was calculated using Equation 3:

$$R(\%) = \left( \frac{A - B}{A} \right) \times 100$$

In which A is the negative control and B the treated sample [18].

### 2.2.3 Transmission Electron Microscopy (TEM)

Samples of NC-NP-treated and untreated bacteria were washed and resuspended with Phosphate Buffer Saline (PBS). A drop of this suspension was deposited on nickel grids covered with Formvar and dried at room temperature. Samples were counterstained for 10 minutes with 0.5% uranyl acetate solution and observed at 80 kV (JEM-1400, JEOL, USA inc.).

## 3. Results and Discussion

### *Physicochemical characterization of AuNP-Pomegranate*

In this study, AuNPs were produced through green synthesis, in which the stabilizing and reducing agent was the pomegranate peel extract. Uniform AuNP formation was initially observed by the color of the solution changing from colorless to pink-red, a color characteristic of surface plasmonic resonance (SPR) emitted by Au<sup>0</sup>. The UV-Vis absorption spectrum showed that the synthesized AuNPs had an absorption peak at 530 nm (Fig. 1). Similar results were reported by Manna et al., who used pomegranate peel alcoholic extract as a reducing agent, obtaining AuNPs with optical spectra with a dominant plasmonic band centered at 525 nm (Manna et al., 2019). The position, intensity, and shape of the surface plasmonic band peak depend on factors such as shape, size, composition, and dielectric constant of the surrounding medium (Haiss et al.,

2007; Martínez et al., 2012). The peak at 373 nm suggests the presence of  $\beta$ -Punicalagin isomers on the surface of AuNPs.  $\beta$ -Punicalagin – an ellagitannin present in pomegranate peels – is a potent antioxidant because of its ability to undergo *in vivo* and *in vitro* hydrolysis (Mehra et al., 2022).

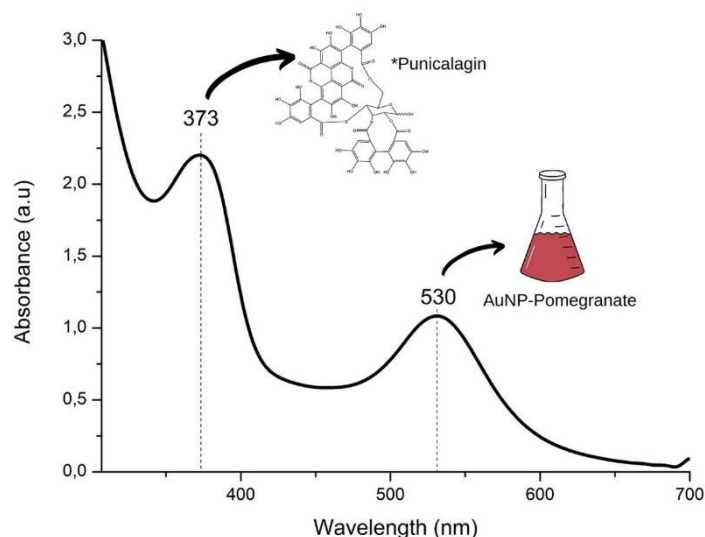


**Fig. 1.** UV-Vis AuNP-Pomegranate absorption spectrum. \*The peak at 373 nm suggests the presence of  $\beta$ -Punicalagin isomers on the surface of AuNPs.

To verify the chemical components and the functional groups present in the AuNP-Pomegranate, Fourier transform infrared (FTIR) measures of the pomegranate peel extract and the colloid extract were performed. There are similarities in the location of some bands of the Pomegranate peel extract and AuNP-Pomegranate spectra and also some differences (Fig. 2). Differences in the position and intensity of the bands between the extract and the AuNP-Pomegranate reflect the interaction of Au ions with the functional groups of the pomegranate coat extract, which lead to the reduction of gold and the formation of a capping layer around the resulting AuNPs (Hussein, et al., 2021). The FTIR spectra of the extract and AuNP-pomegranate show bands representative of functional groups of various compounds available in the pomegranate peel, such as amino acids, phenols, ellagic tannins and esters of gallic and ellagic acid (Table 1) (Goudarzi et al., 2016; Omer et al., 2019).

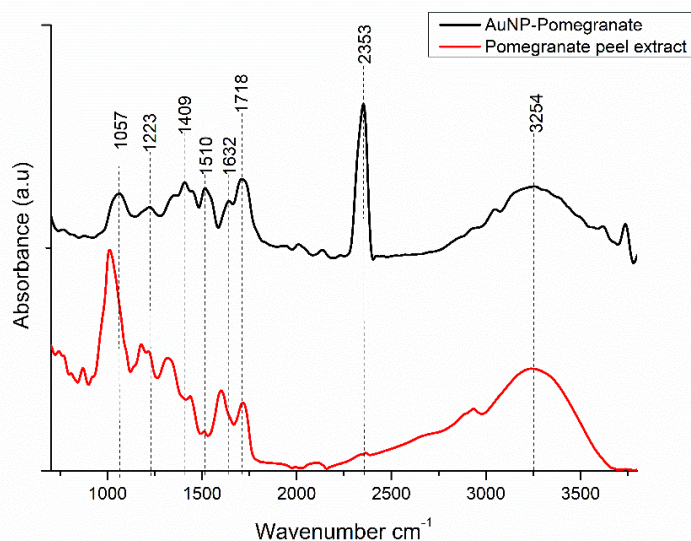


**Fig. 2.** Fourier transform infrared (FTIR) spectra of AuNP-Pomegranate (black) and Pomegranate peel extract (red).

**Table 1.** FTIR spectroscopy interpretation of *P. granatum* plant extracts and AuNP-Pomegranate.

Wavelength cm <sup>-1</sup>	Wavelength cm <sup>-1</sup> (Reference article)	Functional group assignment	Phyto-compounds identified	Reference
3254	3570-3200	O-H stretch, Hydroxy group	Poly Hydroxy compound	Sharif et al., 2020
2353	3500-2400	O-H stretch, Acidic	Carboxylic acids	Sharif et al., 2020; Deepashree et al., 2012
1718	1700-1725	C=O stretch Carbonyl group	Carboxylic acids	Naeem et al., 2020; Gubitosa et al., 2018
1632	1650-1600	C=O stretching vibration, Ketone group	Ketone compound	Sharif et al., 2020
1510	1510-1450	C=C_C, Aromatic ring stretch	Aromatic compound	Sharif et al., 2020; Salem et al., 2017
1409	1390-1420	Aromatic ring vibration	Aromatic compound	Naeem et al., 2020
1223	1250-1020	C-N stretching	Amine	Sharif et al., 2020
1057	1250-1020	C-N stretching	Amine	Sharif et al., 2020

The hydrodynamic size pattern of the nanoparticles was confirmed through DLS analysis, having been found to be 48.40 nm (Fig. 3A). The zeta potential of the AuNPs in water was -30.88 mV, indicating that, when in aqueous solution, AuNPs have a negative charge and the colloidal solution is quite stable, with the particles not easily aggregating (Vinay et al., 2018; Ivanov et al., 2009).

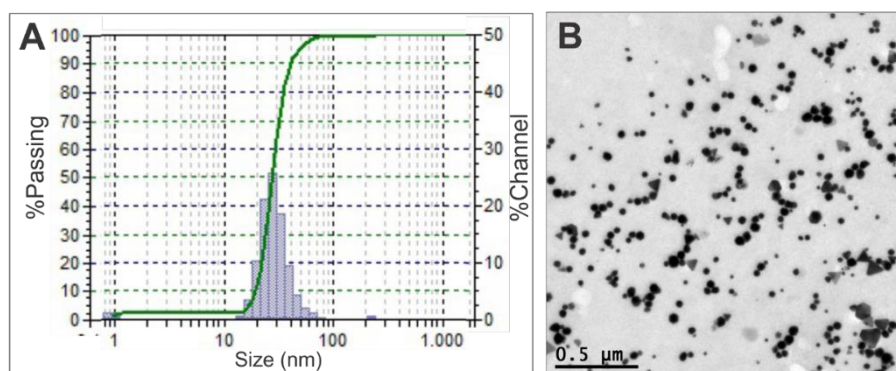


**Fig. 3.** A) DLS of AuNP-Pomegranate. B) Images of the AuNP-Pomegranate obtained by TEM.

The images obtained by TEM revealed that the particles are distributed in a polydisperse way, presenting little variation in size and having, for the most part, an approximately spherical shape, with an average diameter of 20 nm (Fig. 3B).

Nanoparticles of similar appearance, using pomegranate peel alcoholic extract as reducing agent, were synthesized by Manna et al., who obtained mostly round AuNPs, also with an average diameter of 20 nm (Manna et al., 2019). The morphology and composition of nanoparticles are extremely important for the biological application of nanomaterials, since the cellular absorption and toxicity of nanoparticles depend mainly on their size, shape, and surface chemistry (Jin et al., 2013; Albanese et al., 2012).

The ICP-MS analysis showed that the concentration of reduced gold with the green synthesis was 42.70 μg/mL. The concentration of Pomegranate extract present in AuNP was 380 μg/mL, according to the standard curve (Table S1, Fig. S2).



### *Evaluation of the cytotoxicity of AuNP-Pomegranate*

Potential cytotoxic effects of Pomegranate-AuNP were evaluated in L-929 ATCC ® CRL-6364™ normal fibroblasts and HaCat MRC-5 ATCC ® CCL cells, using the MTT colorimetric method. Cells were exposed to different concentrations of nanoparticles and, at the end of treatment, viability was evaluated. The degree of cytotoxicity was analyzed considering the standardized protocol ISO 10993-5 (2009), which considers a substance cytotoxic when cell viability is < 70% in relation to the untreated control. Through the cytotoxicity test, we observed that the AuNPs were not cytotoxic to either of the two strains tested, at any concentration.

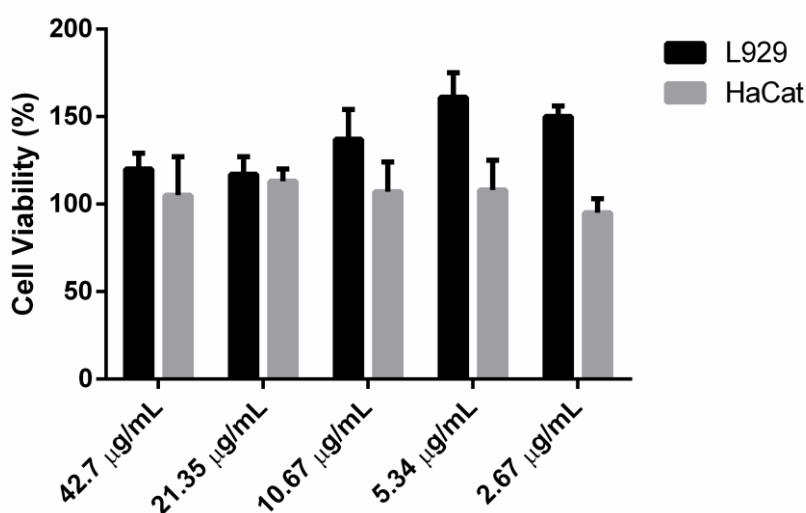


**Fig. 4.** Evaluation of the cytotoxicity of AuNP-Pomegranate.

### *Characterization of the AuNP-Pomegranate +NFC complex*

The CNF TEM images (Fig. 5) show cellulose nanofibers impregnated with AuNPs. The inorganic nanoparticles are homogeneously distributed along the nanofibers, and the content of nanoparticles in the CNF increases with increasing concentrations of AuNPs.

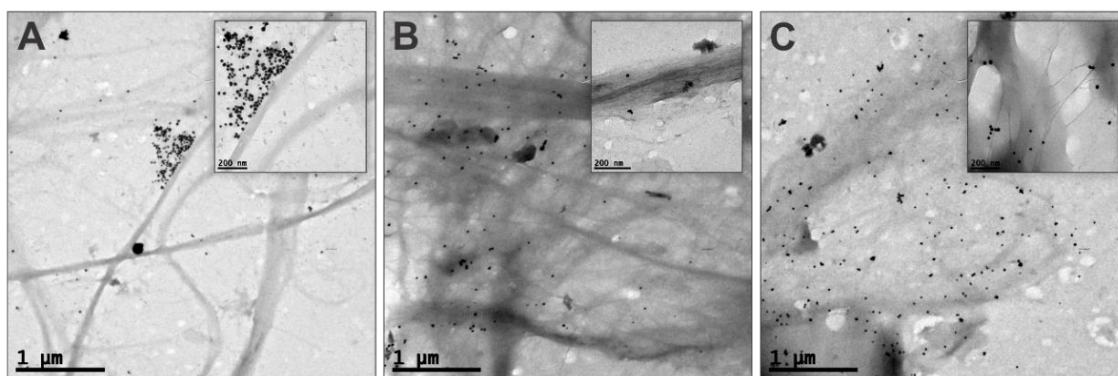


**Fig. 5.** TEM images of CNF impregnated with three different concentrations of AuNP-Pomegranate. A) AuNP-Pomegranate\_C1; B) AuNP-Pomegranate\_C2; C) AuNP-Pomegranate\_C3.

The spectra obtained by EDS of CNF and the AuNP-Pomegranate+CNF complex show the presence of Au only after the complex is formed (Fig. 6 A-D). In the chemical elements distribution map (EDS/SEM) one can observe the dispersion of the elemental components (C, O, and Au) over the complex (Fig. 6E).

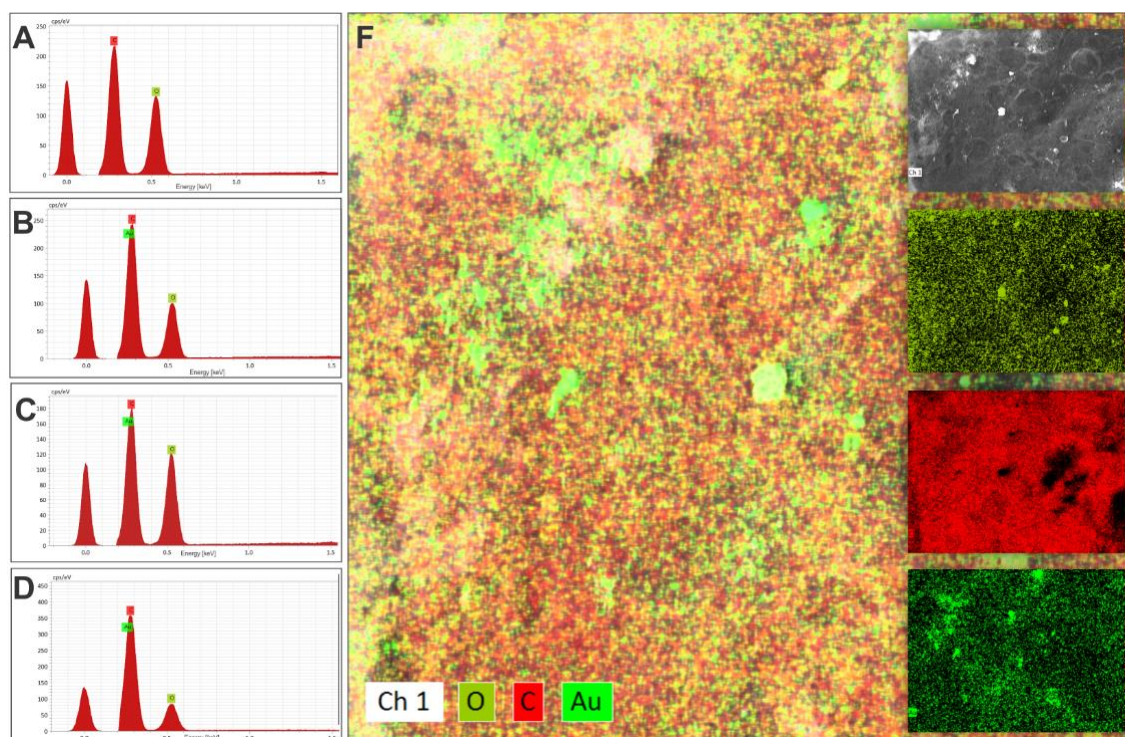


**Fig. 6.** EDS analysis of fibers without AuNP-Pomegranate (A) and with three different concentrations of AuNP (B - AuNP-Pomegranate\_C1; C - AuNP-Pomegranate\_C2; D - AuNP-Pomegranate\_C3). (E) Distribution map of chemical elements (EDS/SEM) present in the AuNP-Pomegranate + CNF complex.

The quantitative analysis of the AuNP content present in the AuNP-Pomegranate + CNF complex was performed by ICP-MS and that of the pomegranate extract content present in the nanofibers by UV-Vis. Table 2 shows the actual amount of

AuNPs and Pomegranate extract present in the AuNP-Pomegranate + CNF complex.

**Table 2.** Analysis of the concentration of Au and pomegranate extract present in the AuNP-Pomegranate + CNF complex.

Sample	Au concentration (µg/mL)	Pomegranate extract concentration (µg/mL)
AuNP-Pomegranate _C1 + CNF	0.77	380
AuNP-Pomegranate _C2 + CNF	0.98	921
AuNP-Pomegranate _C3 + CNF	2.31	1349

The DLS analysis of the AuNP-Pomegranate\_C3 + CNF sample reveals the presence of different populations with different sizes. This is due to AuNP and CNF having different sizes. It is important to note that, although DLS is widely used to obtain the statistical size distribution of suspended nanoparticles, it considers that all particles are spherical, and their sizes therefore depend on the orientation of the suspended nanofibers (Jimenez et al., 2017).

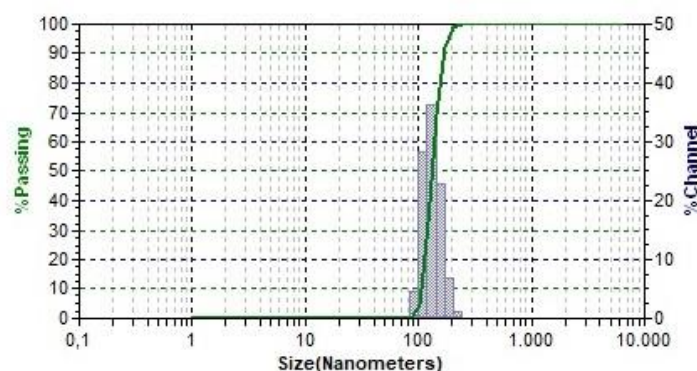


**Fig. 7.** DLS of the AuNP-Pomegranate\_C3 + CNF complex.

#### *Antimicrobial action of the AuNP-Pomegranate + CNF complex*

Because of low toxicity and good biocompatibility, the nanocellulose matrix allows numerous applications related to antibacterial and biomedical materials after being incorporated with antibacterial nanoparticles such as Ag, ZnO, and TiO<sub>2</sub> (Zhang et al., 2020). Despite having greater stability in relation to other metallic nanoparticles, AuNPs have lower antibacterial action. Thus, here we use

pomegranate peel extract not only to reduce and stabilize AuNPs, but also to improve the antibacterial action of these nanoparticles and complex them with CNF. We observed that CNF alone does not induce a significant percentage of CFU reduction in any bacteria (Fig. 8). On the other hand, when AuNP-Pomegranate is added to CNF, forming the AuNP-Pomegranate + CNF complex, excellent antimicrobial activity against *S. aureus*, *E. coli*, and *P. aeruginosa* and low antimicrobial activity against *Enterococcus faecalis* – clinical sample – were achieved. The data obtained are consistent with the results reported by Negi et al. and Prashanth et al. when analyzing the antibacterial activity of pomegranate peel extracts.

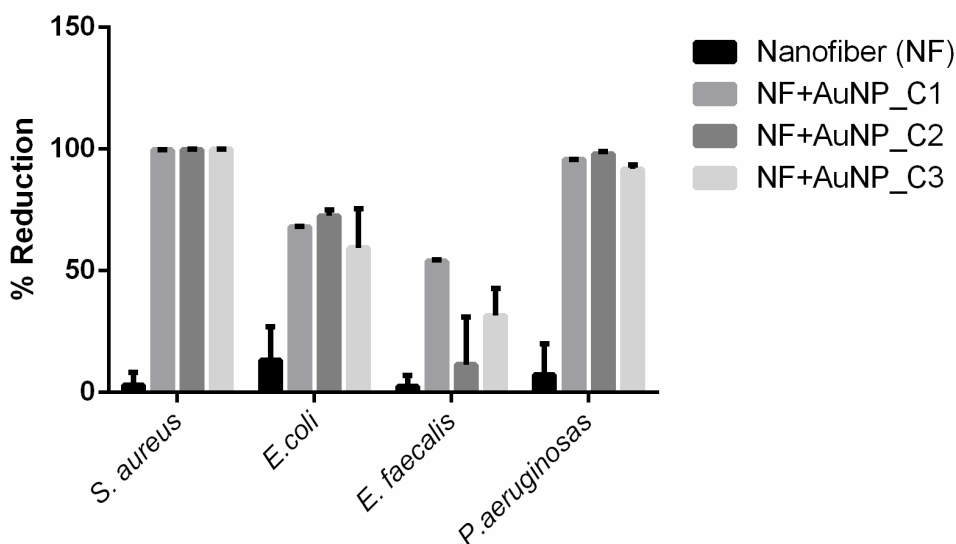


**Fig. 8.** Percentage of reduction in Colony Forming Units (CFU) of *S. aureus*, *E. faecalis*, *E. coli*, and *P. aeruginosa* bacteria, when treated with AuNP-Pomegranate + CNF complex.

The images obtained by TEM show the interaction between the AuNPs present in the AuNP-Pomegranate + CNF complex and the bacteria (Fig. 9).

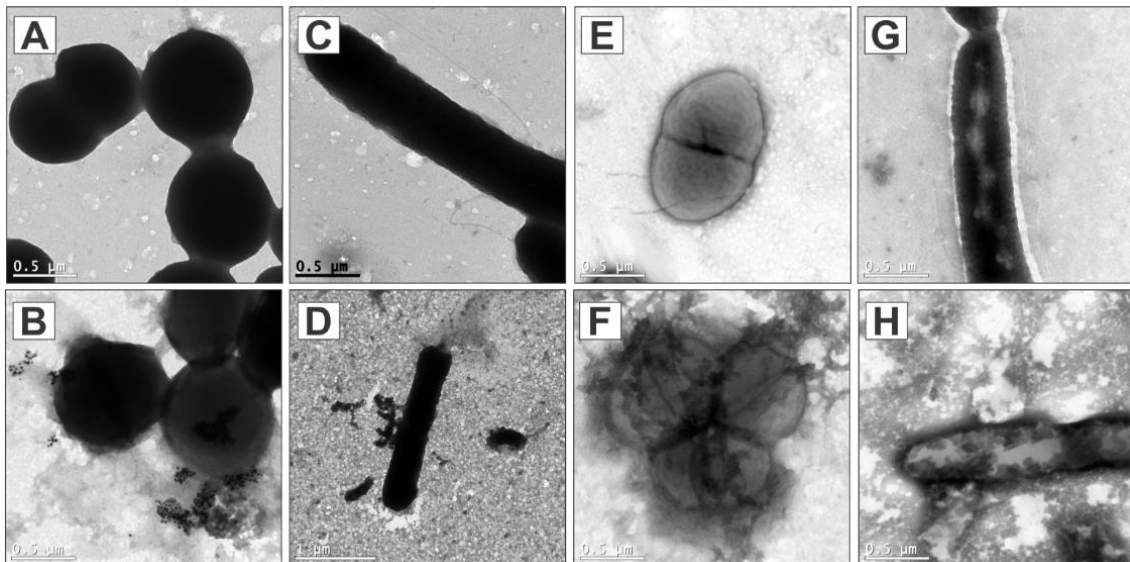


**Fig. 9.** Images obtained by TEM of the interaction between AuNPs present in the AuNP-Pomegranate + CNF complex and bacteria. A) *S. aureus* control; B) *S. aureus* in contact with AuNP-Pomegranate + CNF complex; C) *E. coli* control, D) *E. coli* in contact with AuNP-Pomegranate + CNF complex; E) *E. faecalis* control; F) *E. faecalis* in AuNP-Pomegranate + CNF complex contact; G) *P. aeruginosa* control; F) *P. aeruginosa* in contact with AuNP-Pomegranate + CNF complex.

The antibacterial properties of AuNPs can be attributed to the production of reactive oxygen species that induce oxidative stress within bacterial cells. Thus, compounds formed by the combination of AuNPs with other antibacterial agents aim to enhance the antimicrobial activity of these nanoparticles (Hussein et al., 2021). Pomegranate peel extract is rich in polyphenols, including ellagitannins, phenolic acids, and flavonoids, which have strong antiseptic and antibacterial activity against gram-negative and gram-positive bacteria (Al-Zoreky et al., 2009). Many studies have shown the biological efficacy of *Punica granatum*, such as its potential to inhibit the growth of gram-positive bacteria, especially *S. aureus* (Lokina et al., 2014).

Ellagitannins are the main class of tannins present in pomegranate peel extracts. Punicalagin isomers ( $\alpha$  and  $\beta$ ), ellagic acid, and punicalin are the main ellagitannins found in these extracts (Akhtar et al., 2015; Yan et al., 2017). Pomegranate peel polyphenols display a variety of pharmacological and physiological activities, such as anticancer (Li et al., 2019; Ma et al., 2015),

antioxidant (Zhao et al., 2016; Guo et al., 2007), anti-inflammatory (Glazer et al., 2012; Du et al., 2019) and antibacterial (Sun et al., 2021; Yemis et al., 2019).

Ruan et al. isolated 10 phenolic compounds from pomegranate peel and tested the antimicrobial activity of each of them by disk diffusion against the microorganisms *Candida albicans*, *E. coli*, and *S. aureus*. They observed that only punicalagin, ursolic acid, arjunolic acid, and punicatannin C3 extracted from pomegranate peels showed antimicrobial bioactivity.

Wattrelot et al. suggest that tannins are highly reactive and can readily combine with sulfhydryl (SH) groups of peptidoglycans and, therefore, interact with proteins. Indeed, many microbial enzymes present in culture filtrates were inhibited when mixed with tannins.

Tannins also have a strong ability to bind iron, an element necessary for microbial cells, as they reduce the ribonucleotide precursor of bacterial DNA (Akiyama et al., 2001). In addition, the phenolic groups of these compounds are good hydrogen bond donors and, therefore, can form strong hydrogen bonds with the amide carbonyl groups of peptide chains, which is likely to occur with peptidoglycans of bacterial cell membranes (Hagerman, 1992).

#### **4. Conclusion**

The green synthesis of AuNP-Pomegranate allows not only Au reduction but also confers bioactive properties to AuNPs. We observed that even when complexed with CNF, AuNP-Pomegranate maintains its antimicrobial activity against gram-positive and gram-negative bacteria, whether ATCC or clinical samples. Therefore, our results demonstrate the possibility of using this bioactive and non-cytotoxic nanocomplex in products aimed at the health, textile, and pharmacological areas.

#### **CRedit authorship contribution statement**

**L. P. C. Silva:** Conceptualization, Investigation, Data curation, Methodology, Experiment, Validation, Visualization, Writing-original draft. **N. A. Oliveira:**

Formal analysis, Experiment. **R. S. Valotto:** Experiment, Methodology. **F. C. Monteiro:** Data curation, Investigation. **L. A. Contreras:** Data curation, Investigation, Experiment. **W. J. Keijok:** Methodology, Visualization, Software, Formal analysis. **T. E. C. Zanardo:** Resources, Methodology, Software. **R. Shuenk:** Investigation, Resources, Formal analysis. **J. P. Oliveira:** Methodology, Investigation, Resources. **M. C. C. Guimarães:** Conceptualization, Methodology, Validation, Visualization, Software, Writing—review and Editing, Funding acquisition, Project administration, Resources, Supervision. All authors read and approved the final manuscript.

### **Declaration of competing interest**

The authors declare that they have no known competing financial interests or personal relationships that could have appeared to influence the work reported in this paper.

### **Acknowledgements**

We are grateful for the supports by the Federal University of Espírito Santo, Coordination for the Improvement of Higher Education Personnel (CAPES), and Foundation for Research Support and Innovation of Espírito Santo (FAPES).

### **References**

- [1] Kumari, P., Pathak, G., Gupta, R., et al., 2019. Cellulose nanofibers from lignocellulosic biomass of lemongrass using enzymatic hydrolysis: characterization and cytotoxicity assessment. *DARU J. Pharm. Sci.*, 27, 683–693. <https://doi.org/10.1007/s40199-019-00303-1>.
- [2] Benini, K., Voorwald, H., Cioffi, M., et al., 2018. Preparation of nanocellulose from *Imperata brasiliensis* grass using Taguchi method, *Carbohydr. Polym.*, 192, 337-346. <https://doi.org/10.1016/j.carbpol.2018.03.055>.
- [3] Roig-Sanchez, S., Jungstedt, E., Anton-Sales, I., et al., 2019. Nanocellulose films with multiple functional nanoparticles in confined spatial distribution. *Nanoscale Horiz.*, 4, 634-641. <https://doi.org/10.1039/C8NH00310F>.
- [4] Zhang, Q., Zhang, L., Wu, W., et al., 2020. Methods and applications of nanocellulose loaded with inorganic Nanomater.: a review. *Carbohydr. Polym.*, 229, 115454. <https://doi.org/10.1016/j.carbpol.2019.115454>.
- [5] Bacakova, L., Pajorova, J., Tomkova, M., et al., 2020. Applications of nanocellulose/nanocarbon composites: focus on biotechnology and medicine. *Nanomater.*, 10, 196. <https://doi.org/10.3390/nano10020196>.

- [6] Mokammel, M., Islam, M., Hasanuzzaman, M., et al., 2022. Nanoscale materials for self-cleaning and antibacterial applications, *Encyclopedia of Smart Materials*, 3, 315-324. <https://doi.org/10.1016/B978-0-12-803581-8.11585-1>.
- [7] Naeem, G., Muslim, R., Rabeea, M., et al., 2020. *Punica granatum* L. mesocarp-assisted rapid fabrication of gold nanoparticles and characterization of nano-crystals. *Environ. Nanotechnol. Monit. Manag.*, 14, 100390. <https://doi.org/10.1016/j.enmm.2020.100390>.
- [8] Gad, H., Tayel, A., Al-Saggaf, M., et al., 2021. Phyto-fabrication of selenium nanorods using extract of pomegranate rind wastes and their potentialities for inhibiting fish-borne pathogens. *Green Process. Synth.*, 10, 529–537. <https://doi.org/10.1515/gps-2021-0049>.
- [9] Zhou, J., Hu, Z., Zabihi, F., et al., 2020. Progress and perspective of antiviral protective material, *Adv. Fiber Mater.*, 2, 123–139. <https://doi.org/10.1007/s42765-020-00047-7>.
- [10] Abdalkarim, S., Chen, L.-M., Yu, H.-Y., et al., 2021. Versatile nanocellulose-based nanohybrids: a promising-new class for active packaging applications, *Int. J. Biol. Macromol.*, 182, 1915-1930. <https://doi.org/10.1016/j.ijbiomac.2021.05.169>.
- [11] Zhou, X., Zhao, Z., He, Y., et al., 2018. Photoinduced synthesis of gold nanoparticle-bacterial cellulose nanocomposite and its application for in-situ detection of trace concentration of dyes in textile and paper, *Cellul.*, 25, 3941–3953. <https://doi.org/10.1007/s10570-018-1850-z>.
- [12] Tian, Y., Jia, D., Dirican, M., et al., 2022. Highly soluble and stable, high release rate nanocellulose codrug delivery system of curcumin and AuNPs for dual chemo-photothermal therapy. *Biomacromol.*, 23, 960–971. <https://doi.org/10.1021/acs.biomac.1c01367>.
- [13] Jiang, Q., Ghim, D., Cao, S., et al., 2019. Photothermally active reduced graphene oxide/bacterial nanocellulose composites as biofouling-resistant ultrafiltration membranes. *Environ. Sci. Technol.*, 53, 412–421. <https://doi.org/10.1021/acs.est.8b02772>.
- [14] Nezhad-Mokhtari, P., Akrami-Hasan-Kohal, M., Ghorbani, M., 2020. An injectable chitosan-based hydrogel scaffold containing gold nanoparticles for tissue engineering applications. *Int. J. Biol. Macromol.*, 154, 198–205. <https://doi.org/10.1016/j.ijbiomac.2020.03.112>.
- [15] Ahmad, N., Sharma, S., 2012. Biosynthesis of silver nanoparticles from biowaste pomegranate peels, *Int. J. Nanoparticles*, 5, 185-195. <https://doi.org/10.1504/ijnp.2012.048013>.
- [16] Mosmann, T., 1983. Rapid colorimetric assay for cellular growth and survival: application to proliferation and cytotoxicity assays. *J. Immunol. Methods*, 65, 55–63, [https://doi.org/10.1016/0022-1759\(83\)90303-4](https://doi.org/10.1016/0022-1759(83)90303-4).
- [17] Tong, W., Abdullah, A., Rozman, N., et al., 2018. Antimicrobial wound dressing film utilizing cellulose nanocrystal as drug delivery system for curcumin. *Cellul.*, 25, 631–638. <https://doi.org/10.1007/s10570-017-1562-9>.
- [18] Jafary, R., Mehrizi, M., Hekmatimoghaddam, S., et al., 2015. Antibacterial property of cellulose fabric finished by allicin-conjugated nanocellulose, *J. Text. Inst.*, 106, 683-689. <https://doi.org/10.1080/00405000.2014.954780>.
- [19] Manna, K., Mishra, S., Saha, M., et al., 2019. Amelioration of diabetic nephropathy using pomegranate peel extract-stabilized gold nanoparticles: assessment of NF- $\kappa$ B and Nrf2 signaling system, *Int. J. Nanomedicine*, 14, 1753–1777, <https://doi.org/10.2147/IJN.S176013>.



- [20] Haiss, W., Thanh, N., Aveyard, J., et al., 2007. Determination of size and concentration of gold nanoparticles from UV-Vis spectra. *Anal. Chem.*, 79, 4215-4221. <https://doi.org/10.1021/ac0702084>.
- [21] Martínez, J., Chequer, N., González, J., et al., 2012. Alternative methodology for gold nanoparticles diameter characterization using PCA technique and UV-VIS spectrophotometry. *Nanosci. Nanotechnol.*, 2, 184-189. <https://doi.org/10.5923/j.nn.20120206.06>.
- [22] Mehra, A., Chauhan, S., Jain, V., et al., 2022. Nanoparticles of punicalagin synthesized from pomegranate (*Punica granatum* L.) with enhanced efficacy against human hepatic carcinoma cells. *J. Clust. Sci.*, 33, 349–359. <https://doi.org/10.1007/s10876-021-01979-9>.
- [23] Hussein, M., Grinholc, M., Dena, A., et al., 2021. El-Sherbiny, M. Megahed, Boosting the antibacterial activity of chitosan–gold nanoparticles against antibiotic–resistant bacteria by *Punica granatum* L. extract. *Carbohydr. Polym.*, 256, 117498. <https://doi.org/10.1016/j.carbpol.2020.117498>.
- [24] Goudarzi, M., Mir, N., Mousavi-Kamazani, M., et al. 2016. Biosynthesis and characterization of silver nanoparticles prepared from two novel natural precursors by facile thermal decomposition methods. *Sci. Rep.*, 6, 32539. <https://doi.org/10.1038/srep32539>.
- [25] Omer, H.A.A., Abdel-Magid, S.S., Awadalla, I.M., 2019. Nutritional and chemical evaluation of dried pomegranate (*Punica granatum* L.) peels and studying the impact of level of inclusion in ration formulation on productive performance of growing Ossimi lambs. *Bull. Natl. Res. Cent.*, 43, 182. <https://doi.org/10.1186/s42269-019-0245-0>
- [26] Sharif, M., Ansari, F., Malik, A., et al., 2020. Fourier-Transform Infrared Spectroscopy, Antioxidant, Phytochemical and Antibacterial Screening of N-Hexane Extracts of *Punica granatum*, A Medicinal Plant. *Genet. Mol. Res.*, 19, 1-17.
- [27] Deepashree, C.L., Kumar, J., Prasad, A.G., et al., 2012. FTIR spectroscopic studies on Cleome gynandra –comparative analysis of functional group before and after extraction. *Rom. J. Biophys.*, 22, 137–143.
- [28] Gubitosa, J., Rizzi, V., Lopedota, A., et al., 2018. One pot environmental friendly synthesis of gold nanoparticles using *Punica granatum* juice: a novel antioxidant agent for future dermatological and cosmetic applications. *J. Colloid Interface Sci.*, 521, 50-61. <https://doi.org/10.1016/j.jcis.2018.02.069>.
- [29] Salem, N., Albanna, L., Awwad, A., 2017. Nano-structured zinc sulfide to enhance *Cucumis sativus* (Cucumber) plant growth. *ARPN J. Agric. Biol. Sci.*, 12, 167-173.
- [30] Vinay, C., Goudanavar, P., Acharya, A., 2018. Development and characterization of pomegranate and orange fruit peel extract based silver nanoparticles. *J. Manmohan Mem. Inst. Health Sci.*, 4, 72–85, <https://doi.org/10.3126/jmmihs.v4i1.21146>.
- [31] Ivanov, M., Bednar, H., Haes, A., 2009. Investigations of the mechanism of gold nanoparticle stability and surface functionalization in capillary electrophoresis. *ACS Nano*, 3, 386–394. <https://doi.org/10.1021/nn8005619>.
- [32] Jin, S., Ma, X., Ma, H., et al., 2013. Surface chemistry-mediated penetration and gold nanorod thermotherapy in multicellular tumor spheroids. *Nanoscale*, 5, 143–146, <https://doi.org/10.1039/C2NR31877F>.

- [33] Albanese, A., Tang, P., Chan, W., 2012. The effect of nanoparticle size, shape, and surface chemistry on biological systems. *Annu. Rev. Biomed. Eng.*, 14, 1–16. <https://doi.org/10.1146/annurev-bioeng-071811-150124>.
- [34] Jimenez, A., Jaramillo, F., Hemraz, U., et al., 2017. Effect of surface organic coatings of cellulose nanocrystals on the viability of mammalian cell lines. *Nanotechnol. Sci. Appl.*, 10, 123-136. <https://doi.org/10.2147/NSA.S145891>.
- [35] Negi, P., Jayaprakasha, G., 2003. Antioxidant and antibacterial activities of *Punica granatum* peel extracts. *J. Food Sci.*, 68, 1473-1477. <https://doi.org/10.1111/j.1365-2621.2003.tb09669.x>.
- [36] Prashanth, D., Asha, M., Amit, A., 2001. Antibacterial activity of *Punica granatum*. *Fitoterapia*, 72, 171-173. [https://doi.org/10.1016/s0367-326x\(00\)00270-7](https://doi.org/10.1016/s0367-326x(00)00270-7).
- [37] Al-Zoreky, N., 2009. Antimicrobial activity of pomegranate (*Punica granatum* L.) fruit peels. *Int. J. Food Microbiol.*, 134, 244–248. <https://doi.org/10.1016/j.ijfoodmicro.2009.07.002>.
- [38] Lokina, S., Suresh, R., Giribabu, K., et al., 2014. Spectroscopic investigations, antimicrobial, and cytotoxic activity of green synthesized gold nanoparticles. *Spectrochim. Acta A Mol. Biomol. Spectrosc.*, 129, 484-490. <https://doi.org/10.1016/j.saa.2014.03.100>.
- [39] Akhtar, S., Ismail, T., Fraternali, D., et al., 2015. Pomegranate peel and peel extracts: chemistry and food features. *Food Chem.*, 174, 417–425. <https://doi.org/10.1016/j.foodchem.2014.11.035>.
- [40] Yan, L., Zhou, X., Shi, L., et al., 2017. Phenolic profiles and antioxidant activities of six Chinese pomegranate (*Punica granatum* L.) cultivars. *Int. J. Food Prop.*, 20, S94–S107. <https://doi.org/10.1080/10942912.2017.1289960>.
- [41] Li, J., Wang, G., Hou, C., et al. 2019. Punicalagin and ellagic acid from pomegranate peel induce apoptosis and inhibits proliferation in human HepG2 hepatoma cells through targeting mitochondria. *Food Agric. Immunol.*, 30, 897–912. <https://doi.org/10.1080/09540105.2019.1642857>.
- [42] Ma, G.-Z., Wang, C.-M., Li, L., et al., 2015. Effect of pomegranate peel polyphenols on human prostate cancer PC-3 cells *in vivo*. *J. Food Sci. Biotechnol.*, 24, 1887–1892. <https://doi.org/10.1007/s10068-015-0247-0>.
- [43] Zhao, C., Sakaguchi, T., Fujita, K., et al., 2016. Pomegranate-derived polyphenols reduce reactive oxygen species production via SIRT3-mediated SOD2 activation. *Oxid. Med. Cell. Longev.*, 2016. [https://doi.org/2927131](https://doi.org/10.1155/2016/2927131).
- [44] Guo, S., Deng, Q., Xiao, J., et al., 2007. Evaluation of antioxidant activity and preventing DNA damage effect of pomegranate extracts by chemiluminescence method. *J. Agric. Food Chem.*, 55, 3134–3140. <https://doi.org/10.1021/jf063443g>.
- [45] Glazer, I., Masaphy, S., Marciano, P., et al., 2012. Partial identification of antifungal compounds from *Punica granatum* peel extracts. *J. Agric. Food Chem.*, 60, 4841–4848. <https://doi.org/10.1021/jf300330y>.
- [46] Du, L., Li, J., Zhang, X., et al., 2019. Pomegranate peel polyphenols inhibits inflammation in LPS-induced RAW264.7 macrophages via the suppression of TLR4/NF-κB pathway activation. *Food Nutr. Res.*, 63, 3392. <http://dx.doi.org/10.29219/fnr.v63.3392>.
- [47] Sun, S., Huang, S., Shi, Y., et al., 2021. Extraction, isolation, characterization and antimicrobial activities of non-extractable polyphenols from pomegranate

- peel. Food Chem., 351, 129232. <https://doi.org/10.1016/j.foodchem.2021.129232>.
- [48] Yemis, G., Bach, S., Delaquis, P., 2019. Antibacterial activity of polyphenol-rich pomegranate peel extract against *Cronobacter sakazakii*. Int. J. Food Prop., 22, 985–993. <https://doi.org/10.1080/10942912.2019.1622564>.
- [49] Ruan, J.-H., Li, J., Adili, G., et al., 2022. Phenolic compounds and bioactivities from pomegranate (*Punica granatum* L.) peels. J. Agric. Food Chem., 70, 3678–3686. <https://doi.org/10.1021/acs.jafc.1c08341>.
- [50] Watrelot, A., Schulz, D., Kennedy, J., 2017. Wine polysaccharides influence tannin–protein interactions. Food Hydrocoll., 63, 571–579. <https://doi.org/10.1016/j.foodhyd.2016.10.010>.
- [51] Akiyama, H., Fujii, K., Yamasaki, O., et al., 2001. Antibacterial action of several tannins against *Staphylococcus aureus*. J. Antimicrob. Chemother., 48, 487–491. <https://doi.org/10.1093/jac/48.4.487>.
- [52] Hagerman, A. Tannin-protein interactions, in: C.-T. Ho, C. Lee, M.-T. Huang (Eds.), Phenolic compounds in food and their effects on health I: Analysis, occurrence, and chemistry. American Chemical Society, Washington, 1992: pp. 236–247, 10.102.

## 6. CHAPTER 4 – SMART TEXTILES

### Paper 4. Antibacterial properties of cotton fabric coated with cellulose nanofibers conjugated with pomegranate nanoparticles

Laryssa Pinheiro Costa Silva<sup>1</sup>, Natane Aparecida de Oliveira<sup>1</sup>, Rafaela Spessemille Valotto<sup>1</sup>, Flávio Cunha Monteiro<sup>1</sup>, Luiz Alberto Caldeiras<sup>1</sup>, Letícia Miranda Cesário<sup>1</sup>, Tadeu Ériton Caliman Zanardo, Ricardo Shuenk<sup>2</sup>, Jairo Pinto de Oliveira<sup>1</sup> and Marco Cesar Cunegundes Guimarães<sup>1\*</sup>

<sup>1</sup> Federal University of Espírito Santo, Av Marechal Campos1468, Vitória, ES 29.040-090, Brazil.

\* Corresponding author: [marco.quimaraes@ufes.br](mailto:marco.quimaraes@ufes.br)

#### Abstract

In recent years, the functionalization of textile materials with nanoparticles has become increasingly important because of the demand for high value-added and durable products, having several applications. In this study, we coated a cotton fabric with a bioactive complex composed of cellulose nanofibers and gold nanoparticles synthesized with pomegranate peel extract (CNF+AuNP<sub>Pomegranate</sub>), to improve its functional properties and produce an antibacterial fabric. The physicochemical properties of the CNF+AuNP<sub>Pomegranate</sub> complex (MET, FTIR, and ICP-MS) and the coated fabric (AFM, SEM, and EDS) were analyzed, as well as the antibacterial action of the fabric against *Staphylococcus aureus*, *Escherichia coli*, and *Enterococcus faecalis*. The physicochemical analyses showed that the CNF+AuNP<sub>Pomegranate</sub> complex has fatty acids, phenols, ellagic tannins, and gallic and ellagic acid esters in its composition and is able to adhere to the cotton fabric, giving the surface of the fabric a rougher texture. As for the analysis of antibacterial activity, we verified that the cotton fabric preserved the antibacterial properties of the pomegranate extract and AuNPs. Thus, the application of this nanomaterial in the textile and health industry is feasible.

**Keywords:** Cotton fabric, Pomegranate, Gold nanoparticles, Cellulose nanofibers, Antibacterial activity.

## 1. Introduction

Cotton fiber is a common type of natural fiber, made up of more than 95% cellulose. It is widely used in the textile industry because of its excellent softness, biodegradability, air permeability, hygroscopicity, and comfortable wear (Yang et al. 2020). However, cotton fiber is more sensitive to bacterial colonization than synthetic fibers because it has a hydrophilic porous structure, retains water, and allows the easy diffusion of oxygen and nutrients, providing an ideal environment for bacterial growth. Thus, modification of textile materials – especially cotton fabrics – with antimicrobial substances, is necessary (Jafary et al. 2015).

In recent decades, metallic nanoparticles have attracted great attention in many fields because of their unique optical and electrical properties and good catalytic effects. For antimicrobial purposes, gold nanoparticles (AuNPs) have been of particular interest. These nanoparticles present biocompatibility, ease of surface functionalization, intense plasmonic resonance, and adequate chemical stability both in atmospheric conditions and in living cotton fabrics, being resistant to oxidation (Roy et al. 2016).

The conjugation of AuNPs with other agents such as chitosan, antibiotics, antimicrobial enzymes (lysozyme), and plant extracts (which act both as reducing agents and have antimicrobial effect) is common, as it increases the antimicrobial activity of these nanoparticles in textile composites (Mehravani et al. 2021). Extracts of *Punica granatum L.* have been widely used for the synthesis of AuNP (Gubitosa et al. 2018; Lydia et al. 2020; Naeem et al. 2020). *Punica granatum L.*, commonly known as pomegranate, is a fruit native to the Mediterranean region currently cultivated and consumed throughout the world as fresh fruit, extracted juice, jam, and infusion. It has been used in folk medicine since ancient times and is known for its antioxidant, anti-inflammatory, anticancer, antidiabetic, and antimicrobial properties (Andrade et al., 2019). Pomegranate rinds are particularly rich in hydrolysable tannins such as ellagitannins, flavonoids, lignans, triterpenoids, phytosterols, organic acids, and phenolic acids (Gosset-Erard et al. 2021).

The use of metallic nanoparticles in the coating of textile fibers poses challenges. These nanoparticles usually become thermodynamically unstable and tend to

aggregate because of their large surface area. In addition, there may be electrostatic repulsion between the colloidal particles and textile fibers. Thus, cellulose nanofibers (CNFs) appear as excellent tools to adhere textile fibers to the colloid and stabilize metallic nanoparticles, by promoting the nucleation of nanoparticles and thus preventing their agglomeration (Zhang et al. 2022).

Herein we sought to develop pomegranate-based nanocomposites to improve the functional properties of cotton fabrics. To do so, we produced a bioactive CNF+AuNP<sub>Pomegranate</sub> complex and impregnated cotton fabrics with it. Pomegranate peel extract was used to produce AuNP-Pomegranate and coconut fibers were used to produce cellulose nanofibers. Next, the nanocomposites coated on cotton fabrics were assessed as to their antibacterial nature against *Staphylococcus aureus* (ATCC 29213), *Escherichia coli* (ATCC 25922) and *Enterococcus faecalis* (ATCC 29212) strains.

## 2. Materials and Methods

### 2.1 Synthesis and characterization of the CNF+AuNP<sub>Pomegranate</sub> complex

#### 2.1.1 Pomegranate extract preparation

To obtain the aqueous extract of pomegranate peel, 10 g of crushed peels was added to 50 mL of ultrapure water at 90 °C (Ahmad et al. 2012). The system was kept under orbital agitation (400 rpm) in a round-bottomed flask coupled with a Graham condenser for 20 minutes. The solution was filtered through 0.45 µm quantitative filter paper to remove the husks. The filtrate was submitted to vacuum filtration with a 0.22 µm membrane and reserved for the preparation of AuNP<sub>Pomegranate</sub>.

#### 2.1.2 Synthesis and characterization of AuNP<sub>Pomegranate</sub>

A 100-µL sample of the extract was added to 10 mL of  $2.5 \times 10^{-4}$  mol.L<sup>-1</sup> HAuCl<sub>4</sub> solution (Sigma-Aldrich) at 56 °C and kept under agitation at 400 rpm for 5 minutes. The solution was cooled in an ice bath and the color changed from colorless to pink-red. The formation of AuNPs was confirmed through the spectrum obtained by UV-Vis spectrophotometry (Evolution® 300 ThermoScientific) with a resolution of 1 nm and a sweep of 230-800 nm. The size and morphology of AuNP<sub>Pomegranate</sub> were determined through images obtained by

transmission electron microscopy (JEOL, JEM1400, operating at 120 V with a filament of lanthanum hexaboride (LAB6)).

### 2.1.3 Synthesis and characterization of the CNF+AuNP<sub>Pomegranate</sub> complex

A total of 3.26 g of cellulose extracted from coconut fiber was mixed with 100 mL ultrapure water and 62 g of glass spheres (4 mm) and submitted to ball grinding at 250 rpm in an orbital shaker at 25 °C. After milling, the samples were centrifuged five times at 4000 rpm for 5 minutes. The pellet was lyophilized and stored protected from moisture. Nanofibers (0.001 g) were added to 1 mL of AuNP<sub>Pomegranate</sub> (42.7 µg/mL) and kept under agitation at 150 rpm and 25 °C for 24 h, protected from light. Next, the material was centrifuged twice at 4000 rpm for 5 min and resuspended in ultrapure water to remove possible AuNP<sub>Pomegranate</sub> that did not adhere to CNFs. The material was dried in an oven at 37 °C for 36 h. The adhesion of AuNP<sub>Pomegranate</sub> to CNFs was observed through images obtained by transmission electron microscopy (JEOL, JEM1400, operating at 120 V with a filament of Lanthanum hexaboride (LAB6)). The total concentration of AuNP-Pomegranate present on the surface of CNFs was determined using Inductively Coupled Plasma Mass Spectrometry (ICP-MS – model NEXION300D from Perkin Elmer, model Optima 7000, USA).

### 2.2 Preparation of cotton fabrics coated with CNF+AuNP<sub>Pomegranate</sub> complex

Cotton fabric samples (5×5 mm), previously washed with neutral soap (5gpl) and oven-dried at 50 °C, were sprayed with 0.625 mL of a homogeneous solution of CNF+AuNP<sub>Pomegranate</sub> complex (C1: 2 mg/mL; C2: 1 mg/mL and C3: 0.5 mg/mL). The fabric was then dried at 30 °C for 2 hours.

### 2.3 Characterization of cotton fabrics coated with CNF+AuNP<sub>Pomegranate</sub> complex

#### 2.3.1 Scanning Electron Microscopy - Energy-Dispersive X-ray spectroscopy (SEM-EDX)

The dried samples were analyzed as to the disposition of the CNF+AuNP<sub>Pomegranate</sub> complex on the cotton fabric and elemental composition, by Scanning Electronic Microscopy (ZEISS, EVO MA10) coupled with Energy-Dispersive X-ray spectroscopy (Oxford Instruments-EDX). EDX analyses are

built-in features of SEM. However, for EDX analyses, the samples were not metallized.

### 2.3.2 Atomic Force Microscope (AFM)

The surface of cotton fabrics coated with CNF+AuNP<sub>Pomegranate</sub> complex was analyzed by AFM (AFMAlpha 300 Witec), using a resonance frequency of 300 kHz. The size of the assessed areas was 2 × 2 μm.

## 2.4 Antimicrobial analysis of cotton fabrics

### 2.4.1 Hohenstein challenge test

In this study we used two Gram-positive [*Staphylococcus aureus* (ATCC 29213) and *Enterococcus faecalis* (ATCC 29212)] and one Gram-negative [*Escherichia coli* (ATCC 25922)] bacteria strains. To ensure the sterility of the test, cotton fabric samples were previously autoclaved (121 °C/40 minutes) and the CNF+AuNP<sub>Pomegranate</sub> complex was subjected to UV radiation for 15 minutes. The antimicrobial efficacy of cotton fabrics impregnated with CNF+AuNP<sub>Pomegranate</sub> was evaluated according to the Hohenstein challenge test (AATCC-100) (Tong et al. 2017). Cotton fabric samples impregnated with CNF+AuNP<sub>Pomegranate</sub> complex were added to 1 mL of nutrient broth containing 1.0 × 10<sup>3</sup> CFU/mL of bacteria (Jafary et al., 2015). The flasks were incubated at 37 °C for 10 h, with a rotation speed of 120 rpm. After the incubation period, viable cells were counted using the drop technique, by inoculating 10 μL of the sample diluted in nutrient agar. The antimicrobial activity of the cotton fabrics was evaluated by making a plate count of each sample at 12 h. The tests were performed in triplicate. The antimicrobial efficiency of the sample in terms of percentage of growth was determined in relation to the negative control (cotton fabrics without the complex). The percentage reduction in bacterial colonies was calculated using Equation (1):

$$R(\%) = \left( \frac{A - B}{A} \right) \times 100$$

In which A is the negative control and B the treated sample (Jafary et al. 2015).

### 2.4.2 Scanning electron microscopy (SEM)



Following the antimicrobial test, the control and cotton fabric samples were observed using a scanning electron microscope (ZEISS, EVO MA10) with electronic acceleration varying between 10 and 20 kV.

### **3. Result and discussion**

#### **3.1 Physicochemical characterization of AuNP<sub>Pomegranate</sub> and Cellulose Nanofibers (CNF)**

During the synthesis, the color of the colloid changed from transparent to pink, evidencing the formation of nanoparticles as described by Turkevich et al. 1954. The UV-vis spectrum of AuNP<sub>Pomegranate</sub> is shown in Fig. 1A. AuNP<sub>Pomegranate</sub> exhibit absorbance in the UV region at 530 nm. The spectrum also reveals a peak at 373 nm, which suggests the presence of  $\beta$ -Punicalagin-type ellagitannins on the surface of AuNP<sub>Pomegranate</sub>.  $\beta$ -Punicalagin is widely present in pomegranate peel extracts and is a potent antioxidant because of its ability to undergo hydrolysis in vivo and in vitro (Mehra et al. 2022). The images obtained by TEM show that the AuNP<sub>Pomegranate</sub> are distributed in a polydisperse way, present little variation in size (approximately 20nm), and are mostly spherical, although some particles are shaped as triangles and hexagons (Figure 3B). The ICP-MS analysis showed that the reduced gold concentration obtained using the green synthesis was 42.70  $\mu\text{g/mL}$ .

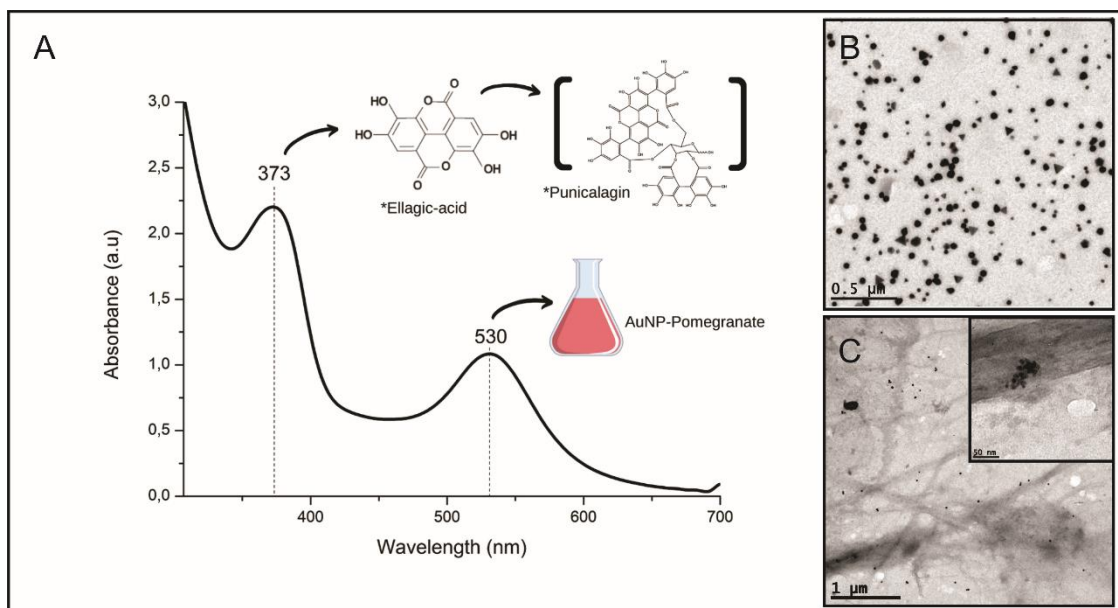


**Figure 1.** A) AuNP<sub>Pomegranate</sub> UV-Vis absorption spectrum. \*Peak at 373 nm suggestive of the presence of punicalagin. B) Images of AuNP<sub>Pomegranate</sub> obtained by transmission electron microscopy (TEM). C) Nanocellulose fibers impregnated with AuNP<sub>Pomegranate</sub>.

TEM images of the CNF+AuNP<sub>Pomegranate</sub> complex depict the AuNP<sub>Pomegranate</sub> adsorbed on the cellulose nanofibers (Figure 1C). One can observe that the inorganic nanoparticles are homogeneously distributed along the nanofibers. The quantitative analysis of the AuNP content in the CNF+AuNP<sub>Pomegranate</sub> complex, performed by ICP-MS, revealed that 1 mg of CNF+AuNP<sub>Pomegranate</sub> contains 0.77 μg of AuNP.

The FTIR spectra (Figure 2) show absorption bands at 876 cm<sup>-1</sup> (referring to O=C=O groups in carboxylic acids) (Salem et al. 2017), 1009 cm<sup>-1</sup> (referring to phosphate ions), 1173 cm<sup>-1</sup> (referring to C-N stretching of amine groups) (Sharif et al. 2020), 1322 - 1435 cm<sup>-1</sup> (referring to vibrations of aromatic rings) (Naeem et al. 2020), 1604 cm<sup>-1</sup> (referring to C=O stretching vibration of ketone groups) (Sharif et al. 2020), 2353 - 2930 cm<sup>-1</sup> (referring to O-H stretching of carboxylic acids) (Deepashree et al. 2012), and 3245 cm<sup>-1</sup> (referring to O-H stretching of Hydroxyl groups present in polyhydroxy compounds) (Sharif et al. 2020). The bands that appear in the FT-IR spectra of the pomegranate peel extract, AuNP<sub>Pomegranate</sub>, and CNF+AuNP<sub>Pomegranate</sub> complex are representative of functional groups of several compounds available in the pomegranate peel, such as phenols, ellagic tannins, and esters of gallic and ellagic acid (Goudarzi et al.2021).

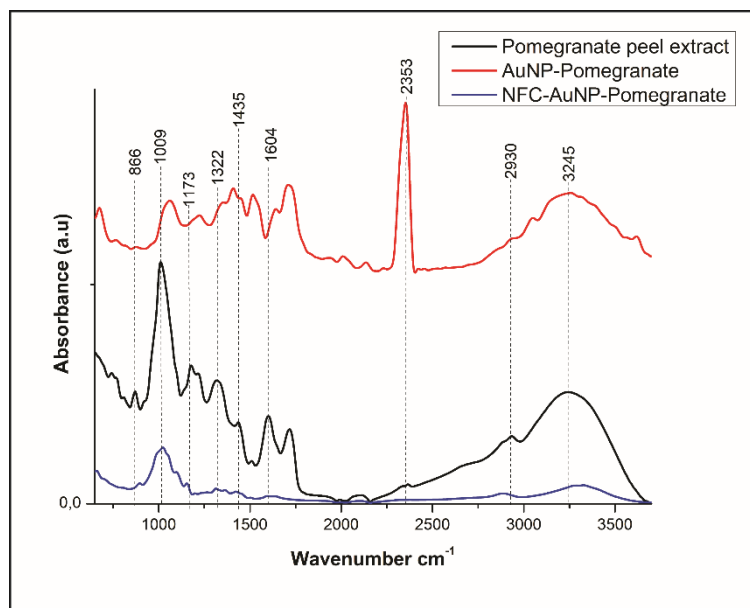


**Figure 2.** Fourier transform infrared (FTIR) of pomegranate peel extract (black), AuNP<sub>Pomegranate</sub> (red), and CNF+AuNP<sub>Pomegranate</sub> complex (blue).

### 3.1 Characterization of cotton fabrics with Cellulose Nanofibers (CNF) and CNF+AuNP<sub>Pomegranate</sub> complex

The surface morphology of cotton fabrics with and without the CNF+AuNP<sub>Pomegranate</sub> complex was observed by SEM (Figure 2A-B). The untreated cotton fabric has a typical longitudinal fibrillar structure, with a natural twist and some grooves on its surface (Figure 3A). After coating with CNF+AuNP<sub>Pomegranate</sub>, the surface of the cotton fiber tends to be smoother because of the formation of a covering film on the surface of the cotton fiber (Figure 3B). This film is due to the presence of cellulose nanofiber. In fact, Yang et al 2020 found similar morphological results regarding the presence of nanocellulose on cotton fabrics and observed that as the nanocellulose size increases, the surface of the film becomes rougher because of the aggregation of particles. The EDS spectra of the cotton fabric and the fabric with the CNF+AuNP<sub>Pomegranate</sub> complex show the presence of Au only in the latter (Figure 3 C-F), thus indicating the presence of AuNP<sub>Pomegranate</sub> on the surface of the fabric.

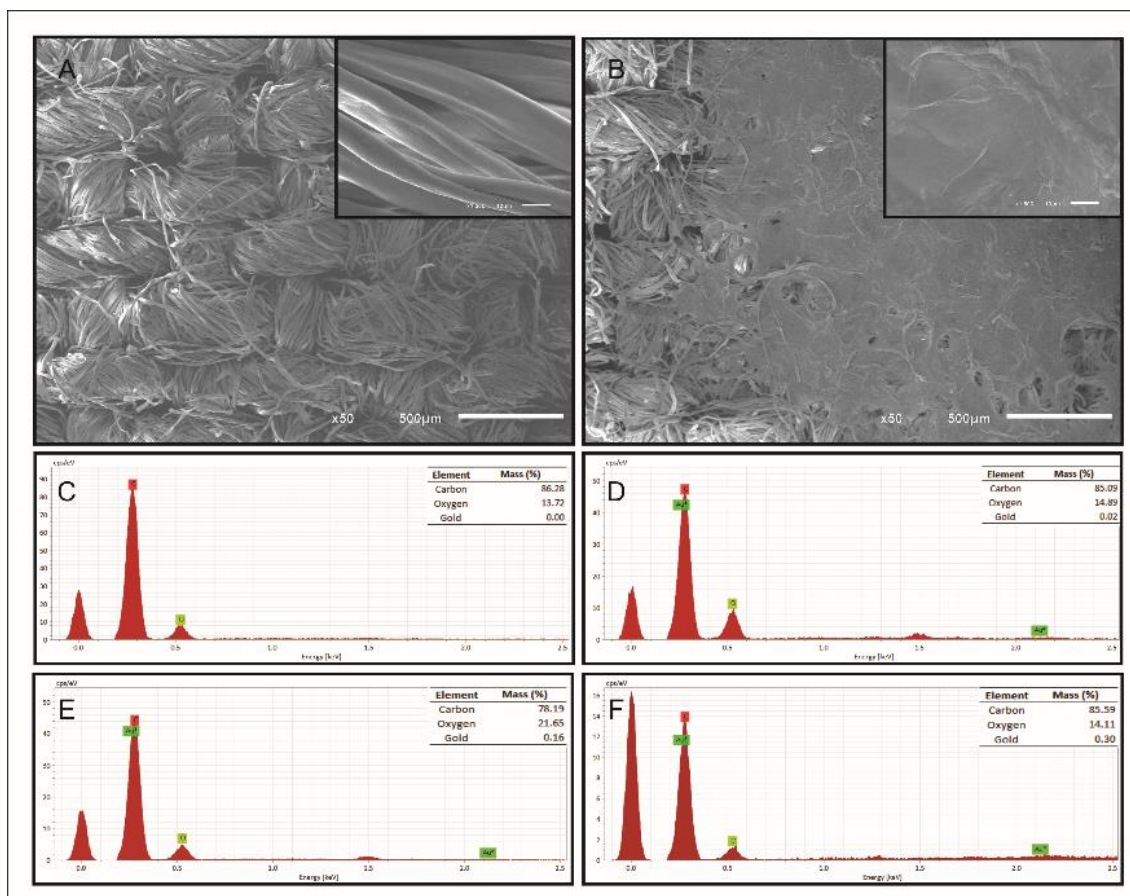


**Figure 3.** SEM images of the cotton fabric (A) and the cotton fabric with CNF+AuNP<sub>Pomegranate</sub> (B). EDS analysis of the cotton fabric without CNF+AuNP<sub>Pomegranate</sub> (C) and with three different concentrations of CNF+AuNP<sub>Pomegranate</sub> (D – 2 mg/mL CNF+AuNP<sub>Pomegranate</sub>; E – 1 mg/ CNF+AuNP<sub>Pomegranate</sub>; F – 0.5 mg/mL CNF+AuNP<sub>Pomegranate</sub>).

To analyze the cotton fabric surface before and after the addition of the CNF+AuNP<sub>Pomegranate</sub> complex, we used topography and phase contrast images obtained by AFM (Figure 4). Topography images and cotton fabric cross-sectional roughness profiles obtained before and after addition of the CNF+AuNP<sub>Pomegranate</sub> complex are shown in Figure 4 A-C. The addition of CNF (Figure 4B) and the CNF+AuNP<sub>Pomegranate</sub> complex (Figure 4C) clearly reduces the depth of naturally existing valleys in the cotton fabric, thus demonstrating the formation of a film on the cotton fabric. However, these images alone do not establish whether the CNF film and the CNF+AuNP<sub>Pomegranate</sub> complex are chemically different. Thus, for a better understanding of the surface, phase contrast images were analyzed (Figure 4D-F).

On a surface with uniform composition, the resulting phase contrast image corresponds to variations in surface friction. However, when surface composition is variable, the phase contrast includes information about such variations, friction, and topographic adhesion (Pang et al 2000; Ye et al. 2010; Kim et al. 1992). As expected, the phase contrast image of the untreated cotton fabric (Figure 4C) does not add any information to the topographic image, because the surface of the material is relatively smooth. However, in the image of the cotton fabric treated with CNF (Figure 4E) and CNF+AuNP<sub>Pomegranate</sub> complex (Figure 4F), the phase contrast revealed fine details of rough surfaces, which are normally obscured in topographical images. This is because the phase contrast in these materials can be attributed to the greater adhesion of the tip in a region of greater contact area, such as grain boundary or triple junction step (Pang et al 2000). Figures 4 D-F show phase contrast images of uncoated cotton fabric, fabric coated with CNF, and with CNF+AuNP<sub>Pomegranate</sub> complex. Figures 4 E-F show the phase difference with slight darkening, in relation to the untreated cotton fabric (Figure 4D), which is probably determined by the roughness of the film. As can be seen in figures 4 E-F, the addition of CNF+AuNP<sub>Pomegranate</sub> makes the image darker, which indicates a significant change in the phase of the probe's oscillation. This is the result of gold having 73 more electrons than carbon atoms, so the interaction potential of the probe's atoms with these two elements is significantly different, which leads to a sharp contrast in the image. This contrast depends on the phase shift of the probe's oscillation, which depends directly on the energy of the dissipative interaction of the probe with the sample according to the law  $\sin(\varphi) \sim E/\pi kA$ , in which E is the energy that compensates for the losses during the dissipative interaction, A and k are the amplitude of the cantilever oscillations and the Boltzmann constant, respectively (Ryaguzov et al. 2022).

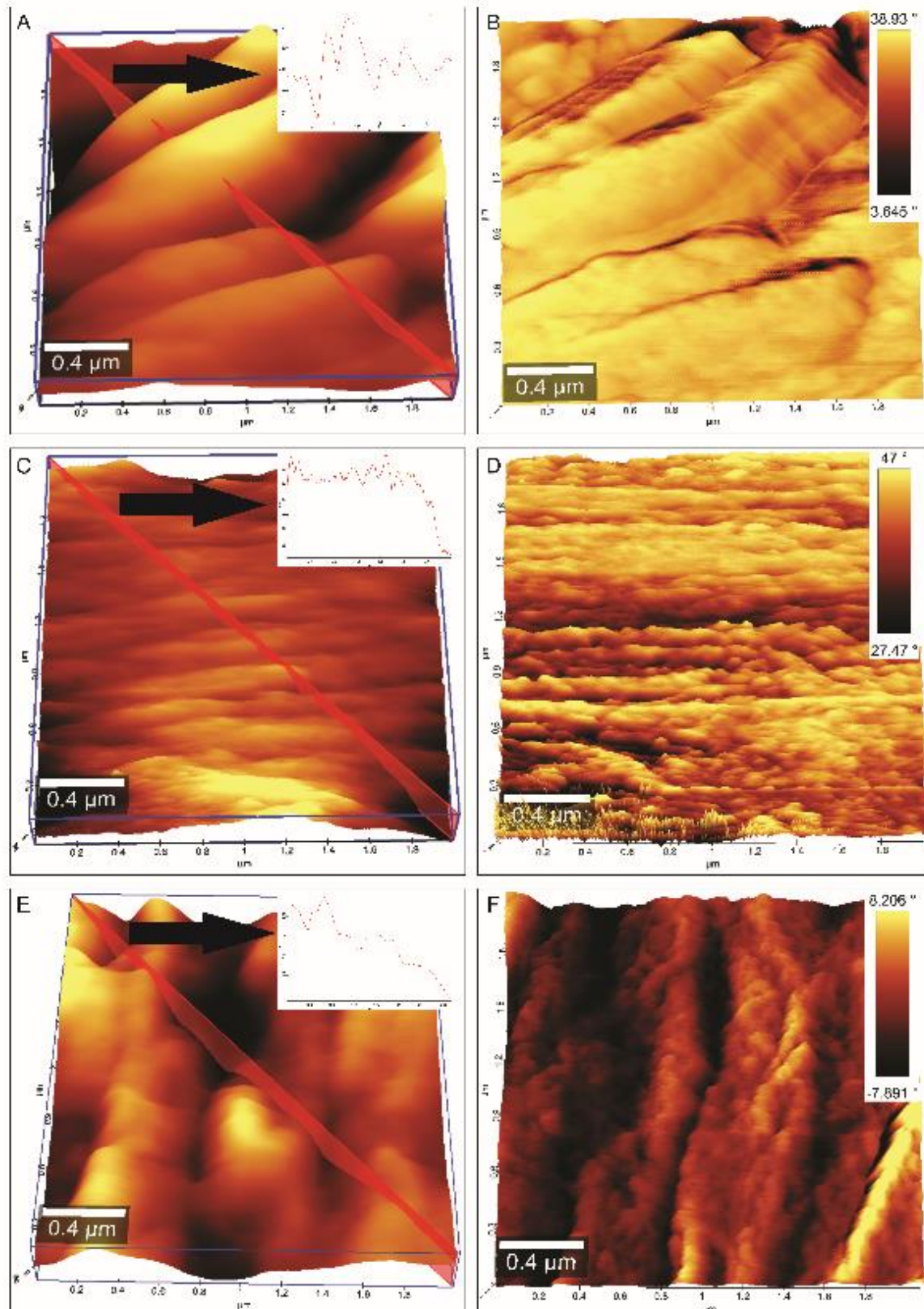
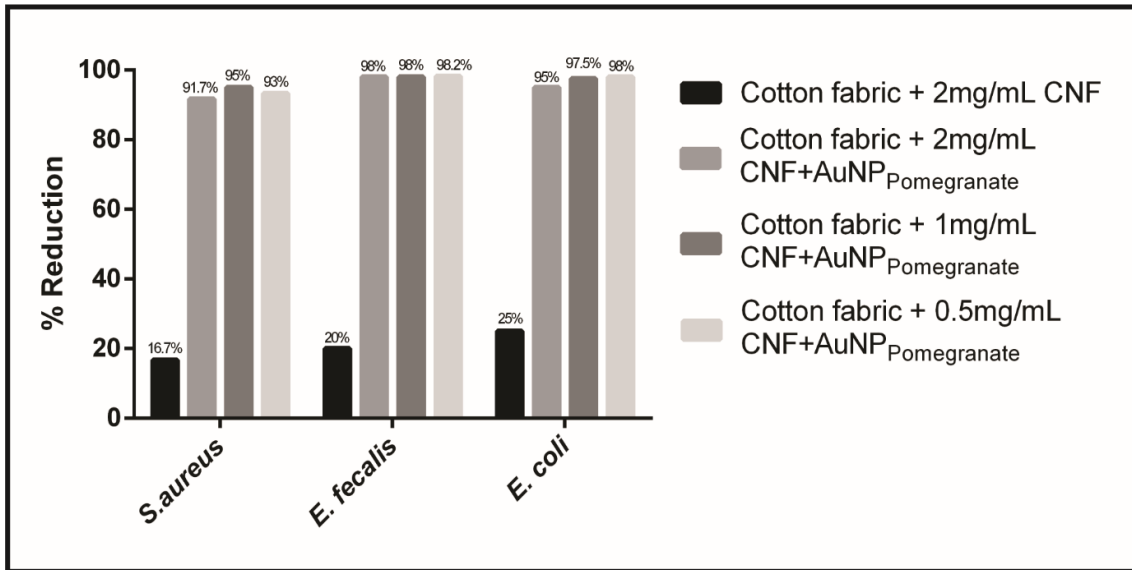


Figure 4. Topography and roughness (insert) AFM images of the cotton fabric surface cross section. a) Untreated cotton fabric, b) after the addition of CNF, and c) after the addition of the CNF+AuNP<sub>Pomegranate</sub> complex. Cotton fabric surface phase contrast AFM images. d) Untreated cotton fabric, e) after the addition of CNF, and d) after the addition of the CNF+AuNP<sub>Pomegranate</sub> complex.

### *3.2 Analysis of the antimicrobial action of cotton fabrics coated with the CNF+AuNP<sub>Pomegranate</sub> complex*

The antibacterial activities of cotton fabrics coated with CNF and CNF+AuNP<sub>Pomegranate</sub> complex are shown in Figure 5. As expected, there was a significant reduction of bacterial growth in cotton fabric coated with CNF+AuNP<sub>Pomegranate</sub> complex in relation to cotton fabric coated only with CNF. This is the result of the complex having AuNP<sub>Pomegranate</sub>, which, as shown in Figures 1A and 2, present on their surface phytochemical compounds such as phenols, ellagic tannins, and esters of gallic and ellagic acid derived from the pomegranate peel extract. Among the ellagic tannins, punicalagin  $\alpha$  and  $\beta$  – phenolic compounds formed by multiple esters of gallic acid and glucose – stand out. These compounds are known for their antioxidant, antimicrobial, and anti-inflammatory properties (Foss et al., 2014; Kharchoufi et al., 2018; Pagliarulo et al., 2016). Gallic acid, also identified on the surface of AuNP<sub>Pomegranate</sub>, has antibacterial action as well. Rattanata et al. 2016 observed that AuNP-gallic acid adhere to and penetrate the bacterial cell wall, disrupting the cellular environment and leading to cell lysis due to leakage of cellular components. A careful observation of the results obtained here revealed no statistically significant differences among fabrics coated with different concentrations of the CNF+AuNP<sub>Pomegranate</sub> complex.



**Figure 5.** Reduction percentage in Colony Forming Units (CFU) of *S. aureus*, *E. faecalis*, and *E. coli* bacteria, when treated with cotton fabric + CNF and cotton fabric + CNF+AuNP<sub>Pomegranate</sub> complex.

Images obtained by SEM (Figure 6) show that the bacterial membrane was wrinkled and damaged after direct contact with the cotton fabric impregnated with CNF+AuNP<sub>Pomegranate</sub> complex for 12 hours (Figure 6 D-F). AuNPs exhibit intense electrostatic attraction to the bacterial wall, accumulate on cell surfaces, and interact with the cell membrane (Shaikh et al. 2019). Thus, the phenolic compounds present in AuNP<sub>Pomegranate</sub> can penetrate the bacterial membrane and promote bacterial lysis (Moreno et al. 2006).



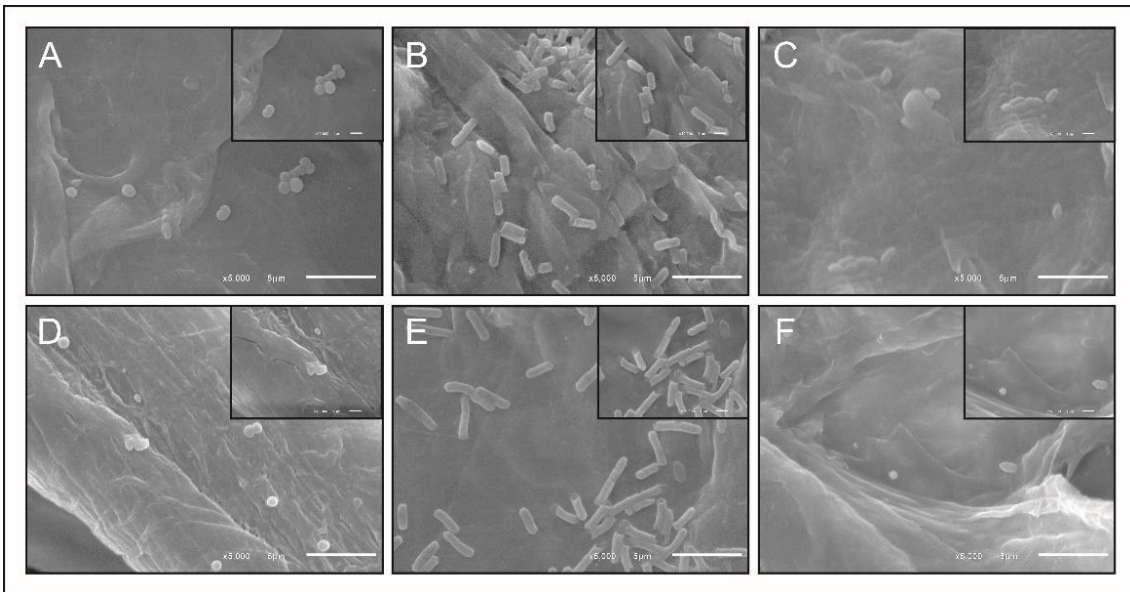


Figure 6. SEM images of cotton fabrics impregnated with CNF alone: a) *S. aureus*, b) *E. coli*, and c) *E. faecalis*; and cotton fabrics impregnated with the CNF+AuNP<sub>Pomegranate</sub> complex: d) *S. aureus*, e) *E. coli*, and f) *E. faecalis*.

#### 4. Conclusion

The CNF+AuNP<sub>Pomegranate</sub> complex successfully coated the fibers of cotton fabrics. Cotton fabrics coated with CNF+AuNP<sub>Pomegranate</sub> complex showed antimicrobial activity against *S. aureus*, *E. coli*, and *E. faecalis*. Thus, one can conclude that the medicinal property of Pomegranate can be transferred to textile fabrics via CNF+AuNP<sub>Pomegranate</sub> coating on the surface. Antimicrobial textiles have diverse applications, such as in health and hygiene products, infection control, and as barrier materials. They can, therefore, be applied in biomedical and textile industries.

#### Acknowledgment

The authors would like to thank LabPetro (UFES, Brazil) for performing FTIR, UV-Vis, Fluorescence measurements (Technical Cooperation Agreements nos. 0050.0022844.06.4), and XRD measurements (Technical Cooperation Agreements nos. CT-Infra 01/2007-FINEP 0202/08).

#### Declaration of interests

The authors declare that they have no known competing financial interests or personal relationships that could have appeared to influence the work reported in this paper.

### Disclosure statement

No potential conflict of interest was reported by authors.

### References

- Ahmad, N., Sharma, S., Rai, R. Rapid green synthesis of silver and gold nanoparticles using peels of *Punica granatum*. *Advanced materials letters*, 3 (5), 1-13.
- Andrade, M. A., Lima, V., Sanches Silva, A., Vilarinho, F., Castilho, M. C., Khwaldia, K., Ramos, F. (2019). Pomegranate and grape by-products and their active compounds: Are they a valuable source for food applications? *Trends in Food Science & Technology*, 86, 68–84. <https://doi.org/10.1016/j.tifs.2019.02.010>
- Deepashree, C. L., Kumar, J., Prasad, A. G., Zarei, M., Gopal, S. (2012). FTIR spectroscopic studies on *Cleome gynandra* –comparative analysis of functional group before and after extraction. *Romanian Journal of Biophysics*, 22, 137–143.
- Foss, S. R., Nakamura, C. V., Ueda-Nakamura, T., Cortez, D. A., Endo, E. H., Dias Filho, B. P. (2014). Antifungal activity of pomegranate peel extract and isolated compound punicalagin against dermatophytes. *Annals of Clinical Microbiology and Antimicrobials*, 13 (32), 1-6. <https://doi.org/10.1186/s12941-014-0032-6>
- Gosset-Erard, C., Zhao, M., Lordel-Madeleine, S., Ennahar, S. (2021). Identification of punicalagin as the bioactive compound behind the antimicrobial activity of pomegranate (*Punica granatum* L.) peels. *Food chemistry*, 352, 129396. <https://doi.org/10.1016/j.foodchem.2021.129396>
- Goudarzi, M., Mir, N., Mousavi-Kamazani, M., Bagheri, S., Salavati-Niasari, M. (2016). Biosynthesis and characterization of silver nanoparticles prepared from two novel natural precursors by facile thermal decomposition methods. *Scientific Reports*, 6, 32539, <https://doi.org/10.1038/srep32539>
- Gubitosa, J., Rizzi, V., Lopodota, A., Fini, P., Laurenzana, A., Fibbi, G., Fanelli, F., Petrella, A., Laquintana, V., Denora, N., Comparelli, R., Cosma, P. (2018). One pot environmental friendly synthesis of gold nanoparticles using *Punica Granatum* Juice: A novel antioxidant agent for future dermatological and cosmetic applications. *Journal of Colloid and Interface Science*, 521, 50-61. <https://doi.org/10.1016/j.jcis.2018.02.069>
- Jafary, R., Mehrizi, M., Hekmatimoghaddam, S., Jebali, A. (2015). Antibacterial property of cellulose fabric finished by allicin-conjugated nanocellulose. *The*

*Journal of The Textile Institute*, 106, 683-689.  
<https://doi.org/10.1080/00405000.2014.954780>

Kharchoufi, S., Licciardello, F., Siracusa, L., Muratore, G., Hamdi, M., Restuccia, C. (2018). Antimicrobial and antioxidant features of 'Gabsi' pomegranate peel extracts. *Industrial Crops and Products*, 111, 345–352.  
<https://doi.org/10.1016/j.indcrop.2017.10.037>

Kim, Y., Lieber, C. M. (1992). Machining Oxide Thin Films with an Atomic Force Microscope: Pattern and Object Formation on the Nanometer Scale. *Science*, 257 (5068), 375-377. <https://doi.org/10.1126/science.257.5068.375>

Lydia, D. E., Khusro, A., Immanuel, P., Esmail, G. A., Al-Dhabi, N. A., Arasu, M. V. (2020). Photo-activated synthesis and characterization of gold nanoparticles from *Punica granatum* L. seed oil: An assessment on antioxidant and anticancer properties for functional yoghurt nutraceuticals. *Journal of Photochemistry and Photobiology B: Biology*, 206, 111868.  
<https://doi.org/10.1016/j.jphotobiol.2020.111868>

Mehra, A., Chauhan, S., Jain, V., Nagpal, S. (2022). Nanoparticles of punicalagin synthesized from pomegranate (*Punica granatum* L.) with enhanced efficacy against human hepatic carcinoma cells, *Journal of Cluster Science*, 33, 349–359.  
<https://doi.org/10.1007/s10876-021-01979-9>

Mehravani, B., Ribeiro, A. I., Zille, A. (2021). Gold Nanoparticles Synthesis and Antimicrobial Effect on Fibrous Materials. *Nanomaterials (Basel, Switzerland)*, 11(5), 1067. <https://doi.org/10.3390/nano11051067>

Moreno, S., Scheyer, T., Romano, C. S., Vojnov, A. A. (2006). Antioxidant and antimicrobial activities of rosemary extracts linked to their polyphenol composition. *Free radical research*, 40(2), 223–231.  
<https://doi.org/10.1080/10715760500473834>

Naeem, G. A., Muslim, R. F., Rabeea, M. A., Owaid, M. N., Abd-Alghafour, N. M. (2020). *Punica granatum* L. mesocarp-assisted rapid fabrication of gold nanoparticles and characterization of nano-crystals. *Environmental Nanotechnology, Monitoring & Management*, 14, 100390.  
<https://doi.org/10.1016/j.enmm.2020.100390>

Pagliarulo, C., De Vito, V., Picariello, G., Colicchio, R., Pastore, G., Salvatore, P., Volpe, M. G. (2016). Inhibitory effect of pomegranate (*Punica granatum* L.) polyphenol extracts on the bacterial growth and survival of clinical isolates of pathogenic *Staphylococcus aureus* and *Escherichia coli*. *Food Chemistry*, 190, 824–831. <https://doi.org/10.1016/j.foodchem.2015.06.028>

Pang, G. K. H., Baba-Kishi, K. Z., Patel, A. (2000). Topographic and phase-contrast imaging in atomic force microscopy. *Ultramicroscopy*, 81 (2), 35-40.  
[https://doi.org/10.1016/S0304-3991\(99\)00164-3](https://doi.org/10.1016/S0304-3991(99)00164-3)

Rattanata, N., Klaynongsruang, S., Leelayuwat, C., Limpai boon, T., Lulitanond, A., Boonsiri, P., Chio-Srichan, S., Soontaranon, S., Rugmai, S., Daduang, J. (2016). Gallic acid conjugated with gold nanoparticles: antibacterial activity and mechanism of action on foodborne pathogens. *International Journal of Nanomedicine*, 27(11), 3347-3356. <https://doi.org/10.2147/IJN.S109795>

- Roy, S., Das, T.K., Maiti, G.P., Basu, U. (2016). Microbial Biosynthesis of Nontoxic Gold Nanoparticles. *Materials Science & Engineering B*, 203, 41–51.
- Ryaguzov, A. P., Assembayeva, A. R., Myrzabekova, M. M., Nemkayeva, R. R., Guseinov, N. R. (2022). Study of the influence of palladium nanoparticles on the structure of DLC films synthesized on silicon (100) substrates. *Diamond and Related Materials*, 126, 109125. <https://doi.org/10.1016/j.diamond.2022.109125>
- Salem, N., Albanna, L., Awwad, A. (2017). Nano-structured zinc sulfide to enhance Cucumis sativus (Cucumber) plant growth. *ARP Journal of Agricultural and Biological Science*, 12, 167-173.
- Shaikh, S., Nazam, N., Rizvi, S. M. D., Ahmad, K., Baig, M. H., Lee, E. J., Choi, I. (2019). Mechanistic Insights into the Antimicrobial Actions of Metallic Nanoparticles and Their Implications for Multidrug Resistance. *International Journal of Molecular Sciences*, 20(10), 2468. <https://doi.org/10.3390/ijms20102468>
- Sharif, M., Ansari, F., Malik, A., Ali, Q., Hasan, Z., Khan, N.U.H. (2020). Fourier-Transform Infrared Spectroscopy, Antioxidant, Phytochemical and Antibacterial Screening of N-Hexane Extracts of Punica granatum. *A Medicinal Plant, Genetics and Molecular Research*, 19, 1-17.
- Tong, W., Abdullah, A., Rozman, N., Wahid, M., Hossain, M., Ring, L., Lazim, Y., Tan, W.-N. (2018). Antimicrobial wound dressing film utilizing cellulose nanocrystal as drug delivery system for curcumin, *Cellulose*, 25, 631–638, <https://doi.org/10.1007/s10570-017-1562-9>
- Turkevich, J., Garton, G., Stevenson, P. C. (1954). The color of colloidal gold. *Journal of Colloid Science*, 9, 26–35.
- Yang, X., Wang, Z., Zhang, Y., Liu, W. (2020). A Biocompatible and Sustainable Anti-ultraviolet Functionalization of Cotton Fabric with Nanocellulose and Chitosan Nanocomposites. *Fibers and Polymers*, 21, 2521–2529. <https://doi.org/10.1007/s12221-020-1339-x>
- Ye, Z., Zhao, X. (2010). Phase imaging atomic force microscopy in the characterization of biomaterials. *Journal of Microscopy*, 238 (1), 27-35. <https://doi.org/10.1111/j.1365-2818.2009.03282.x>
- Zhang, Q., Zhang, L., Wu, W., Xiao H. (2020). Methods and applications of nanocellulose loaded with inorganic nanomaterials: A review. *Carbohydrate Polymers*, 229, 115454. <https://doi.org/10.1016/j.carbpol.2019.115454>

## 7. Conclusions and future prospects

Using the DOE statistical tool, we determined the ideal condition for extracting cellulose from coconut fibers and producing nanocellulose.

The present work elaborated a cellulose extraction route using low amounts of chemical reagents and produced nanocellulose without chemical reagents, thus obtaining an ecologically correct product that can be functionalized with other nanomaterials with known biological activity.

Non-cytotoxic gold nanoparticles obtained by green synthesis with pomegranate peel extract (AuNP-Pomegranate) with antibacterial activity, as described in previous studies carried out by our research group (data not shown), were used.

AuNP-Pomegranate were able to adhere to cellulose nanofibers, forming the nanocomplex CNF+ AuNP-Pomegranate. In addition, these nanoparticles conferred antibacterial action to the nanocomplex, mainly against strains of *S. aureus* and *P. aeruginosa*.

The nanocomplex produced successfully adhered to cotton fabric fibers, conferring antibacterial action to the fabric.

The smart fabric produced here validates a new approach to manufacture smart fabrics that can be applied in healthcare, such as in the production of Personal Protective Equipment -PPE-, hospital bedding, and anti-odor clothing.

## References

Abdelmonema, A.M.; Aminb, R.M. Rapid Green Synthesis of Metal Nanoparticles using Pomegranate Polyphenols. **International Journal of Sciences:Basic and Applied Research**, 15 (1), 57-65, 2014.

Abouzeid, R. E.; Khiari, R.; El-Wakil, N.; Dufresne, A. Current State and New Trends in the Use of Cellulose Nanomaterials for Wastewater Treatment. **Biomacromolecules**, 20, 2, 573–597, 2019. DOI: 10.1021/acs.biomac.8b00839.

Abral, H.; Ariksha, J.; Mahardika, M.; Handayani, D.; Aminah, I.; Sandrawati, N.; Pratama, A. B.; Fajri, N.; Sapuan, S. M.; Ilyas, R. A. Transparent and antimicrobial cellulose film from ginger nanofiber. **Food Hydrocolloids**, 98, 105266, 2020. DOI: 10.1016/j.foodhyd.2019.105266.

Albinante, S. R.; Pacheco, E. B. A. V.; Visconte, L. L. Y.; Tavares, M. I. B. Caracterização de fibras de bananeira e de coco por ressonância magnética nuclear de alta resolução no estado sólido. **Polímeros**, 22(5), 460-466, 2012. DOI: 10.1590/S0104-14282012005000057.

Alexandre, E.M.C.; Silva, S.; Santos, S.A.O.; Silvestre, A.J.D.; Duarte, M.F.; Saraiva, J.A.; Pintado, M. Antimicrobial activity of pomegranate peel extracts performed by high pressure and enzymatic assisted extraction. **Food Research International**, 115, 167-176, 2019. DOI: 10.1016/j.foodres.2018.08.044

Almeida, T. M.; Bispo, M. D.; Cardoso, A. R.; Migliorini, M. V.; Schena, T.; de Campos, M. C.; Machado, M. E.; López, J. A.; Krause, L. C.; Caramão, E. B. Preliminary studies of bio-oil from fast pyrolysis of coconut fibers. **Journal of agricultural and food chemistry**, 61, 28, 6812–6821, 2013. DOI: 10.1021/jf401379s.

Alonso-Lerma, B.; Barandiaran, L.; Ugarte, L.; Larraza, I.; Reifs, A.; Olmos-Juste, R.; Barrietabeña, N.; Amenabar, I.; Hillenbrand, R.; Eceiza, A.; Perez-Jimenez, R. High performance crystalline nanocellulose using an ancestral endoglucanase. **Communications Materials**, 1, 57, 1-10, 2020. DOI: 10.1038/s43246-020-00055-5.

Angamuthu, D.; Purushothaman, I.; Kothandan, S.; Swaminathan, R. Antiviral study on Punica granatum L., Momordica charantia L., Andrographis paniculata Nees, and Melia azedarach L., to Human Herpes Virus-3. **European Journal of Integrative Medicine**, 28, 98-108, 2019. DOI: 10.1016/j.eujim.2019.04.008

Badhe, R.V.; Godse, A.; Ahinkar, A. Biomaterials in 3D printing: a special emphasis on nanocellulose. **Indian Journal of Pharmaceutical Education and Research**, 54, 526–540, 2020. DOI: 10.5530/ijper.54.3.101.

Balea, A; Fuente, E; Blanco, A; Negro, C. Nanocelluloses: Natural-Based Materials for Fiber-Reinforced Cement Composites. A Critical Review. **Polymers (Basel)**, 11(3), 2019. DOI: 10.3390/polym11030518.

Baptista, C.; Robert, D.; Duarte, A. P. Relationship between lignin structure and delignification degree in *Pinus pinaster* kraft pulps. **Bioresource technology**, 99(7), 2349–2356, 2008. DOI: 10.1016/j.biortech.2007.05.012.

Basavegowda, N.; Sobczak-Kupiec, A.; Fenn, R. I.; Dinakar, S. Bioreduction of chloroaurate ions using fruit extract *Punica granatum* (Pomegranate) for synthesis of highly stable gold nanoparticles and assessment of its antibacterial activity. **Micro & Nano Letters**, 8 (8), 400–404, 2013. DOI:10.1049/mnl.2013.0137

Benini, K.; Voorwald, H.; Cioffi, M.; Rezende, M. C.; Arantes, V. Preparation of nanocellulose from *Imperata brasiliensis* grass using Taguchi method. **Carbohydrate polymers**, 192, 337–346, 2018. DOI: 10.1016/j.carbpol.2018.03.055.

Bhat, A. H.; Khan, I.; Usmani, M. A.; Umapathi, R.; Al-Kindy, S. Cellulose an ageless renewable green nanomaterial for medical applications: An overview of ionic liquids in extraction, separation and dissolution of cellulose. **International journal of biological macromolecules**, 129, 750–777, 2019. DOI: 10.1016/j.ijbiomac.2018.12.190.

Bilal, M.; Iqbal, H. M. N. Naturally-derived biopolymers: potential platforms for enzyme immobilization. **International journal of biological macromolecules**, 130, 462–482, 2019. DOI: 10.1016/j.ijbiomac.2019.02.152.

Brainer, M.S. de C. P. Produção de coco: o nordeste é destaque nacional. **Caderno Setorial ETENE**, 3, 61, 2018.

Bundschuh, M.; Filser, J.; Lüderwald, S.; McKee, M. S.; Metreveli, G.; Schaumann, G. E.; Schulz, R.; Wagner, S. Nanoparticles in the environment: where do we come from, where do we go to? **Environmental Sciences Europe**, 30, 6, 1-17, 2018. DOI: 10.1186/s12302-018-0132-6.

Cao, Y.; Zavaterra, P.; Youngblood, J.; Moon, R.; Weiss, J. The influence of cellulose nanocrystal additions on the performance of cement paste. **Cement and Concrete Composites**, 56, 73-83, 2015. DOI: 10.1016/j.cemconcomp.2014.11.008.

Carpenter, A. W.; de Lannoy, C.-F.o.; Wiesner, M. R. Cellulose nanomaterials in water treatment technologies. **Environmental Science & Technology**, 49 (9), 5277–5287, 2015. DOI: 10.1021/es506351r.

Chantereau, G.; Sharma, M.; Abednejad, A.; Vilela, C.; Costa, E.M.; Veiga, M.; Antunes, F.; Pintado, M.M.; Sèbe, G.; Coma, V.; Freire, M.G.; Freire, C.S.R.; Silvestre, A.J.D. Bacterial nanocellulose membranes loaded with vitamin B-based ionic liquids for dermal care application. **Journal of Molecular Liquids**, 302, 1-10, 2020. DOI: 10.1016/j.molliq.2020.112547.

Chattopadhyay, D. P.; Patel, B. H. Synthesis, Characterization and Application of Nano Cellulose for Enhanced Performance of Textiles. **Journal of Textile Science & Engineering**, 6, 248-256, 2016. DOI: 10.4172/2165-8064.1000248.

Chauve, G.; Bras, J. Industrial Point of View of Nanocellulose Materials and Their Possible Applications. *In*: Oksman, K.; Mathew, A. P.; Bismarck, A.; Rojas, O.; Sain, M. **Handbook of Green Materials**. San Diego: World Scientific, 2014, p. 233-251. DOI: 10.1142/8975.

Chen, W. J.; Zhao, B. C.; Cao, X.F.; Yuan, T. Q.; Shi, Q.; Wang, S.F.; Sun, R.C. Structural Features of Alkaline Dioxane Lignin and Residual Lignin from *Eucalyptus grandis* × *E. urophylla*. **ACS Journal of Agricultural and Food Chemistry**, 67, 3, 968-974, 2019. DOI: 10.1021/acs.jafc.8b05760.

Colom X, Carrillo F. Crystallinity changes in lyocell and viscosetype fibres by caustic treatment. **European Polymer Journal**, 38:2225, 2002.

Corradini, E.; Rosa, M. de F.; Macedo, B. P. de; Paladin, P. D.; Mattoso, L. H. C. Composição química, propriedades mecânicas e térmicas da fibra de frutos de cultivares de coco verde. **Revista Brasileira de Fruticultura**, 31, 3, 837-846, 2009.

Cruz-Tato, P.; Ortiz-Quiles, E. O.; Vega-Figueroa, K.; Santiago-Martoral, L.; Flynn, M.; Díaz-Vázquez, L. M.; Nicolau, E. Metalized Nanocellulose Composites as a Feasible Material for Membrane Supports: Design and Applications for Water Treatment. **Environmental science & technology**, 51(8), 4585–4595, 2017. DOI: 10.1021/acs.est.6b05955.

Dahham, S.S.; Ali, M.N.; Tabassum H.; Khan, M. Studies on Antibacterial and Antifungal Activity of Pomegranate (*Punica granatum* L.). **American-Eurasian Journal of Agricultural & Environmental Sciences**, 9 (3): 273-281, 2010.

de Andrade, M. R.; Nery, T. B. R.; de Santana E Santana, T. I.; Leal, I. L.; Rodrigues, L. A. P.; de Oliveira Reis, J. H.; Druzian, J. I.; Machado, B. A. S. Effect of Cellulose Nanocrystals from Different Lignocellulosic Residues to Chitosan/Glycerol Films. **Polymers**, 11(4), 658, 2019. DOI: 10.3390/polym11040658.

De France, K.J.; Hoare, T.; Cranston, E.D. Review of Hydrogels and Aerogels Containing Nanocellulose. **Chemistry of Materials**, 29, 11, 4609-4631, 2017. DOI: 10.1021/acs.chemmater.7b00531.

Derami, H. G.; Jiang, Q.; Ghim, D.; Cao, S.; Chandar, Y. J.; Morrissey, J. J.; Jun, Y.-S.; Singamaneni, S. A Robust and Scalable Polydopamine/Bacterial Nanocellulose Hybrid Membrane for Efficient Wastewater Treatment. **ACS Applied Nano Materials**, 2, 1092–1101, 2019. DOI: 10.1021/acsanm.9b00022.

Elshafei, A.; El-Zanfaly, H. T. Application of Antimicrobials in the Development of Textiles. **Asian Journal of Applied Sciences**, 4, 585-595, 2011. DOI: 10.3923/ajaps.2011.585.595

Emam, H.E. Antimicrobial cellulosic textiles based on organic compounds. **3 Biotech**, 9, 29 (2019). DOI: 10.1007/s13205-018-1562-y

Eslahi, N.; Mahmoodi, A.; Mahmoudi, N.; Zandi, N.; Simchi, A. Processing and properties of nanofibrous bacterial cellulose-containing polymer composites: a



review of recent advances for biomedical applications. **Polymers**, 60, 144–170, 2020. DOI: 10.1080/15583724.2019.1663210.

Forsman, N.; Lozhechnikova, A.; Khakalo, A.; Johansson, L.-S.; Vartiainen, J.; Osterberg, M. Layer-by-layer assembled hydrophobic coatings for cellulose nanofibril films and textiles, made of polylysine and natural wax particles. **Carbohydrate Polymers**, 173, 392–402, 2017. DOI: <https://doi.org/10.1016/j.carbpol.2017.06.007>.

Gawande, M. B.; Goswami, A.; Asefa, T.; Guo, H.; Biradar, A. V.; Peng, D. L.; Zboril, R.; Varma, R. S. Core–shell nanoparticles: synthesis and applications in catalysis and electrocatalysis. **Chemical Society Reviews**, 44, 21, 7540–7590, 2015. DOI: 10.1039/C5CS00343A.

Giese, M.; Blusch, L. K.; Khan, M. K.; MacLachlan, M. J. Functional materials from cellulose-derived liquid-crystal templates. **Angewandte Chemie** (International ed. in English), 54, 10, 2888–2910, 2015. DOI: 10.1002/anie.201407141.

Golmohammadi, H.; Morales-Narváez, E.; Naghdi, T.; Merkoçi, A. Nanocellulose in Sensing and Biosensing. **Chemistry of Materials**, 29 (13), 5426-5446, 2017. DOI: 10.1021/acs.chemmater.7b01170.

Gour, A.; Jain, N.K. Advances in green synthesis of nanoparticles. **Artificial Cells, Nanomedicine, and Biotechnology**, 47, 1, 844-851, DOI: 10.1080/21691401.2019.1577878.

Halib, N.; Ahmad, I. Nanocellulose: insight into health and medical applications. In: Martínez, L. M. T.; Kharissova, O. V.; Kharisov, B. I. **Handbook of Ecomaterials**. Springer International Publishing, 2018, 1-19. DOI: 10.1007/978-3-319-48281-1\_5-1.

Hamdy, M. E.; Del Carlo, M.; Hussein, H. A.; Salah, T. A.; El-Deeb, A. H.; Emara, M. M.; Pezzoni, G.; Compagnone, D. Development of gold nanoparticles biosensor for ultrasensitive diagnosis of foot and mouth disease virus. **Journal of Nanobiotechnology**, 16, 48, 1-12, 2018. DOI: 10.1186/s12951-018-0374-x.

Hassan, B. S.; Islam, G. M. N.; Haque, A. N. M. A. Applications of Nanotechnology in Textiles: A Review. **Advance Research in Textile Engineering**, 4 (2), 1038-1047, 2019.

Hindeleh, A.M.; Johnson, D.J. Crystallinity and crystallite size measurement in polyamide and polyester fibers. **Polymer**, 19:27, 1978.

Honarvar, M.G.; Latifi, M. Overview of wearable electronics and smart textiles. **Journal of the Textile Institute**, 108:631, 2017.

Hu, L.; Du, H.; Liu, C.; Zhang, Y.; Yu, G.; Zhang, X.; Zhang, X. Comparative Evaluation of the Efficient Conversion of Corn Husk Filament and Corn Husk Powder to Valuable Materials via a Sustainable and Clean Biorefinery Process. **ACS Sustainable Chemistry & Engineering**, 7, 1, 1327-1336, 2018. DOI: 10.1021/acssuschemeng.8b05017

Huang, Z.H.; Kang, F.Y.; Zheng, Y.P.; Yang, J.B.; Liang, K.M. Adsorption of trace polar methy-ethyl-ketone and non-polar benzene vapors on viscose rayon-based activated carbon fibers. **Carbon**, 40:1363, 2002.

Hussein, M.A.M.; Grinholc, M.; Dena, A.S.A.; El-Sherbiny, I.M.; Megahed, M. Boosting the antibacterial activity of chitosan–gold nanoparticles against antibiotic–resistant bacteria by Punicagranatum L. extract. **Carbohydrate Polymers**, 256,117498, 2021. DOI: 10.1016/j.carbpol.2020.117498

Idumah, C.I. Influence of nanotechnology in polymeric textiles, applications, and fight against COVID-19. **The Journal of The Textile Institute**,1-21, 2020. DOI: 10.1080/00405000.2020.1858600.

Indústria Brasileira de Árvores. Histórico de desempenho. São Paulo: IBÁ, 2020. Disponível em: < <https://iba.org/historico-de-desempenho#celulose-1> >. Acesso em: 11 de junho de 2020.

Ishizaki, M. H.; Visconte, L. L. Y.; Furtado, C. R. G.; Leite, M. C. A. M.; Leblanc, J. L. Caracterização mecânica e morfológica de compósitos de polipropileno e fibras de coco verde: influência do teor de fibra e das condições de mistura. **Polímeros**, 16, 3, 182-186, 2006.

Jamkhande, P. G.; Ghule, N. W.; Bamer, A. H.; Kalaskar, M. G. Metal nanoparticles synthesis: An overview on methods of preparation, advantages and disadvantages, and applications. **Journal of Drug Delivery Science and Technology**, 53, 1-11, 2019. DOI: 10.1016/j.jddst.2019.101174.

Jebali, A.; Hekmatimoghaddam, S.; Behzadi, A. Rezapour, I; Mohammadi, B. H.; Jasemizad, T.; Yasini, S. A.; Javadzadeh, M.; Amiri, A.; Soltani, M.; Rezaei, Z.; Sedighi, N.; Seyfi, M.; Rezaei, M.; Sayadi, M. Antimicrobial activity of nanocellulose conjugated with allicin and lysozyme. **Cellulose**, 20, 2897–2907, 2013. DOI: 10.1007/s10570-013-0084-3.

Johar, N.; Ahmad, I.; Dufresne, A. Extraction, preparation and characterization of cellulose fibres and nanocrystals from rice husk. **Industrial Crops and Products**, 37, 1, 93–99, 2012. DOI: 10.1016/j.indcrop.2011.12.016.

Junka, K.; Guo, J.; Filpponen, I.; Laine, J.; Rojas, O. J. Modification of cellulose nanofibrils with luminescent carbon dots. **Biomacromolecules**, 15, 3, 876–881, 2014. DOI: 10.1021/bm4017176.

Keijok, W.J.; Pereira, R.H.A.; Alvarez, L.A.C.; Prado, A. R.; da Silva, A. R.; Ribeiro, J.; de Oliveira, J. P.; Guimarães, M. C. C. Controlled biosynthesis of gold nanoparticles with Coffea arabica using factorial design. **Scientific Reports**, 9, 2019. DOI: 10.1038/s41598-019-52496-9.

Kishor, R.; Purchase, D.; Saratale, G. D.; Saratale, R. G.; Ferreira, L.F.R.; Bilal, M.; Chandra, R.; Bharagava, R.N. Ecotoxicological and health concerns of persistent coloring pollutants of textile industry wastewater and treatment approaches for environmental safety. **Journal of Environmental Chemical Engineering**, 9, 2, 2213-3437, 2021. DOI: 10.1016/j.jece.2020.105012.

Klemm, D.; Heublein, B.; Fink, Hans-Peter; Bohn, A. Cellulose: Fascinating Biopolymer and Sustainable raw material. **Angewandte Chemie International**, 44, 3358 – 3393, 2005. DOI: 10.1002/anie.200460587.

Klemm, D.; Cranston, E.D.; Fischer, D.; Gama, M.; Kedzior, S.A.; Kralisch, D.; Kramer, F.; Kondo, T.; Lindström, T.; Nietzsche, S.; Petzold-Welcke, K.; Rauchfu, F. Nanocellulose as a natural source for groundbreaking applications in materials science: Today's state. **Materials Today**, 21, 7, 720-748, 2018. DOI: 10.1016/j.mattod.2018.02.001.

Klemm, D.; Heublein, B.; Fink, H. P.; Bohn, A. Cellulose: fascinating biopolymer and sustainable raw material. **Angewandte Chemie (International ed. in English)**, 44, 22, 3358–3393, 2005. DOI: 10.1002/anie.200460587.

Kokol, V.; Vivod, V.; Peršin, Z.; Čolić, M.; Matjaž, K. Antimicrobial properties of viscose yarns ring-spun with integrated amino-functionalized nanocellulose. **Cellulose**, 28, 6545–6565, 2021. DOI: 10.1007/s10570-021-03946-z(0123456789().,-volV()0123456789().,-volV).

Lam, E.; Male, K. B.; Chong, J. H.; Leung, A. C.; Luong, J. H. Applications of functionalized and nanoparticle-modified nanocrystalline cellulose. **Trends in biotechnology**, 30(5), 283–290, 2012. DOI: 10.1016/j.tibtech.2012.02.001.

Le, D. H.; Lee, K. L.; Shukla, S.; Commandeur, U.; Steinmetz, N. F. Potato virus X, a filamentous plant viral nanoparticle for doxorubicin delivery in cancer therapy. **Nanoscale**, 9, 6, 2348–2357, 2017. DOI: 10.1039/c6nr09099k.

Lee, H. V.; Hamid, S. B.; Zain, S. K. Conversion of lignocellulosic biomass to nanocellulose: structure and chemical process. **The Scientific World Journal**, 2014, 631013, 2014. DOI: 10.1155/2014/631013.

Li, J.; Cha, R.; Mou, K.; Zhao, X.; Long, K.; Luo, H.; Zhou, F.; Jiang, X. Nanocellulose-Based Antibacterial Materials. **Advanced Healthcare Materials**, 7, 20, 2018. DOI: 10.1002/adhm.201800334.

Li, J.; Wei, X.; Wang, Q.; Chen, J.; Chang, G.; Kong, L.; Su, J.; Liu, Y. Homogeneous Isolation of Nanocellulose from Sugarcane Bagasse by High Pressure Homogenization. **Carbohydrate Polymers**, 90, 4, 1609–1613, 2012. DOI: 10.1016/j.carbpol.2012.07.038.

Li, M.; Farooq, A.; Jiang, S.; Zhang, M.; Mussana, H.; Liu, L. Functionalization of cotton fabric with ZnO nanoparticles and cellulose nanofibrils for ultraviolet protection. *California Management Review*, 91(19-20):117-137, 2021. DOI:10.2307/41166438

Liang, H.; Hu, X. A quick review of the applications of nano crystalline cellulose in wastewater treatment. **Journal of Bioresources and Bioproducts**, 1, 4, 199–204, 2016. DOI: 10.21967/jbb.v1i4.65.

Liu, K.; Du, H.; Zheng, T.; Liu, H.; Zhang, M.; Zhang, R.; Li, H.; Xie, H.; Zhang, X.; Ma, M.; Si, C. Recent advances in cellulose and its derivatives for oilfield

applications. **Carbohydrate Polymers**, 259, 1-13, 2021. DOI: 10.1016/j.carbpol.2021.117740.

Lokina, S.; Suresh, R.; Giribabu, K.; Stephen, A.; Lakshmi Sundaram, R.; Narayanan, V. Spectroscopic investigations, antimicrobial, and cytotoxic activity of green synthesized gold nanoparticles. **Spectrochimica Acta Part A: Molecular and Biomolecular Spectroscopy**, 129, 484-490, 2014. DOI: 10.1016/j.saa.2014.03.100

Lynd, L. R.; Weimer, P. J.; van Zyl, W. H.; Pretorius, I. S. Microbial cellulose utilization: fundamentals and biotechnology. **Microbiology and molecular biology reviews**, 66(3), 506–577, 2002. DOI: 10.1128/MMBR.66.3.506-577.2002.

Machado, B. A.; Reis, J. H.; Cruz, L. A.; Leal, I. L.; Barbosa, J. D.; Azevedo, J. B.; Druzian, J. I. Characterization of cassava starch films plasticized with glycerol and strengthened with nanocellulose from green coconut fibers. **African Journal of Biotechnology**, 16, 1567-1578, 2017. DOI:10.5897/AJB2017.15943.

Machado, B.A.S.; Reisb, J.H.O.; da Silva, J.B.; Cruz, L.S.; Nunes, I.L.; Pereira, F.V.; Druzian, J. I. Obtenção de nanocelulose da fibra de coco verde e incorporação em filmes biodegradáveis de amido plastificados com glicerol. **Química Nova**, 37, 8, 1275-1282, 2014.

Maldonado-Bustamante, S.R., Mondaca-Fernández, I., Caro-Reyes, R.B., Gámez-Gutierrez, L.A., Santos- Villalobos, S. de los, Meza-Montenegro, M.M., & Balderas-Cortés, J.J. Selección de cepas productoras de enzimas ligninolíticas nativas del Valle del Yaqui. **Nova scientia**, 9(19), 24-36, 2017. DOI: 10.21640/ns.v9i19.893.

Martin-Martinez F. J. Designing nanocellulose materials from the molecular scale. **Proceedings of the National Academy of Sciences of the United States of America**, 115(28), 7174–7175, 2018. DOI: 10.1073/pnas.1809308115.

Mishra, S.; Kharkar, P. S.; Pethe, A. M. Biomass and waste materials as potential sources of nanocrystalline cellulose: Comparative review of preparation methods (2016 – Till date). **Carbohydrate Polymers**, 207, 418-427, 2019. DOI: 10.1016/j.carbpol.2018.12.004.

Mohamed, M. A.; Abd Mutalib, M.; Mohd Hir, Z. A.; M Zain, M. F.; Mohamad, A. B.; Jeffery Minggu, L.; Awang, N. A.; W Salleh, W. N. An overview on cellulose-based material in tailoring bio-hybrid nanostructured photocatalysts for water treatment and renewable energy applications. **International journal of biological macromolecules**, 103, 1232–1256, 2017. DOI: 10.1016/j.ijbiomac.2017.05.181.

Mondal, D.; Perween, M.; Srivastava, D.N.; Ghosh, P.K. Unconventional Electrode Material Prepared from Coir Fiber through Sputter Coating of Gold: A Study toward Value Addition of Natural Biopolymer. **ACS Sustainable Chemistry & Engineering**, 2, 3, 348–352, 2014. DOI: 10.1021/sc400389u.

Morais, J. P. S.; Rosa, M. de F.; de Souza Filho, M. de sa M.; Nascimento, L. D.; do Nascimento, D.M.; Cassales, A. R. Extraction and Characterization of Nanocellulose Structures from Raw Cotton Linter. **Carbohydrate Polymers**, 91 (1), 229–235, 2013. DOI: 10.1016/j.carbpol.2012.08.010.

Moura, D.; Souza, M.T.; Liverani, L.; Rella, G.; Luz, G.M.; Mano, J.F.; Boccaccini, A.R. Development of a bioactive glass-polymer composite for wound healing applications. **Materials Science and Engineering: C**, 76, 224–232, 2017. DOI: 10.1016/j.msec.2017.03.037.

Murthy, K.N.C.; Jayaprakasha, G.K.; Singh, R.P. Studies on Antioxidant Activity of Pomegranate (*Punica granatum*) Peel Extract Using in Vivo Models. **Journal of Agricultural and Food Chemistry**, 50 (17), 4791–4795, 2002. DOI: 10.1021/jf0255735

Mussato, I.S.; Roberto, I.C. Produção biotecnológica de xilitol a partir da palha de arroz. **Biotecnologia Ciência & Desenvolvimento**, 28, 24-39, 2002.

Nadagouda, M.N.; Iyanna, N.; Lalley, J.; Han, C.; Dionysiou, D.D.; Varma, R.S. Synthesis of Silver and Gold Nanoparticles Using Antioxidants from Blackberry, Blueberry, Pomegranate, and Turmeric Extracts. **ACS Sustainable Chemistry & Engineering**, 2 (7), 1717–1723, 2014. DOI: 10.1021/sc500237k

Nadi, A.; Boukhriss, A.; Bentis, A.; et al. Evolution in the surface modification of textiles: a review. **Textile Progress**, 50:67–108, 2018. DOI: 10.1080/00405167.2018.1533659

Ngô, C.; Van de Voorde, M. Nanotechnology for the Textile Industry. *In*: Ngô, C.; Van de Voorde, M. **Nanotechnology in a Nutshell**. Atlantis Press, 2014, p. 321–329. DOI: 10.2991/978-94-6239-012-6\_19.

Norrrahim, M. N. F.; Kasim, N. A. M.; Knight, V. F.; Ujang, F. A.; Janudin, N.; Razak, M. A. I. A.; Shah, N. A. A.; Noor, S. A. M.; Jamal, S. H.; Ong, K. K.; Yunus, W. M. Z.W. Nanocellulose: the next super versatile material for the military. **Materials Advances**, 2, 1485–1506, 2021a. DOI: 10.1039/D0MA01011A.

Norrrahim, M. N. F.; Nurazzi, N. M.; Jenol, M. A.; Farid, M. A. A.; Janudin, N.; Ujang, F. A.; Yasim-Anuar, T. A. T.; Najmuddin, S. U. F. S.; Ilyas, R. A. Emerging development of nanocellulose as an antimicrobial material: an overview. **Materials Advances**, 2, 3538–3551, 2021. DOI: 10.1039/d1ma00116g.

Nunes, M. U. C.; dos Santos, J. R.; dos Santos, T. C. Tecnologia para Biodegradação da Casca de Coco Seco e de Outros Resíduos do Coqueiro. Aracaju: **Embrapa Agroindústria Tropical**, Circular Técnica, 46; 2007.

OpenStax. Biology 2e. Houston, Texas, 2018. Disponível em: <<https://openstax.org/books/biology-2e/pages/3-2-carbohydrates>> Acesso em: 16 de junho de 2020.

Patel, M.; Siddiqi, N.J.; Sharma, P.; Alhomida, A.S.; Khan, H.A. Reproductive toxicity of pomegranate peel extract synthesized gold nanoparticles: A

multigeneration study in *C. elegans*. **Journal of Nanomaterials**, 2019 , 8767943, 2019. DOI:10.1155/2019/8767943

Pere, J.; Tammelin, T.; Niemi, P.; Lille, M.; Virtanen, T.; Penttilä, P.A.; Ahvenainen, P.; Grönqvist, S. Production of High Solid Nanocellulose by Enzyme-Aided Fibrillation Coupled with Mild Mechanical Treatment. **ACS Sustainable Chemistry & Engineering**, 8, 51, 18853–18863, 2020. DOI: 10.1021/acssuschemeng.0c05202.

Phanthong, P.; Reubroycharoen, P.; Hao, X.; Xu, G.; Abudula, A.; Guan, G. Nanocellulose: Extraction and application. **Carbon Resources Conversion**, 1, 1, 32-43, 2018. DOI: 10.1016/j.crcon.2018.05.004.

Polos de Fruticultura – Coco. Incaper, 2016. Disponível em: < <https://incaper.es.gov.br/fruticultura-coco>>. Acesso em: 30 de junho de 2020.

Power, G.; Loh, J. Organic compounds in the processing of lateritic bauxites to alumina: Addendum to Part 1: Origins and chemistry of organics in the Bayer process. **Hydrometallurgy**, 108, 1–2, 149-151, 2011). DOI: 10.1016/j.hydromet.2011.03.011.

Prashanth, D.; Asha, M.K.; Amit, A. Antibacterial activity of *Punica granatum*. **Fitoterapia**, 72 (2), 171-173, 2001. DOI: 10.1016/S0367-326X(00)00270-7

Raghav, N.; Sharma, M. R.; Kennedy, J. F. Nanocellulose: A mini-review on types and use in drug delivery systems. **Carbohydrate Polymer Technologies and Applications**, 2, 1-10, 2021. DOI: 10.1016/j.carpta.2020.100031.

Rajabairavi, N.; Raju, C. S.; Karthikeyan, C.; Varutharaju, K.; Nethaji, S.; Hameed, A. S. H.; Shajahan, A. Biosynthesis of novel zinc oxide nanoparticles (ZnO NPs) using endophytic bacteria *Sphingobacterium thalpophilum*. **Recent trends in materials science and applications**, 189, 245–254, 2017. DOI: 10.1007/978-3-319-44890-9\_23.

Rajinipriya, M.; Nagalakshmaiah, M.; Robert, M.; Elkoun, S. Importance of Agricultural and Industrial Waste in the Field of Nanocellulose and Recent Industrial Developments of Wood Based Nanocellulose: A Review. **ACS Sustainable Chemistry & Engineering**, 6, 3, 2807–2828, 2018. DOI: 10.1021/acssuschemeng.7b03437.

Rana, A.; Yadav, K.; Jagadevan, S. A comprehensive review on green synthesis of nature-inspired metal nanoparticles: Mechanism, application and toxicity. **Journal of Cleaner Production**, 272, 1-25, 2020. DOI: 10.1016/j.jclepro.2020.122880.

Rasheed, M.; Jawaid, M.; Parveez, B.; Zuriyati, A.; Khan, A. Morphological, chemical and thermal analysis of cellulose nanocrystals extracted from bamboo fibre. **International journal of biological macromolecules**, 160, 183–191, 2020. DOI: 10.1016/j.ijbiomac.2020.05.170.

Rencoret, J.; Ralph, J.; Marques, G.; Gutiérrez, A.; Martínez, Á.; del Río, J. C. Structural characterization of lignin isolated from coconut (*Cocos nucifera*) coir

fibers. **Journal of agricultural and food chemistry**, 61, 10, 2434–2445, 2013. DOI: 10.1021/jf304686x.

Ricci, D.; Giamperi, L.; Bucchini, A.; Fraternali, D. Antioxidant activity of Punica granatum fruits. **Fitoterapia**, 77, 310 – 312, 2006.

Rivero, P.J.; Urrutia, A.; Goicoechea, J.; Arregui, F.J. Nanomaterials for Functional Textiles and Fibers. **Nanoscale Research Letters**, 10(1):501, 2015. doi: 10.1186/s11671-015-1195-6.

Rosa, M. F.; Medeiros, E. S.; Malmonged, J. A.; Gregorskib, K. S.; Wood, D. F.; Mattoso, L. H. C.; Glenn, G.; Orts, W. J.; Imam, S. H. Cellulose nanowhiskers from coconut husk fibers: Effect of preparation conditions on their thermal and morphological behavior. **Carbohydrate Polymers**, 81, 1, 83-92, 2010. DOI: 10.1016/j.carbpol.2010.01.059.

Roy, A.; Bulut, O.; Some, S.; Mandal, A. K.; Yilmaz, M. D. Green synthesis of silver nanoparticles: biomolecule-nanoparticle organizations targeting antimicrobial activity. **RSC Advances**, 9, 2673-2702, 2019. DOI: 10.1039/C8RA08982E.

Ruiz, N.T. **Derivatização de celulose sob condições homogêneas de reação**. Dissertação (Mestrado em Química) – Instituto de Química, Universidade de São Paulo. São Paulo, p. 25. 2004.

Salem, S. S.; Fouda, A. Green Synthesis of Metallic Nanoparticles and Their Prospective Biotechnological Applications: an Overview. **Biological Trace Element Research**, 199, 1, 344-370, 2021. DOI: 10.1007/s12011-020-02138-3.

Salimi, S.; Sotudeh-Gharebagh ,R.; Zarghami, R.; Chan, S. Y.; Yuen, K. H. Production of Nanocellulose and Its Applications in Drug Delivery: A Critical Review. **ACS Sustainable Chemistry & Engineering**, 7, 15800–15827, 2019. DOI: 10.1021/acssuschemeng.9b02744.

Salles, T.S.; Meneses, M.D.F.; Caldas, L.A.; Sá-Guimarães, T.E.; Oliveira, D.M.; Ventura, J.A.; Azevedo, R.C.; Kuster, R.M.; Soares, M.R.; Ferreira, D.F. Virucidal and antiviral activities of pomegranate (Punica granatum) extract against the mosquito-borne Mayaro virus. **Parasites Vectors**, 14, 443, 2021. DOI: 10.1186/s13071-021-04955-4

Santos, F. A.; Queiróz, J. H. de; Colodette, J. L.; Fernandes, S. A.; Guimarães, V. M.; Rezende, S. T. Potencial da palha de cana-de-açúcar para produção de etanol. **Química Nova**, 35(5), 1004-1010, 2012. DOI: 10.1590/S0100-40422012000500025.

Shah, M. A.; Pirzada, B. M.; Price, G.; Shibiru, A. L.; Qurashi, A. Applications of nanotechnology in smart textile industry: A critical review. **Journal of Advanced Research**, 38, 55-75, 2022. DOI: 10.1016/j.jare.2022.01.008.

Shahbazi, Y.; Shavisi N. Characterization of active nanochitosan film containing natural preservative agents. **Nanomedicine Research Journal**, 3 (2), 109-116, 2018. DOI: 10.22034/nmrj.2018.02.008

Sharma, C.; Bhardwaj, N.K. Fabrication of natural-origin antibacterial nanocellulose films using bio-extracts for potential use in biomedical industry. **International Journal of Biological Macromolecules**, 145 914–925, 2020. DOI: 10.1016/j.ijbiomac.2019.09.182.

Shaygannia, E.; Bahmani, M.; Zamanzad, B.; Rafieian-Kopaei, M. A Review Study on *Punica granatum* L. **Journal of Evidence-Based Complementary & Alternative Medicine**, 21(3), 221-227, 2016. DOI: 10.1177/2156587215598039

Shi, Q., Sun, J., Hou, C. *et al.* Advanced Functional Fiber and Smart Textile. **Advanced Fiber Materials**, 1, 3–31, 2019. DOI: 10.1007/s42765-019-0002-z

Silva, L. P. C.; Oliveira, J. P.; Keijok, W.J.; da Silva, A. R.; Aguiar, A. R.; Guimarães, M. C. C.; Ferraz, C. M.; Araújo, J. V.; Tobias, F. L.; Braga, F. R. Extracellular biosynthesis of silver nanoparticles using the cell-free filtrate of nematophagous fungus *Duddingtonia flagrans*. **International Journal of Nanomedicine**, 12, 6373-6381, 2017. DOI: 10.2147/IJN.S137703.

Silva, R.; Haraguchi, S. K.; Muniz, E. C.; Rubira, A.F. Aplicações de fibras lignocelulósicas na química de polímeros e em compósitos. **Química Nova**, 32(3), 661-671, 2009. DOI: 10.1590/S0100-40422009000300010.

Simão, L.; Hotza, D.; Raupp-Pereira, F.; Labrincha, J. A.; Montedo; O. R. K. Wastes from pulp and paper mills - a review of generation and recycling alternatives. **Cerâmica**, 64, 371, 443-453, 2018. DOI: 10.1590/0366-69132018643712414.

Simoni P. Advanced biosensors for monitoring astronauts' health during longduration space missions. **Biosensors and Bioelectronics**, 111, 18–26, 2018. DOI: 10.1016/j.bios.2018.03.062.

Sinsinwar, S.; Sarkar, M. K.; Suriya, K. R.; Nithyanand, P.; Vadivel, V. Use of agricultural waste (coconut shell) for the synthesis of silver nanoparticles and evaluation of their antibacterial activity against selected human pathogens. **Microbial Pathogenesis**, 124, 30-37, 2018. DOI: 10.1016/j.micpath.2018.08.025.

Soares, B.; Tavares, D. J. P.; Amaral, J. L.; Silvestre, A. J. D.; Freire, C. S. R.; Coutinho, J. A. P. Enhanced Solubility of Lignin Monomeric Model Compounds and Technical Lignins in Aqueous Solutions of Deep Eutectic Solvents. **ACS Sustainable Chemistry & Engineering**, 5, 5, 4056-4065, 2017. DOI: 10.1021/acssuschemeng.7b00053.

Subhedar, A.; Bhadauria, S.; Ahankari, S.; Kargarzadeh, H. Nanocellulose in biomedical and biosensing applications: A review. **International Journal of Biological Macromolecules**, 166, 587-600, 2021. DOI: 10.1016/j.ijbiomac.2020.10.217.

Taflick, T.; Schwendler, L. A.; Rosa, S.; Bica, C.; Nachtigall, S. Cellulose nanocrystals from acacia bark-Influence of solvent extraction. **International journal of biological macromolecules**, 101, 553–561, 2017. DOI: 10.1016/j.ijbiomac.2017.03.076.



Tang, J.; Song, Y.; Zhao, F.; Spinney, S.; da Silva Bernardes, J.; Tam, K. C. Compressible cellulose nanofibril (CNF) based aerogels produced via a bio-inspired strategy for heavy metal ion and dye removal. **Carbohydrate polymers**, 208, 404–412, 2019. DOI: 10.1016/j.carbpol.2018.12.079.

Thakur, V.; Guleria, A.; Kumar, S.; Sharmad, S.; Singh, K. Recent advances in nanocellulose processing, functionalization and applications: a review. **Materials Advances**, 2, 1872–1895, 2021. DOI: 10.1039/D1MA00049G.

Tripathi, A.; Ferrer, A.; Khan, S.A.; Rojas, O.J. Morphological and Thermochemical Changes upon Autohydrolysis and Microemulsion Treatments of Coir and Empty Fruit Bunch Residual Biomass to Isolate Lignin-Rich Micro- and Nanofibrillar Cellulose. **ACS Sustainable Chemistry & Engineering**, 5, 2483–2492, 2017. DOI: 10.1021/acssuschemeng.6b02838.

Verma, C.; Chhajed, M.; Gupta, P.; Roy, S.; Maji, P. K. Isolation of cellulose nanocrystals from different waste bio-mass collating their liquid crystal ordering with morphological exploration. **International journal of biological macromolecules**, 175, 242–253, 2021. DOI: 10.1016/j.ijbiomac.2021.02.038.

Wang, Q. Q.; Zhu, J. Y.; Gleisner, R.; Kuster, T. A.; Baxa, U.; McNeil, S. E. Morphological Development of Cellulose Fibrils of a Bleached Eucalyptus Pulp by Mechanical Fibrillation. **Cellulose**, 19, 5, 1631–1643, 2012. DOI: 10.1007/s10570-012-9745-x.

Wang, Y.L.; Wan, Y.Z.; Dong, X.H.; Cheng, G.X.; Tao, H.M.; Wen, T.Y. Preparation and characterization of antibacterial viscose-based activated carbon fiber supporting silver. **Carbon**, 36:1567, 1998.

Xu, Y.; Li, S.; Yue, X.; Lu, W. Review of silver nanoparticles (AgNPs)-Cellulose antibacterial composites. **BioResources**, 13, 2150–2170, 2017. DOI: 10.15376/biores.13.1. Xu.

Yusefi, M.; Shameli, K.; Ali, R. R.; Pang, S.–W.; Teow, S.–Y. Evaluating anticancer activity of plant–mediated synthesized iron oxide nanoparticles using Punica Granatum fruit peel extract. **Journal of Molecular Structure**, 1204, 127539, 2020. DOI: 10.1016/j.molstruc.2019.127539

Zhang, Y.; Wu, J.Q.; Li, H.; Yuan, T. Q.; Wang, Y. Y.; Sun, R. C. Heat Treatment of Industrial Alkaline Lignin and its Potential Application as an Adhesive for Green Wood–Lignin Composites. **ACS Sustainable Chemistry & Engineering**, 5 (8), 7269–7277, 2017. DOI: 10.1021/acssuschemeng.7b01485.

Zhu, H.; Luo, W.; Ciesielski, P. N.; Fang, Z.; Zhu, J. Y.; Henriksson, G.; Himmel, M. E.; Hu, L. Wood-derived materials for green electronics, biological devices, and energy applications. **ACS Chemical Reviews**, 116, 9305–9374, 2016. DOI: 10.1021/acs.chemrev.6b00225.

## ANNEX I

### Publications

1. Avila, Sady Roberto Rodriguez ; Schuenck, Gisele Pereira Diniz ; **Silva, Laryssa Pinheiro Costa** ; Keijok, Wanderson Juvencio ; Xavier, Lorena Martins ; Endringer, Denise Coutinho ; Oliveira, Jairo Pinto ; Schuenck,

Ricardo Pinto ; Guimarães, Marco Cesar Cunegundes . High antibacterial in vitro performance of gold nanoparticles synthesized by epigallocatechin 3-gallate. JOURNAL OF MATERIALS RESEARCH, v. 1, p. 1-5, 2021. DOI: 10.1557/s43578-020-00012-5

## **ANNEX II**

### **Conference contributions**

#### **Posters**

- 28º Congresso Brasileiro de Microscopia e Micoanálise. Design of Experiments Approach to nanocellulose production: transforming food waste in nanoprodukt. 2021.
- 27º Congresso Brasileiro de Microscopia. Methods for determining the concentration of green gold nanoparticles. 2019.

### **ANNEX III**

#### **Additional information**

## Economic impact

The present work used coconut fiber as a source of cellulose. Brazil is the fifth largest producer of coconut in the world <sup>1</sup> and among Brazilian states, Espírito Santo stands out as an important producer of the dwarf variety. The state has a planted area of approximately 11 thousand hectares and an annual production of about 134 million fruits, concentrated mainly in the northern region. Cultivation is carried out mainly by small family-based rural producers. The plantation of coconut has great socioeconomic importance, as it is an alternative to coffee monoculture. From the 1960s onwards, there was an increase in tourism on the Espírito Santo coast, generating a greater interest in coconut cultivation, with the purpose of meeting the consumption of green coconut water <sup>2</sup>.

This growing consumption had as an immediate consequence a large production of solid waste, formed by the fibrous coconut husks, which are responsible for 60% of the volume of domestic waste generated in some areas of the Brazilian coast <sup>3</sup>. In the state of Rio de Janeiro, for example, around 12,000 t/month of coconut waste is produced during the summer <sup>4</sup>. In addition, when this material is discarded in landfills and dumps, it is a potential emitter of greenhouse gases (methane) <sup>5</sup>(Nunes et al. 2007).

The great availability of coconut fiber in Brazil, added to the environmental problem it generates, justifies the use of this material as a source of raw material for obtaining nanocellulose. This should turn a public health problem into a source of wealth, since the price of cellulose nanofiber varies between 2-40 \$/g<sup>6</sup>.

---

<sup>1</sup> Brainer, M.S. de C. P. Produção de coco: o nordeste é destaque nacional. Cad. Set. ETENE, 3:61, 2018.

<sup>2</sup> Polos de Fruticultura – Coco. Incaper, 2016. Disponível em: < <https://incaper.es.gov.br/fruticultura-coco>>. Acesso em: 30 de junho de 2020.

<sup>3</sup> Sinsinwar, S.; Sarkar, M.K.; Suriya, K.R.; Nithyanand, P.; Vadivel, V. Use of agricultural waste (coconut shell) for the synthesis of silver nanoparticles and evaluation of their antibacterial activity against selected human pathogens. Microb. Pathog., 124:30-37, 2018.

<sup>4</sup> Ishizaki, M. H.; Visconte, L. L. Y.; Furtado, C. R. G.; Leite, M. C. A. M.; Leblanc, J. L. Caracterização mecânica e morfológica de compósitos de polipropileno e fibras de coco verde: influência do teor de fibra e das condições de mistura. Polímeros, 16(3), 182-186, 2006.

<sup>5</sup> Nunes, M.U.C.; dos Santos, J.R.; dos Santos, T.C. Tecnologia para Biodegradação da Casca de Coco Seco e de Outros Resíduos do Coqueiro. Aracaju: Embrapa Agroindústria Tropical, Circular Técnica, 46; 2007.

<sup>6</sup> 2020 Cellulose Lab Nanocellulose Products Price. Celluloselab. Disponível em:< <https://www.celluloselab.com/price/CelluloseLab%20Product%20Price%20List%202020.htm>>. Acesso em: 20 de agosto de 2022.

### **Socioenvironmental impact**

The smart textile produced is made of a 100%-cotton fabric functionalized with nanomaterials from organic waste, such as pomegranate peel and coconut fiber, extracted through methods that reduce or eliminate the use and generation of chemical pollutants. Thus the circular economy adds value to products that would otherwise be discarded.

## **ANNEX IV**

### **Scientific outreach**

“School of Nano Science”

Social media channel focused on the dissemination of nanoscience to students in the areas of health, engineering, physics and the curious.

